INSTITUTO SUPERIOR TÉCNICO
Universidade Técnica de Lisboa

Energy efficient solutions based on beamforming for UMTS and LTE

Tiago Alexandre Correia Gonçalves

Dissertation submitted for obtaining the degree of
Master in Electrical and Computer Engineering

Jury

Supervisor: Prof. Luís M. Correia

President: Prof. José Bioucas Dias

Members: Prof. Custódio Peixeiro

Prof. Filipe Cardoso

October 2011

To the Ones I really love.

Acknowledgements

First of all, I would like to thank Professor Luís M. Correia for sharing with me, more than his technical expertise and more than the opportunity to develop this work in a forefront application, his commitment for detail, rigor and professionalism that for sure will help me to become a successful professional.

To the EARTH Project, through the Portuguese team of GROW, for all the technical information and support they gave, me and also for the environment created that made me feel as a part of the objective that the EARTH Project is aiming at.

To all GROW members that I have the privilege to know, with all their engineering expertise that comes from years of investment in cutting edge investigation, many thanks for sharing with me their work in several other areas of wireless communications.

To my partners at RF2, also known as “The Basement”, Diogo Silva, João Pinto, Pedro Carreia and Ricardo Batista (without any importance in the order), thank you for enjoyable fellowship and the light and confidence environment that was created when we all were facing the most variable problems in our works. A special thank you to André Silva, who was always ready to discuss the most unbelievable subjects that plagued me during this journey.

Fortunately, I have had the chance to say all those ones that are important for me, how much I love them and how much I want to be close of them, but I cannot finish my acknowledgements without thanking my parents and my brother for all their endeavour in creating the conditions to achieve success in my academic life, and for the responsibility spirit they taught me along my growth.

Abstract

The race for more energy aware systems is motivating the development of solutions that reduce the overall energy spent in telecommunication systems. Looking at the radio interface that UMTS and LTE present, beamforming is studied in order to assess the efficiency in terms of radiated power that is possible to be saved when antenna arrays are placed instead of static sector antennas. Several multiple user scenarios were studied with different users' arrangement. Two simulators, one for UMTS and another for LTE, were developed to evaluate in a statistical way the potential impact that adaptive antenna arrays have to reduce the radiated power, compared with actual BS static sector antennas. UMTS, besides signal improvement, has a lot of interference suppression potential, due to its multiple access technique that separates users by codes in the same carrier frequency. LTE, due to the absence of co-channel intercell interference, is evaluated in terms of desired signal improvement. Through statistical results, it was possible to derive a model for UMTS that describes the power improvement achieved as a function of the number of users and of antenna elements. For UMTS carriers near top capacity, a power reduction of the order of 90% is achievable. For LTE, significant power improvements are reached, especially for antenna arrays with 8 elements, which are able to save near 65%.

Keywords

Beamforming, adaptive antennas, energy efficiency, UMTS, LTE

Resumo

A corrida por sistemas mais conscientes energeticamente está a motivar o desenvolvimento de soluções que reduzam a energia total gasta em sistemas de telecomunicações. Olhando para a interface de rádio de UMTS e LTE, a formação de lobos de radiação é estudada com o objectivo de avaliar a eficiência em termos de potência radiada que é possível obter quando agregados de antenas são colocados em locais onde antes eram usadas antenas sectoriais estáticas. Vários cenários com vários arranjos de utilizadores foram estudados. Dois simuladores, um para UMTS e outro para LTE, foram desenvolvidos para avaliar de forma estatística o impacto potencial que os agregados de antenas adaptativas têm na redução da potência radiada. UMTS, além da melhoria do sinal, tem um grande potencial de supressão de interferências devido à sua técnica de acesso múltiplo que separa os utilizadores por códigos na mesma frequência de portadora. LTE, devido à ausência de interferência de co-canal dentro da mesma célula, é avaliado em relação à melhoria de sinal. Através de resultados estatísticos, foi possível determinar um modelo para UMTS que descreve a melhoria de potência que é alcançada em função dos números de utilizadores e de elementos do agregado. Para UMTS, em portadoras perto de sua capacidade máxima, uma redução da potência da ordem de 90% é alcançável. Para LTE, melhorias significativas são alcançadas, especialmente para agregados com 8 elementos, que são capazes de poupar perto de 65%.

Palavras-chave

Lobos, antenas, adaptativas, eficiência energética, UMTS, LTE

Table of Contents

List of Figures

List of Tables

List of Acronyms

3GPP	Third Generation Partnership Project
ARQ	Automatic Repeat ReQuest
AWGN	Additive White Gaussian Noise
BER	Bit Error Rate
BF	Beamforming
BFU	Beamforming Unit
BPSK	Binary Phase-Shift Keying
BS	Base Station
BTU	British Thermal Unit
CDF	Cumulative Density Function
CDMA	Code Division Multiple Access
CN	Core Networks
CP	Cyclic Prefix
CQI	Channel Quality Information
CS	Circuit-Switched
DBWS	Distributed Broadcast Wireless Networks
DCH	Dedicated Transport Channels
DFTS-OFDM	Discrete Fourier Transform Spreading - OFDM
DL	Downlink
EIA	Energy Information Administration
EIRP	Effective isotropic radiated power
eNB	Evolved-NodeB
EPC	Evolved Packet Core
ETC	Ethiopian Telecommunications Corporation
E-UTRAN	Evolved-UTRAN
FDD	Frequency Division Duplex
HARQ	Hybrid ARQ
HHO	Hard Handover
HSDPA	High-Speed Downlink Packet Access
HS-DSCH	High-Speed Downlink Shared Channel
HSPA	High-Speed Packet Access
HSPA+	High-Speed Packet Access Evolution
HSUPA	High-Speed Uplink Packet Access
IP	Internet Protocol
ISI	Inter-Symbol Interference
LOS	Line-of-Sight
LTE	Long Term Evolution
MAC	Medium Access Control
MIMO	Multiple Input and Multiple Output
MME	Mobility Management Entity

MMSE	Minimum Mean-Square Error
MT	Mobile Terminal
NB	Node B
OFDMA	Orthogonal Frequency Division Multiple Access
OPEX	Operational Expenditure
OSI	Open Systems Interconnection
OVSF	Orthogonal Variable Spreading Factor
PBCCH	Physical Broadcast Control CH
PCFICH	Physical Control Format Indicator Channel
PDCCH	Physical Downlink Control Channel
PDCP	Packet Data Convergence Protocol
PDF	Probability Density Function
PDSCH	Physical Downlink Shared Channel
PDU	Packet Data Unit
P-GW	Packet Data Network Gateway
PHICH	Physical Hybrid-ARQ Indicator CH
PMCH	Physical Multicast Channel
PS	Packet-Switched
P-SCH	Primary-Synchronisation Channel
PSK	Phase-Shift Keying
PUCCH	Physical Uplink Control CH
PUSCH	Physical Uplink Shared CH
QAM	Quadrature Amplitude Modulation
QoS	Quality of Service
QPSK	Quadrature Phase-Shift Keying
RB	Resource Block
RF	Radio Frequency
RLC	Radio Link Control
RNC	Radio Network Controller
RRC	Radio Resource Control
RRM	Radio Resource Management
RS	Reference Signal
SC-FDMA	Single Carrier Frequency Division Multiple Access
SDMA	Spatial Division Multiple Access
SF	Spreading Factor
S-GW	Serving Gateway
SHO	Soft Handover
SIMO	Single Input Multiple Output
SIR	Signal-to-Interference Ratio
SMI	Simple Matrix Inversion
SNR	Signal-to-Noise Ratio
S-SCH	Secondary-Synchronisation Channel
SSHO	Softer Handover
TDD	Time Division Duplex
TTI	Transmission Time Interval
UE	User Equipment
UL	Uplink
UMTS	Universal Mobile Telecommunications System

USIM	UMTS Subscriber Identity Module
UTRAN	UMTS Terrestrial Radio Access Network
WCDMA	Wideband Code Division Multiple Access

List of Symbols

Δf	Radio channel bandwidth
$\Delta P_{TX_{du}}$	Variation of radiated power to serve the desired user
ΔP_{TX_i}	Variation of radiated power to serve user i
$\Delta P_{TX_{total}}$	Power improvement, compared to the reference antenna
$\Delta P_{TX_{total}}{}^{i}$	Power improvement, compared to the reference antenna obtained at simulation number i
$\Delta P_{TX_{total}}{}^{4\ elements}$	Average power improvement for arrays with 4 elements
$\Delta P_{TX_{total}}{}^{8\ elements}$	Average power improvement for arrays with 8 elements
$\overline{\varepsilon^2}$	Mean-square error
ζ_i	Code orthogonality factor of user i
θ_{du}	Angle of arrival of desired user's signal
θ_{i}	Angle of arrival of user's i signal
η_{DL}	DL Load Factor
η_{UL}	UL Load Factor
λ	Wavelength
σ	Standard deviation
σ_{LOS}	Standard deviation of the path loss for LOS
σ_{NLOS}	Standard deviation of the path loss for non-LOS
τ_{TTI}	Time transfer interval
a	Array steering vector
a_{pd}	Average power decay for propagation models
d	Array inter-element spacing
E_b	Average bit energy
F	Noise Figure
Fa_i	Activity factor for user i
f_c	Carrier frequency
g_i	Radiation pattern created to serve user i
g_{ref}	Radiation pattern of the reference antenna

G_{p_i}	Processing gain of user i
G_r	Gain of the receiving antenna
G_t	Gain of the transmitting antenna
$I_{inter\,n}$	Normalised inter-cell interference
$L_{p_{du}}$	Average path loss between desired user and BS
L_{p_i}	Average path loss between user i and BS
$L_{p_{LOS}}$	Average path loss between for LOS
$L_{p_{NLOS}}$	Average path loss between for non-LOS
L_{ref}	Propagation model's reference path loss
M	Modulation's order
$M_I^{UL,DL}$	UL,DL Interference Margin
M_p	Link margin
N	Total noise power at UE
N_a	Number of antenna array elements
N_0	Noise spectral density
N_{RB}	Transmission bandwidth configuration
$N_{RB}/_U$	Number of resource blocks assigned for each used
N_{RF}	Radio frequency noise
n_sim	Number of simulations
$N_{streams}$	Number of parallel streams
$N_{symbols/sub-frame}$	Number of OFDM symbols per sub-frame
N_U	Number of active users
P_b	Bit probability error
P_r	UE's sensitivity
$P_{r_{sub-carrier}}$	UE's sensitivity for sub-carrier
$P_{RX_{du}}$	Power perceived of the desired user's signal, at BS
P_{RX_i}	Power sent by user i received at the antenna array

$P_{TX_{total}}$	Total power spent before adaptive antennas
$P_{TX_i}^{BF}$	Power radiated with adaptive antennas
$P_{TX_{total}}^{BF}$	Total power radiated with adaptive antennas
P_{TX}^{BS}	Power transmitted required at the BS
P_{TX_i}	Power transmitted by BS to serve user i
$P_{TX_{sub-carrier}}$	Transmitting power assigned for each sub-carrier
$\boldsymbol{R}$	Covariance Matrix
R_i	Distance between the user i and the BS
R_b	Bit rate
$R_{b/U}$	Physical layer bit rate required for each user
R_c	Chip Rate
r_{cell}	Radius of a cell
R_{coding}	Channel coding rate
$\boldsymbol{u}$	Total interference signals
u_{du}	UL channel signals sent by the desired user
u_i	UL channel signals sent by user i
$\boldsymbol{v_i}$	Array's propagation vector of user i
$\boldsymbol{w}$	Array weighting vector
w_K	Weight of the K^{th} element of the antenna array
$\boldsymbol{w}_{opt}$	Optimum weighting vector

List of Software

Google Earth	Geographical Information System software
Matworks Matlab	Computational math tool
Microsoft Excel	Calculation tool
Microsoft Visio	Design tool (e.g. flowcharts, diagrams, etc)
Microsoft Word	Text editor tool

Chapter 1

Introduction

This chapter gives a brief overview of the work. Before establishing work targets and original contributions, the scope and motivations are brought up. The current State-of-the-Art concerning the scope of the work is also presented. At the end of the chapter, the work structure is provided.

1.1 Overview

More than ever, the global awareness for energy issues is motivating several trends for efficiency. The telecommunications area is not out of this perspective, with vendors, operators and customers committed to reduce the overall energy bill by adopting green behaviours that, isolated, do not introduce a significant impact, but together can create a major revolution on the cost associated to energy consumption. The environmental awareness is obviously motivated by the effective reduction of the energy bill, which makes the reduction of carbon footprint attractive, especially with petrol consistently rising at international markets. Energy efficiency is, for many reasons, a win-win strategy, which makes it a worldwide trend. Figure 1.1 shows a projection of the energy prices from the Energy Information Administration (EIA) of the US Department of Energy [EarP11b], taken in 2008.

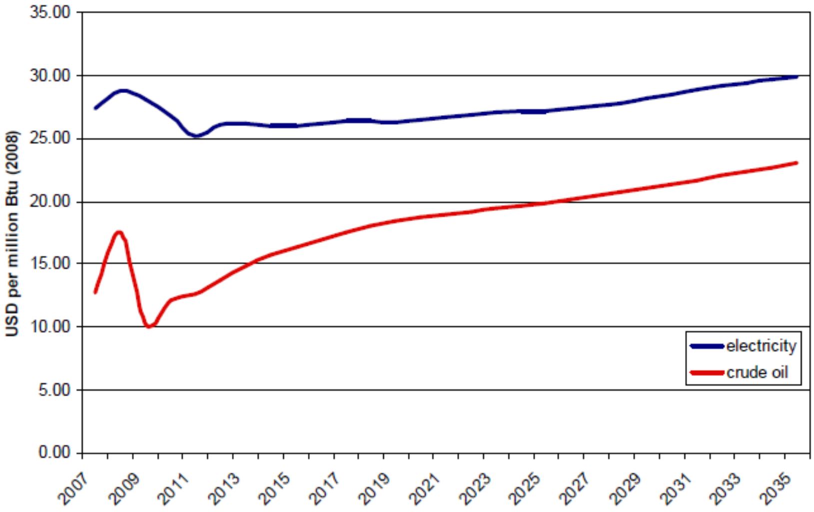

Figure 1.1: Projection of the energy price evolution (extracted from [EarP11b]).

With no surprise, the price of energy, either petrol or electricity, will raise, with special relevance for the fossil source that will likely, at least, double its price in the next twenty years. Also the electricity has its price contaminated by the increasing price of petrol, even with renewable sources' exploration that will for sure attenuate that effect. The impact on operators' profits would not be visible if the profile of utilisation remains the same, with the update on the revenues following the same trend of the increase of energy price. Unfortunately for operators, customers' behaviour is also changing, and the demand for services that require higher data rates is not compatible with older billing models. Figure 1.2 shows the average revenue price (in US dollars) of the mobile data traffic [EarP11b]. The type of data traffic that grows is the one that shows a lower revenue. Operators need, more than ever, to maximise the operational cost of their networks, in order to, competitively, deliver high data rate services that can be affordable to customers and profitable for themselves. An email needs to be as much profitable as a text message, even if it requires more data traffic to be sent over the network. Operators need to be ready for the change of customers' behaviour.

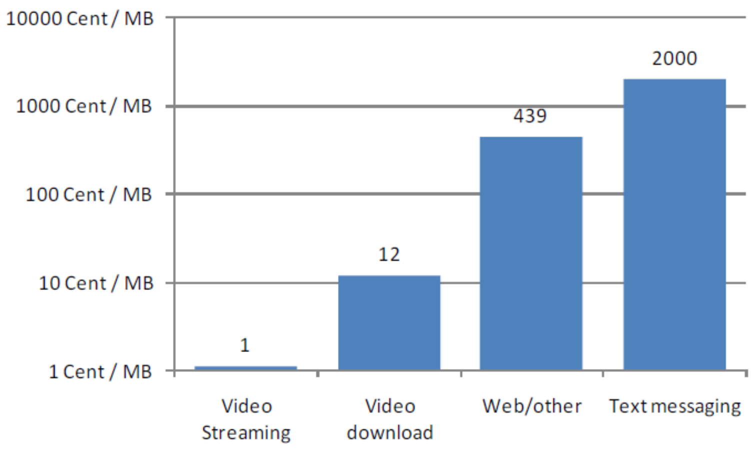

Figure 1.2: Average revenue price of mobile data traffic (extracted from [EarP11b]).

Concerning the telecommunications industry, all entities are committed to reduce their footprints and energy spent by adopting ambitious goals for the future. Taking as example the EARTH Project [EarP11a], its target “is to reduce the energy consumption of mobile systems by a factor of at least 50%” while still “providing high capacity and uncompromised quality of service”. Within the goal of 50% of energy consumption efficiency, the single largest consumers of energy are base stations, where any advances in order to reduce their energy consumption will have immediate benefits in terms of cost. The objective of energy efficiency is to reduce the overall energy bill, which can be seen as more than just a reduction of the money transferred to the energy supplier. Actually, the same amount of energy can be used in a more efficient way, which means providing a better service to more users, while energy cost remains the same.

The impact on energy efficiency and consumption of mobile broadband systems is motivating vendors and operators to exploit new geographical areas, where physical access is hard and the energy grid is not available or is unaffordable to be installed. With network equipment being less hungry for energy, new sources of energy can be reliable and economically attractive to serve remote rural areas or small cities, reducing the need for diesel generators, and consequently reducing the dependence of fossil sources, decreasing the operational expenditure (OPEX). Locally available sources of energy will significantly reduce the need for maintenance and fuel refilling. Once again, energy efficient enhancements are win-win solutions. Although initial installation costs for locally available energy sources exploration could be higher, in a long term analysis, the OPEX reduction will dilute the actual price and, at the same time, the additional income due to the service provided to new customers located in isolated areas will make the investment of base station installation profitable. Probably, in developed countries, hard access locations with no energy supplying do not constitute a significant problem to motivate the research and adoption of more efficient technologies, but in developing countries, the capability to locally provide energy to supply base stations is often the only way to provide outer communications to near communities. Using the example of Ethiopian Telecommunications Corporation (ETC), near 300 sites were installed to cover northern and central parts of the country, which were only possible due to more efficient equipment that could be supplied by solar cells and backup battery packs, as Nokia Siemens Networks announced [NSNC08].

In what concerns technical issues, the goal for more energy efficient systems comprises both their network and radio sides. Focusing on the scope of this thesis, the radio communication between base stations and mobile terminals can be improved by introducing more efficient radio interfaces. Antenna technology can be enhanced in order to provide better reception and transmission, increase data rates and, at the same time, reduce the overall transmitted power. Multiple Input Multiple Output (MIMO) transmission increases the spectral efficiency by exploiting the multipath effects that signals sent spatially apart suffer. Multiple antennas exploit spatial diversity to improve signal's quality from propagation effects. Adaptive antenna arrays exploit spatial locations of users to improve signal and reduce interference, contributing to the overall reduction of radiated power. Alcatel-Lucent's lightradio™ antennas already take advantage of vertical beamforming to increase capacity and reduce energy consumption, by dynamically changing radiation patterns according to cell's load and traffic density [Kemp11].

The objective of this thesis is framed by antenna's developments that make it possible to use users' spatial location to improve the signal and reduce interference in the azimuthal domain. Beamforming is analysed from the view point of achieved energy improvement, compared with ordinary static sector antennas, providing the same service. The goal is to establish a model for the expected power improvements that can be reached in several scenarios. Then, with this model, several everyday scenarios are tested to assess how these smart antennas can be explored in the best way possible. Current and future systems, UMTS and LTE, are the starting point, through their particular radio interfaces and potential for energy efficiency, for the analysis of the improvements that beamforming introduces. Several scenarios, ranges, antenna configurations and cell's load are evaluated in order to find the portion of energy that beamforming is able to save. Instead of long-term radiation patterns dependent on statistics for cell's load and traffic, the goal is to generate individual radiation patterns to serve each user in the most efficient way, expecting to reduce the overall radiated power.

The innovation of this thesis relies on the fact that the achieved efficiency by adaptive antennas is used to reduce the energy consumption instead of increasing services. Current operation standard situations are simulated for the same parameters (users, services, radius, frequency), before with static antennas and after with adaptive antennas. For exactly the same arrangement, the energy saved in DL is quantified.

In order to exploit results as much as possible the current architecture of mobile communications networks, this work addresses single cells in an attempt to find the energy efficiency that is possible to achieve when adaptive antennas are introduced in this situation, no matter the type of antennas used in neighbouring cells.

1.2 Structure

The thesis is structured into 5 chapters. The present one gives the overview and the starting point that motivates the investigation on beamforming applied as an energy efficient solution for UMTS and LTE.

In Chapter 2, systems' background is presented. UMTS and LTE architectures, radio interfaces and coverage and capacity aspects are addressed, with special emphasis on time related issues associated to the radio interface. Multiple access techniques of both systems are analysed, in order to understand how beamforming can be applied into their radio interfaces, and simulated in the more realistically way possible.

Chapter 3 presents the model proposed to evaluate the performance of beamforming in the descripted systems. Multi user models are explained, for UMTS and for LTE, according to their radio interfaces. After the models are described, the simulators that were developed to implement these models are presented. Aspects related to users' generation, algorithms and metrics are addressed as crucial components of the models for the evaluation of the impact of beamforming in UMTS and LTE in terms of energy efficiency.

In Chapter 4, the description of the scenarios where simulations were performed is made, followed by the main results that were obtained for UMTS and LTE. Although the different models for UMTS and LTE are relatively close and addressed together, due to the very different radio interfaces, the results that were obtained are distinguished. Results for the power improvement that is reached by the adaptive antennas for different scenarios, configurations and users are presented separately for both systems. The analysis of the results obtained is presented also in Chapter 4.

This thesis concludes with Chapter 5, where the main conclusions of the work are drawn, and suggestions for future works are pointed out.

Finally, a set of annexes closes the present document with supplementary information, when there is a need for the global comprehension of the described problem.

.

Chapter 2

Basic Aspects

This chapter provides the basic aspects of UMTS and LTE. The radio interface is specially studied, in order to understand how beamforming techniques can be applied at a base station, to become an effective energy saving solution.

2.1 UMTS

From its 1999 version, UMTS has had several improvements that allow operators to offer higher data rates. Firstly in this section, one presentes the basic aspects of Release 99, related to network architecture and specially radio interface, followed by the main enhancements added to the original specifications, in order to achieve higher data rates, namely concerning improvements that constitute HSPA and HSPA+ [Hoto07].

2.1.1 Network Architecture

UMTS network can be grouped in three main functional modules, which are:

- User Equipment (UE).
- UMTS Terrestrial Radio Access Network (UTRAN).
- Core Network (CN).

Figure 2.1 shows these three functional modules and their interconnections.

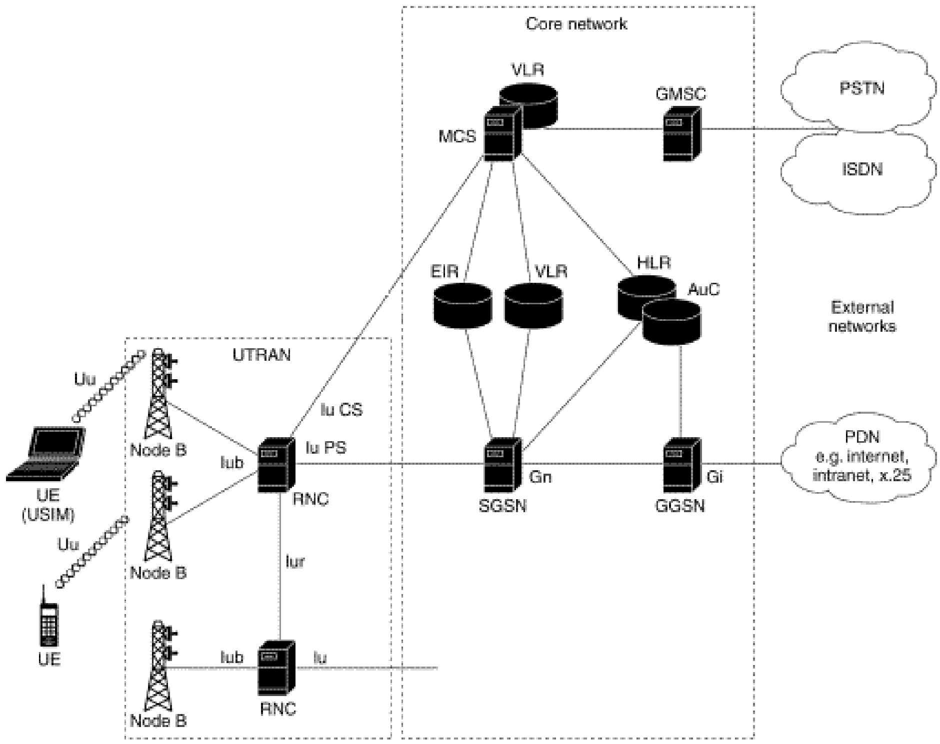

Figure 2.1: UMTS System Architecture (extracted from [Jaci09])

The UE is the interface with the user, composed by the UMTS Subscriber Identity Module (USIM) and the Mobile Terminal (MT). UE is responsible for the radio communications with UTRAN over Uu interfaces. The UE's USIM performs the subscriber's identification, provides authentication, encryption and other information needed at the MT.

UTRAN is responsible for the entire radio interface, and it is composed by Node Bs (NBs), usually known as Base Stations (BSs), charged of multiplexing (demultiplexing) the user's signal from (to) Radio Network Controllers (RNCs), which are responsible for controlling and managing BSs in its covering area as well as Radio Resource Management (RRM) functions.

In what concerns CN, it provides transport, switching, routing and data base functions, and its elements can be grouped in Packet-Switched (PS) and Circuit-Switched (CS).

2.1.2 Radio Interface

UMTS' radio spectrum is defined in between two frequency bands, [1900, 2025] MHz and [2110, 2200] MHz. The Frequency Division Duplex (FDD) mode has two paired bands, with 60 MHz each, [1920, 1980] MHz for uplink and [2110, 2170] MHz for downlink. Figure 2.2 presents the distribution of UMTS' spectrum.

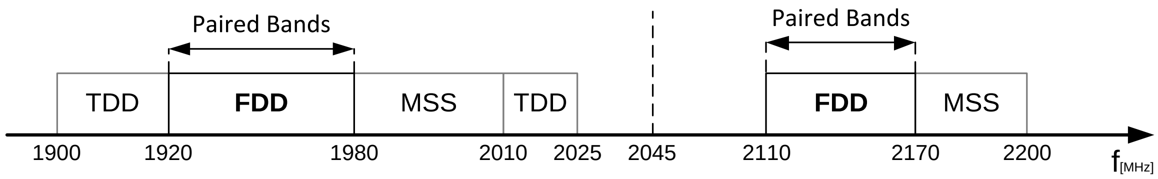

Figure 2.2: Frequency spectrum for UMTS.

To ensure multiple access, UMTS uses Wideband Code Division Multiple Access. In this technique, each user has an orthogonal code, which grants an easy understanding of the information sent to him. In this way, all users are able to operate the same band simultaneously, without causing harmful interference problems to each other, over ideal conditions.

CDMA is based on spreading. Usually, user's data has its power mostly concentrated in a small frequency band, compared with the entire band of the system. In a first step, the information sent by some source is uniquely coded and spread at the frequency domain, by multiplying user's data by a higher rate sequence, the orthogonal code, which spreads sources' power over a larger band and leads to a decrease of power peak value. For a user that has not access to the correct code, signal's power is now at a level that is seen as interference. This stage is known as Channelisation and each symbol generated is called as chip, as well as the symbol rate is chip rate. In UMTS, Channelisation codes have a chip rate of 3.84 Mcps (chips per second). After coding, the spread signal must be submitted to a process responsible for signal separation from different sources. This process is called as Scrambling and it does not affect channelisation properties. Concerning codes, they are all defined (*a priori*) and they are well known, but each user has only permission, at a certain moment, to use one or some ones. Codes are quasi-random and they must be orthogonal in between each other. A code family that has these properties is the Orthogonal Variable Spreading Factor (OVSF) family that has its codes generated by a tree structure. At the nth level of the tree, there are always 2^n orthogonal codes, all with length equal to 2^n. This family has the property to allowing different length codes to be orthogonal, since they are not at lower levels of the same branch. Other interesting characteristic of UMTS comes from Scrambling. Scrambling codes are used to separate signals from different sources.

This means that the same code can be used by different sources (MTs or NBs), since they have a different Scrambling code, i.e., there is no need to coordinate codes between different sources (BSs). Theoretically, OVSF codes can be infinitely expanded to deal with as much users as those within a cell. However, capacity and interference are strongly dependent on the number of users, and the maximum number of users handled by a single BS is a trade-off between capacity and a desirable Quality of Service (QoS).

In UMTS, four types of different channels are defined:

- Radio Channels: they are related with the spectrum division into several frequency slots, each one associated to a carrier. A radio channel has a bandwidth of 4.4 MHz and they are apart from each other by 5 MHz.
- Physical Channels: these channels carry any kind of data and each one is associated to an orthogonal code. Different physical channels can operate at the same radio channel.
- Logical Channels: these channels are responsible for carrying a specific kind of data, which can be associated to traffic information or signalling and control.
- Transport Channels: they are responsible for carrying user´s information from higher layers of the network to the UE and they can be splitted into two subtypes:
  - Common Transport Channels: shared by all users in the cell.
  - Dedicated Transport Channels (DCH): channels used by a single user.

Physical channels correspond to the lower layer (layer 1 or physical layer) of the OSI reference model. Layer 2, or data link layer, can be seen as a Medium Access Control (MAC) layer, and it is responsible for mapping data onto layer 1, through transport channels. All transport channels are defined as unidirectional, which means that the UE can have several transport channels in downlink and one or several in uplink, simultaneously, depending on the service and the state of UE, [3GPP10a].

The basic unit exchanged between MAC and Layer 1 is the Transport Block, similar to the MAC PDU (Packet Data Unit). In a single transport channel, at the same time instant, one or several transport blocks are transferred, which corresponds to the Transport Block Set. The Transmission Time Interval (TTI) is defined as the inter-arrival time of transport block sets, and it is equal to the periodicity at which a transport block set is transferred to the physical layer. MAC layer delivers one Transport Block Set to the physical layer every TTI. UMTS R99 defines several TTIs, from 10 ms to 80 ms. At the radio channel, the basic unit is the radio frame, which is sent every 10 ms (R99), which is why TTI must be always a multiple of the radio frame's duration. The equal size of the transport block sets among a TTI leads to user's data rate kept constant during each TTI. From TTI to TTI, it is possible to change data rate. Figure 2.3 shows an example of transport blocks exchanging between MAC and physical layer, in three parallel transport channels. Note that in each TTI, all transport blocks have the same size. Note also from TTI to TTI, the number of transport blocks and their sizes can change, which confers different data rates in each TTI, [3GPP10a].

UMTS R99 has almost all of the intelligence at the RNC, which is responsible for source coding, scheduling and retransmission assessment. The Node B is only responsible for power control management. A single RNC is most of the times in charge of several NBs (physically apart) and data rates must be downsized in order to deal with variations on the propagation conditions, which cannot be assessed as often as desired. The RNC has no capacity to assess the propagation conditions of all its NBs and, even if it had, propagation conditions change during the communication between a Node B and the RNC. To improve data rates, UTRAN needs to bring more intelligence to the closest element of the radio interface, to NBs, which happens with Release 5 and Release 6 (HSPA).

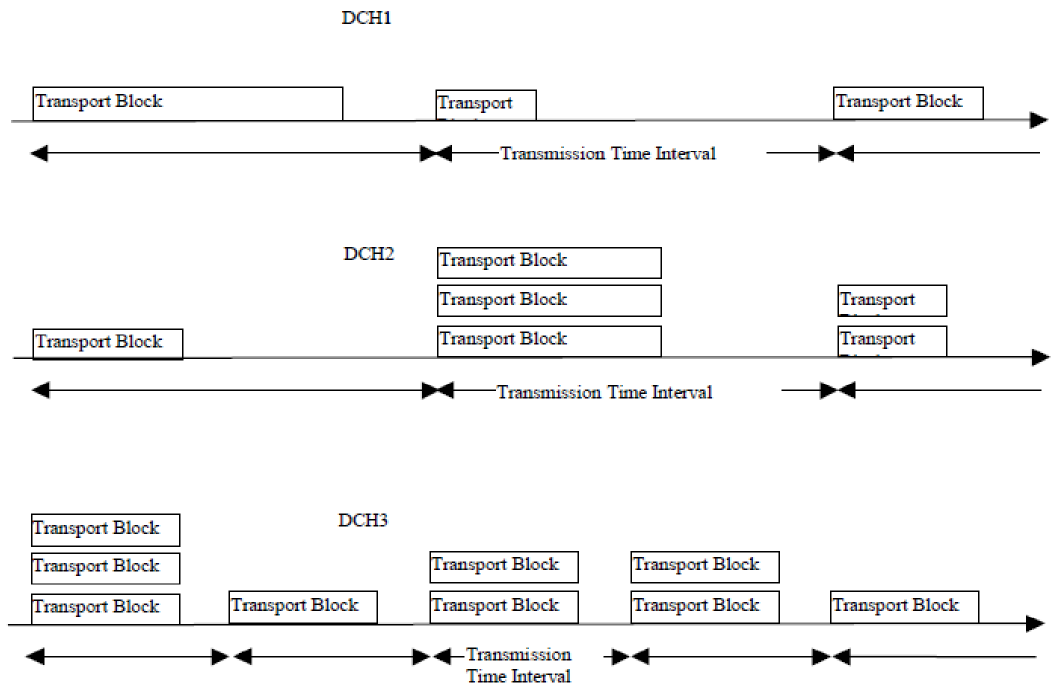

Figure 2.3: Transport blocks exchanging between Mac and physical layer (extracted from [3GPP10a]).

In order to deal with radio channel conditions as soon as they change, HSPA (High Speed Packet Access) introduced scheduling, coding and retransmissions at the Node B. In this way, the Node B is able to set up transmission parameters depending on channel's conditions. Nevertheless, RNC functions are still needed to provide services for those that do not use HSPA, and provide radio resource and mobility management to HSPA services. The main innovations that HSPA brought were:

- Higher order modulation schemes: HSPA is able to use QAM modulation over better propagation conditions, while QPSK can be used when the radio channel is more severe for the signal, bringing strength to link.
- Shared transmission channels: codes and radiated power of a Node B are seen as limited resources, and they are dynamically allocated at either time or code domains, among users. TTI has the same length of the radio frame (they are uniquely invoked) and, at each TTI, MAC only delivers one transport block. The shared transmission channel of the HSDPA is the HS-DSCH (High Speed Downlink Shared Channel) and an example of transport block exchanging between MAC and physical layer can be seen in Figure 2.4.
- Reduction of the radio frame duration (also known as reduction of TTI): shared codes of the shared transmission channel are dynamically (re)allocated every 2 ms, unlike 10ms of R99.

- Automatic Repeat ReQuest (ARQ): when some error is detected, it is possible to request retransmission of the errored transmission block, even before decoding. With TTI's reduction, ARQ is also performed faster and the retransmitted data is more granular, which result in a more efficient process. ARQ is performed at the UE - Node B communication, without RNC intervention.
- Faster adaptation to the propagation conditions: as referred, once transmission is set up at Node B, propagation conditions can be assessed more frequently, with Channel Quality Information (CQI) reports sent periodically to Node B. Faster adaptation of characteristics like modulation, coding and radiated power ensures the same QoS for all users.

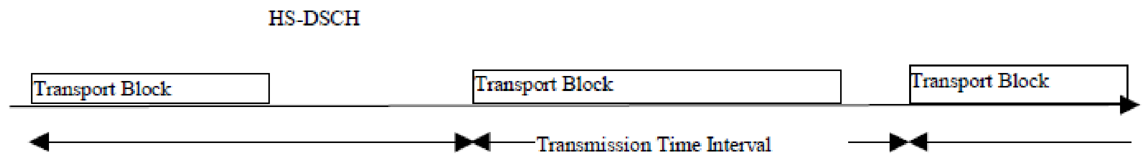

Figure 2.4: Transport blocks exchanging between MAC and physical layer at HS-DSCH (extracted from [3GPP10a]).

High Speed Packet Access Evolution (HSPA+) keeps increasing the modulation order, and the main feature that it introduces at the radio interface is Multiple Input and Multiple Output (MIMO) transmission. MIMO transmits multiple transport blocks in parallel and, on the other hand, it introduces spatial diversity, which explores multipath to contour fading that severely affects the signal received at an antenna by using the signal of another antenna. Thus, with the same bandwidth, it is possible to offer higher data rates due to improved SNR.

Finally, in this introduction to UMTS radio interface, handover is approached. Handover is the process that allows a call not to be interrupted when a UE moves from one cell to another cell, or from one sector to another of the same cell. It can be classified as hard handover (HHO), when a call transits to other Node B without having a simultaneous connection with both Node Bs, as soft handover (SHO), when call is kept in both Node Bs during the transition, and as softer handover (SSHO), similar to SHO but when UE transits between sectors of a same cell. Usually in R99, excepting for SSHO that are performed by Node B, handovers are performed by RNC.

2.1.3 Coverage and Capacity

With systems able to provide different data rates to different users, the coverage of a cell is far from being the average area around the BS that stills has power above receiver's sensibility.

All the parameters that affect capacity can be organised into three main limiting factors:

- Available codes in DL.
- System's load, directly related with interference issues.
- Base station's transmission power.

UMTS has its multiple access technique based on CDMA, with one cell per cluster. The frequency reuse ratio is one and the system usually is interference limited. The number of available codes in DL limits the number of users that can be simultaneously active within a cell. Higher data rates require codes with lower spreading factor. In ideal conditions, codes are orthogonal between each other. However, when mobility and multipath are taken into account, code's orthogonality can be missed and interference between users becomes as much important as more users are active, with impact on cell's coverage. A Node B has a maximum power transmitted to be shared among users, which becomes also a limiting factor, because the received power stills need to be above the sensitivity of the UE.

Considering the same transmitted power for all users and dependent on the system's load, it is possible to estimate the radius of a cell by considering the path-loss given by the most adequate propagation model for the environment.

The load factor depends on the services. It is usual to distinguish between UL and DL, since services provided are, most of the times, asymmetric. The recommended load factors are also different between both. UL load factor should not be higher than 50%, while for the DL, the load factor should not be higher than 70%. Load factors, for UL and DL respectively, have the following expressions:

$$\eta_{UL} = (1 + I_{inter\,n}) \sum_{i=1}^{N_U} \frac{1}{1 + \frac{G_{p_i}}{\left(E_b/N_0\right)_i Fa_i}} \tag{2.1}$$

$$\eta_{DL} = \sum_{i=1}^{N_U} Fa_j \frac{\left(E_b/N_0\right)_i}{G_{p_i}} [(1 - \zeta_i) + I_{inter\,n}] \tag{2.2}$$

where:

- N_U is the number of active users.
- $I_{inter\,n}$ is the normalised inter-cell interference ([40,60]% in UL).
- G_{p_i} is the processing gain of user i.
- Fa_i is the activity factor of user i (50% for voice and 100% for data).
- ζ_i is the code orthogonality factor of user i (typically between 50% and 90%).
- $R_c = 3.83 \text{ Mcps}$.
- E_b is the average bit energy.
- N_0 is the noise spectral density.

The processing gain, G_{p_i}, is a relationship between bit rate and chip rate.

$$G_{p_i} = \frac{R_c}{R_{b_i}} \tag{2.3}$$

where:

- R_{b_i} is the bit rate required by user i.

The interference cause by all of the active users can be represented as an interference margin, M_I, and typically it takes values between 1 and 3 dB. The expression for M_I is given by

$$M_I^{UL,DL}{}_{[\mathrm{dB}]} = -10\,log\left(1 - \eta_{UL,DL}\right) \tag{2.4}$$

Considering M_I, when the system is near its top capacity (η near one), the interference margin goes to infinity, with impact on coverage. The transmitted power required at the Node B is shared among active users and it is assessed through DL load factor, given by:

$$P_{TX}^{BS} = \frac{N_0 . R_c}{1 - \eta_{DL}} \sum_{i=1}^{N_U} Fa_i \therefore L_{p_i} \frac{\left(E_b/N_0\right)_i}{G_{p_i}} \tag{2.5}$$

where:

- L_{p_i} is the average path-loss between user i and Node B.

Considering the total transmitted power required at a Node B as evenly shared among all active users that are performing the same bit rate at the same propagation conditions, user i has, generically, $P_{TX_i}$for himself:

$$P_{TX_i} = \frac{P_{TX}^{BS}}{N_U} \tag{2.6}$$

L_{p_i} is obtained from the propagation model that represents better the scenario. On the UE side, a minimum received power must be accomplished in order to keep bit error probability above a threshold value, which depends on the modulation scheme and the bit rate required. This value, from now on referred to as UE's sensitivity, $P_{r[\mathrm{dBm}]}$, is given by:

$$P_{r[\mathrm{dBm}]} = N_{[\mathrm{dBm}]} - G_{p_{i[\mathrm{dB}]}} + \left(E_b/N_0\right)_{i[\mathrm{dB}]} \tag{2.7}$$

$N_{[\mathrm{dBm}]}$ is the total noise power at UE, and its expression is the following:

$$\begin{aligned} N_{[\mathrm{dBm}]} &= N_{RF_{[\mathrm{dBm}]}} + M_I^{DL}{}_{[\mathrm{dB}]} \\ N_{RF[\mathrm{dBm}]} &= -174 + 10\log_{10}\left(\Delta f_{[\mathrm{Hz}]}\right) + F_{[\mathrm{dB}]} \end{aligned} \tag{2.8}$$

where:

- $F_{[\mathrm{dB}]}$ is the Noise Figure for UE.
- $\Delta f_{[\mathrm{Hz}]}$ is the system's total bandwidth ($\Delta f_{[\mathrm{Hz}]}$ = 4.4 MHz).

The radius of a cell that provides a service not exceeding a specific bit rate R_b is obtained from Friis expression:

$$r_{cell[\mathrm{km}]} = 10^{\frac{P_{TX_i[\mathrm{dBm}]}+G_{t[\mathrm{dBi}]}-P_{r[\mathrm{dBm}]}+G_{r[\mathrm{dBi}]}-L_{ref[\mathrm{dB}]}-M_{p[\mathrm{dB}]}}{10\cdot a_{pd}}} \tag{2.9}$$

where:

- a_{pd} is the average power decay of the propagation model.
- $G_{t[\mathrm{dBi}]}$ and $G_{r[\mathrm{dBi}]}$ are, respectively, the gain of the transmitting and the receiving antennas.
- L_{ref} is the reference path loss of the propagation model, independent on the distance.
- $M_{p[\mathrm{dB}]}$ is the margin where fading (fast and slow), indoor penetration and soft handover gain are accounted.

On an alternative way, it is possible to estimate the capacity within the cell's coverage, with radius d, by assuming a specific power transmitted for each user, the same bit rate for all users and the same modulation scheme/order, so all UEs are requiring the same E_b/N_0. By taking (2.7), (2.8) and (2.9), it is possible to obtain the maximum acceptable interference margin $M_I^{DL}{}_{[\mathrm{dB}]}$.

$$M_I^{DL}{}_{[\mathrm{dB}]} = 10 \cdot a_{pd} \log_{10}(d_{[\mathrm{km}]}) - P_{TX_i[\mathrm{dBm}]} - G_{t[\mathrm{dBi}]} + N_{RF[\mathrm{dBm}]} - G_{p[\mathrm{dB}]} + \left({}^{E_b}/_{N_0}\right)_{i[\mathrm{dB}]} - G_{r[\mathrm{dBi}]} + L_{ref[\mathrm{dB}]} + M_{p[\mathrm{dB}]} \tag{2.10}$$

Using the relationship between interference margin and load factor, (2.4), η_{DL} assumes the following form:

$$\eta_{DL} = 1 - 10^{\left(\frac{10\cdot a_{pd}\log_{10}(d_{[\mathrm{km}]})-P_{TX_i[\mathrm{dBm}]}-G_{t[\mathrm{dBi}]}+N_{RF[\mathrm{dBm}]}-G_{p[\mathrm{dB}]}+\left({}^{E_b}/_{N_0}\right)_{i[\mathrm{dB}]}-G_{r[\mathrm{dBi}]}+L_{ref[\mathrm{dB}]}+M_{p[\mathrm{dB}]}}{10}\right)} \tag{2.11}$$

Finally, through (2.2) and its relationship between η_{DL} and the number of users N_U, the capacity of a cell is obtained:

$$N_U = \frac{1 - 10^{\left(\frac{10\cdot a_{pd}\log_{10}(d_{[\mathrm{km}]})-P_{TX_i[\mathrm{dBm}]}-G_{t[\mathrm{dBi}]}+N_{RF[\mathrm{dBm}]}-G_{p[\mathrm{dB}]}+\left({}^{E_b}/_{N_0}\right)_{i[\mathrm{dB}]}-G_{r[\mathrm{dBi}]}+L_{ref[\mathrm{dB}]}+M_{p[\mathrm{dB}]}}{10}\right)}}{Fa_i \frac{\left({}^{E_b}/_{N_0}\right)_i}{G_{p_i}}\left[(1-\alpha_i)+I_{inter\,n}\right]} \tag{2.12}$$

Concerning ${}^{E_b}/_{N_0}$, it depends on the modulation scheme (PSK, QAM), the modulation order (BPSK, QPSK or 16QAM, 64QAM) and the minimum acceptable Bit Error Ratio (BER) required by the system to operate properly.

The way how Node B power transmitted is distributed among channels must be also taken into account. Common channels take some of the allocated power for signalling and control functions. In R99, common channels represent 25% of the transmitted power, while the remaining 75% are effectively allocated for dedicated channels, those ones that transport user's data. HSPA and HSPA+, due to the increase of data rates and the consequent need of enhanced signalling and control mechanisms, reserve 60% for user's purposes and 40% of power for common channels.

The formulation for coverage assumes that services are performed at constant bit rate, like a voice call, for instance. When bit rates changes from TTI to TTI, and the transmitting characteristics are also adjusted, which is the example of HSDPA, the $\left({E_b}/{N_0}\right)$ metric is not used. In these specific systems, there are implemented metrics depending on terminal capacity categories, like modulation, TTI or number of codes, in order to give some average of the system's capacity.

2.2 LTE

Long Term Evolution emerges from the demand to ensure competitiveness for the 3GPP radio-access technology over a longer time frame, in order to deal with the increase of high data rate applications, provided by a miscellaneous of platforms which offer different types of multimedia content. The success of HSPA is the starting point for the development, with the major drivers focused on offering higher data rates, improving latency, improving capacity and coverage and reducing costs for operators. [3GPP09a]

This section presents an overview of LTE, specially its radio interface, and looks through network architecture, coverage and capacity basic aspects.

2.2.1 Network architecture

Similarly to the enhancements added by the introduction of HSPA in UMTS, in order to reach higher data rates it is imperative to bring more intelligence as near as possible to the radio interface. LTE architecture, as it can be seen in Figure 2.5, is flat and has in its concept the optimisation of packet-based traffic.

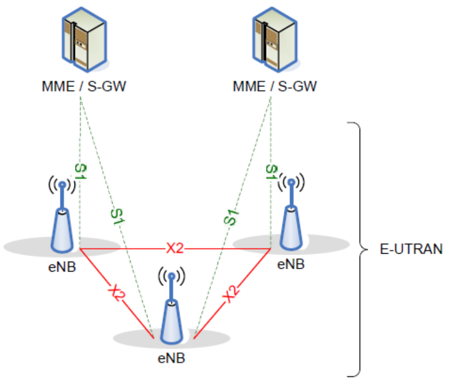

Figure 2.5: overall LTE's architecture (extracted from [3GPP10b]).

The Evolved-UTRAN (E-UTRAN) has one single element, the Evolved-NodeB (eNB), where all functions related to radio aspects are performed. Compared with HSPA, the eNB has new features organised into three main groups: Radio Link Control (RLC) Layer, Radio Resource Control (RRC) and Packet Data Convergence Protocol (PDCP). In this way, eNB performs all RRM operations, as admission control, radio barrier control, or dynamic resource allocation.

eNBs interact with each other through the interface X2. It is assumed there is an X2 interface between eNBs all the time, in order to perform, among other functions, handovers. Therefore, handover are performed at the BS level, with no intervention of any higher level controller.

The link to core network is provided by S1 interface that connects the eNBs to the Evolved Packet Core (EPC). EPC is constituted by the Mobility Management Entity (MME), which performs control plane signalling, the Serving Gateway (S-GW) and the Packet Data Network Gateway (P-GW), both responsible, mainly, for user-plane data processing as well as integration with other radio access and transport technologies. The EPC is the link to the outer world with a strong PS traffic orientation, since the UE is IP addressed. The functional split between E-UTRAN and EPC is presented in Figure 2.6.

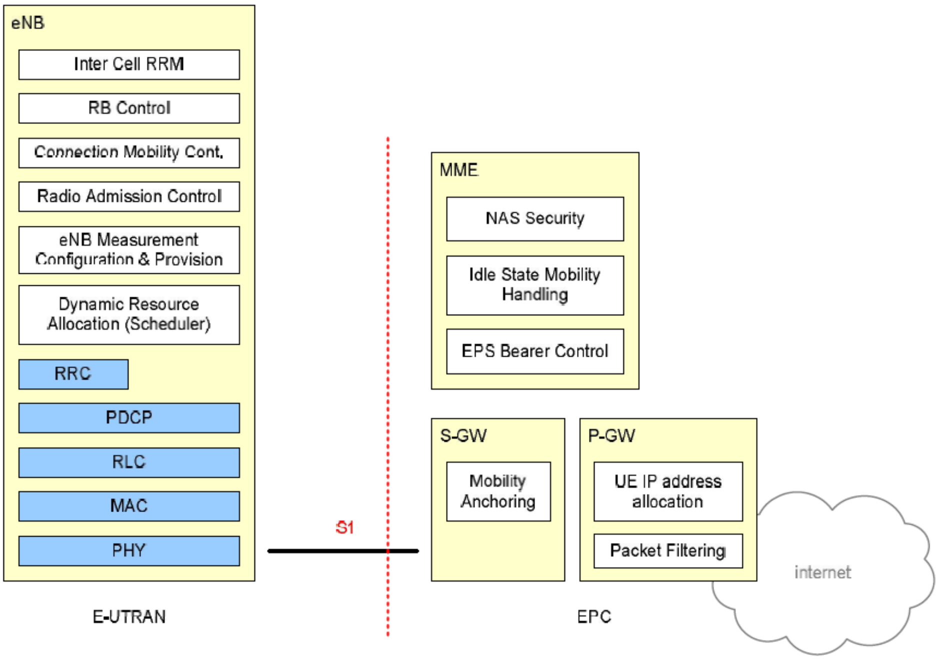

Figure 2.6: functional split between E-UTRAN and EPC (extracted from [3GPP10b]).

2.2.2 Radio Interface

In what radio aspects is concerned, the long-term evolution of the 3GPP's access technologies was designed to co-exist with the former releases, namely with UMTS, which will provide a smooth transition while LTE expands its coverage. LTE was also designed to operate in several arrangements of frequency bands and bandwidths. For Portugal, the regulatory body, ICP-ANACOM, launched in March 2011 an auction to assign spectrum in several bands with no restrictions about the technology to be implemented. LTE is likely to be firstly implemented in 2.6 GHz band, but operators are free to develop solutions operating the 800 MHz, 900 MHz, 1800 MHz or the 2.1 MHz bands, a decision that will depend on the business model and, of course, on the founds they are willing to spend. In this work, due to the range of frequency bands where LTE can be implemented, the analysis of energy efficiency that adaptive antennas bring is performed at the 1800 MHz frequency band. Table 2.1 shows the amount of spectrum compatible with LTE, available for auction in Portugal.

Table 2.1: Portuguese available bands for auction (adapted from [AnMC11]).

Band denomination	Range	Arrangement	Volumes
800 MHz	[791,821]MHz and [832,862]MHZ	Paired: 2 x 30MHz	6 volumes of 2 x 5MHz
900 MHz	[880,890]MHz and [925,935]MHz	Paired: 2 x 10MHz	2 volumes of 2 x 5MHz
1800 MHz	[1710,1740]MHz and [1805,1835]MHz	Paired: 2 x 30MHz	6 Volumes of 2 x 5MHz
2100 MHz	[1900,1910]MHz	Unpaired: 2 x 5MHz	2 volumes of 5MHz
2600 MHz	[2500,2690]MHz	Paired: 2 x 70MHz and Unpaired: 50MHz	14 volumes of 2 x 5MHz and 2 volumes of 25MHz

LTE's radio interface has two duplex modes, FDD and TDD. FDD is optimised to co-exist with 3.84 Mcps UMTS, while TDD is optimised to co-exist with 1.28 Mcps UMTS TDD mode, which is out of the scope of this thesis. This work is focused on LTE's FDD mode. The variety of bandwidths available was conceived in order to grant more flexibility in whichever frequency band the system may be implemented. The allowed channel bandwidths are six: 1.4, 3.0, 5, 10, 15 and 20 MHz. [3GPP09a]

There are different multiple access transmission schemes for DL and UL. DL multiple access is based on Orthogonal Frequency Division Multiple Access (OFDMA), which consists of splitting the channel bandwidth into several smaller sub-bands, corresponding to sub-carriers coded and sent in parallel, in order to explore the different propagation characteristics that affect each sub-band almost independently from each other. Users have some sub-carriers, available in sets, for a certain period of time according to the service they are requesting and, periodically, sub-carriers are reallocated. Every sub-band has the same size, Δf =15 kHz, sufficiently small to not be consider chromatic dispersion, which means the entire sub-band suffers the same propagation effects. Other advantage of this technique is the lower wastage of capacity in case of bad reception, due to the carried data into a sub-band being much lower than it would be if the entire bandwidth was used, and retransmissions are only performed to the data lost in the bad received band(s).

UL transmission scheme is based on Single Carrier Frequency Division Multiple Access (SC-FDMA), more specifically DFTS-OFDM (Discrete Fourier Transform spreading - OFDM). Any kind of multi-carrier technique suffers a large variation in instantaneous power, which decreases efficiency of power amplifiers as well as their consumption. This problem is more critical at UE, due to the need to preserve battery. In this way, SC-FDMA reduces the variation of instantaneous power, while it still preservs the high flexibility to different bandwidths and the high performance with low-complexity receivers of an OFDMA system. The basic principle of SC-FDMA is the transmission of signals over the entire assigned bandwidth. However, the signal transmitted over the entire bandwidth is composed of several sub-carriers, with discrete components at the frequency domain. Every sub-band has the same spacing of the DL scheme, Δf =15 kHz, and they are assigned in sets as well.

Common to UL and DL transmission is the Cyclic Prefix (CP). CP reduces the ISI by being attached between each symbol as guard intervals. CP allows low-complexity equalisers with high performance, and it has two available lengths, depending on the radio channel adversity for the signal. The largest CP corresponds to a worst radio channel. Figure 2.7 shows, at the time domain, the ISI between generic data blocks in the channel output as well as the influence of CP to mitigate ISI impact.

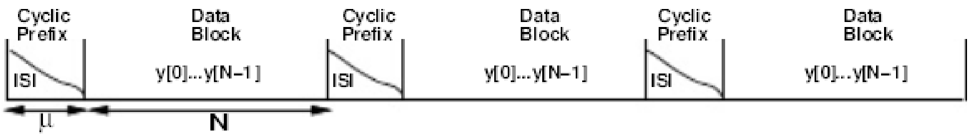

Figure 2.7: ISI between data blocks (extracted from [Gold05]).

The maximum efficiency of LTE for packet-based transmissions led to the abolishment of dedicated transport channels. At physical layer, all transport channels are shared. More signalling and control is added to handle with dynamic resource allocation, synchronisation and, for higher data rates, to improved channel estimation.

No matter the frequency band or channel bandwidth in which the system is operating, transmission has always the same time frame structure. One radio frame corresponds to 10 ms. Each radio frame consists in 20 slots with 0.5 ms each. Two slots comprise a sub-frame, with 1 ms duration, that is coincident with TTI of L2, Figure 2.8. Compared with HSPA, TTI was reduced in half of its duration.

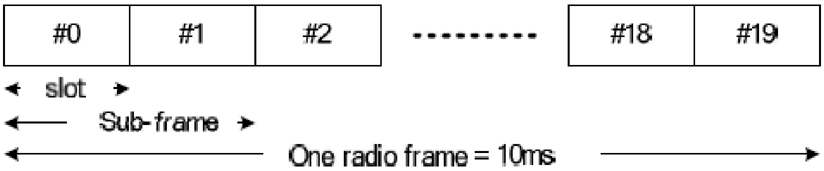

Figure 2.8: FDD frame structure (extracted from [3GPP10b]).

Sub-carriers are allocated into sets for a certain period of time and the basic unit is the resource block. One resource block (RB) corresponds to 12 consecutive sub-carriers (180 kHz) during one slot. The amount of sub-carriers depends on the channel's bandwidth, and they are grouped into sets of 12 consecutive sub-carriers, i.e., the transmission bandwidth configuration (N_{RB}), Table 2.2. N_{RB} varies from 6 for 1.4 MHz channel bandwidth up to 100 for 20 MHz.

Table 2.2: Transmission bandwidth configuration accordingly to system's bandwidth (extracted from [3GPP10c]).

Channel Bandwidth [MHz]	1.4	3	5	10	15	20
transmission bandwidth configuration N_{RB}	6	15	25	50	75	100

The amount of symbols comprised into one slot is fixed, and it only depends on the type of cyclic prefix. In a normal CP, it is possible to send 7 OFDMA symbols over a slot duration, while for extended CP, only 6 OFDMA symbols fit into a slot. Figure 2.9 represents a resource grid for downlink with normal CP. Each small square is an ODFMA symbol of a sub-carrier, so called as Resource Element.

Resources scheduling, i.e., resource blocks allocation, is performed for each radio frame (10 ms). Ended the radio frame, resource blocks are evaluated depending on several parameters, e.g., bit rate demand or service priorities.

Physical channels correspond to a set of resource elements that carries information originated in higher layers. Besides physical DL shared channels for user's data purposes, there are other physical channels related with synchronisation and channel estimations, and they needed to accomplish low latency high data rate performance, mostly to radio frame structure timing requirements and channel estimation. These channels must be mapped onto physical resources over a fixed and well known order, to be correctly understood. Figure 2.10 presents the physical mapping of main DL physical channels onto the frame structure, as well as the reference signal for channel estimation.

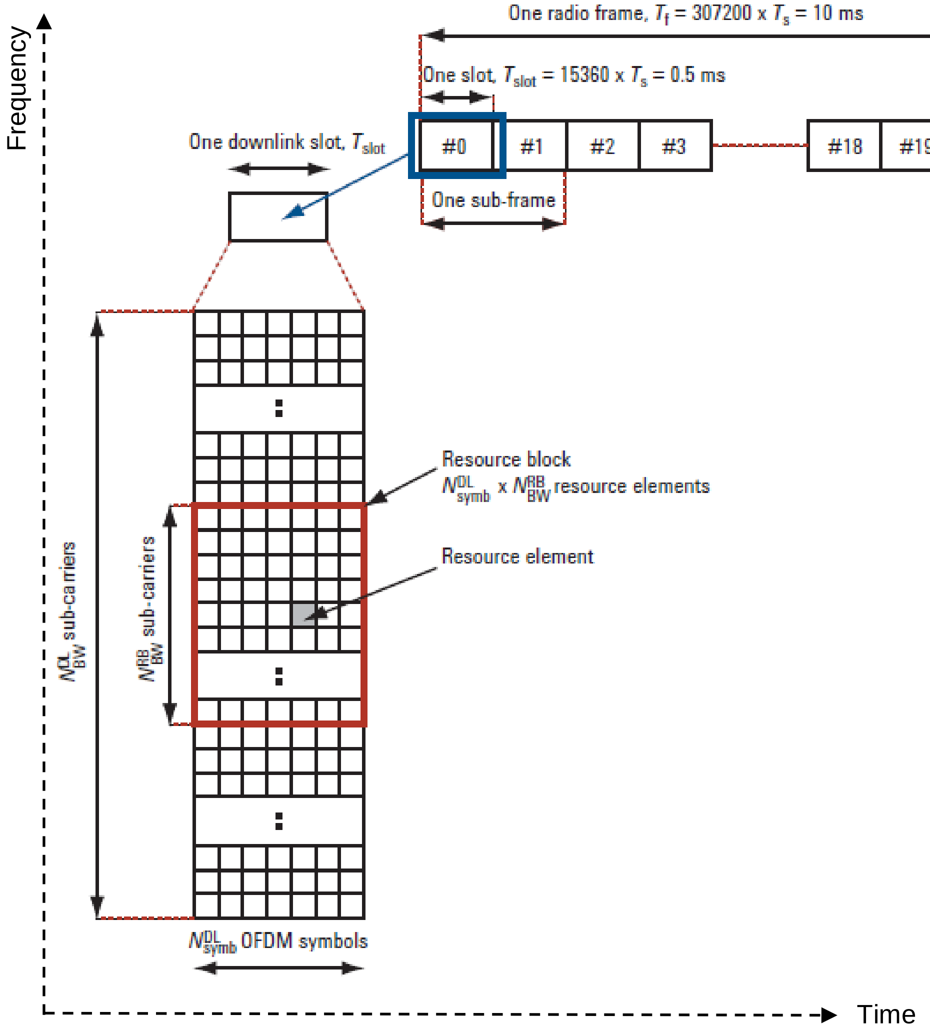

Figure 2.9: Resource Grid for DL (adapted from [Agil07]).

The physical channels represented and their main features are:

- Reference signal (RS): used for channel estimation, mapped over the entire bandwidth in DL, while in UL it is transmitted over the UE's allocation, commonly known as pilots.
- Primary-Synchronisation Channel (P-SCH) and Secondary-Synchronisation Channel (S-SCH): used for cell search and UE network synchronisation.
- Physical Downlink Control Channel (PDCCH): used for scheduling, acknowledgement procedures for error detection and retransmission assessment.
- Physical Control Format Indicator Channel (PCFICH): used to inform which CP is set, i.e., the number of OFDMA symbols per slot.

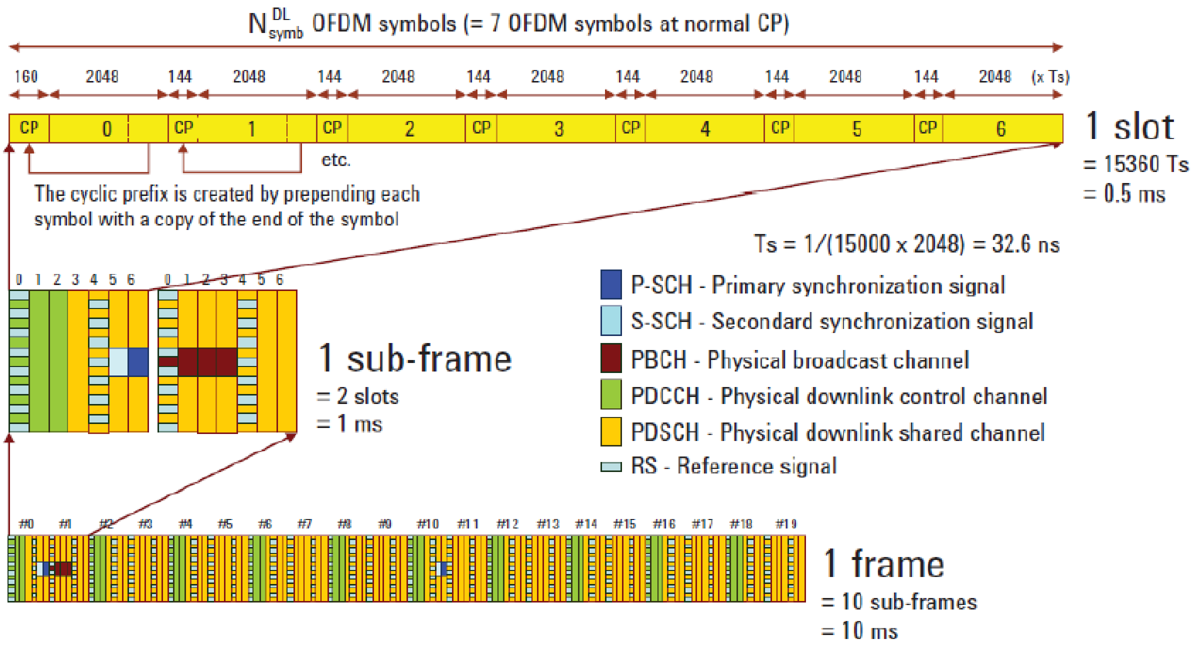

Figure 2.10: DL physical channels mapped into the frame structure (extracted from [Agil07]).

The UL preserves the same frame structures of DL, in terms of slots, sub-frames and radio frames, with the same duration and hierarchy between each other. Control channels in UL are mandatory, since dynamic resource allocation and channel estimation are performed to improve data rates and maximise spectrum efficiency, through different modulations. Physical Uplink Control Channel is mapped onto resource blocks assigned to control purposes and consists on, [3GPP10b]:

- CQI: informs about current channel condition perceived by the UE.
- HARQ (Hybrid ARQ): feedback procedure as response to DL data transmission.
- Scheduling Request.

UL reference signals, used for channel estimation and coherent demodulation, are transmitted in the fourth symbol of the slot, for normal CP. Figure 2.11 shows the UL frame structure and the mapping of the UL reference signal onto the slot.

System's throughput depends on the modulation. As higher the modulation, more bits are carried on each symbol and the higher is the bit rate available. When link conditions are poor, the modulation order must be decreased to accomplish a minimum bit error rate that makes possible the maintenance of connection. LTE accepts a range of modulation orders, depending on the purpose of the physical channel that is sent over the assigned resource element, i.e., the OFDMA assigned symbol. BPSK, QPSK, 16-QAM and 64-QAM are available in either UL or DL.

BPSK is the lower modulation order allowed. Physical Hybrid-ARQ Indicator CH (PHICH) is only BPSK modulated, while Physical Uplink Control CH (PUCCH) can be BPSK or QPSK modulated. Downlink control channels, namely Physical Broadcast Control CH (PBCCH), Physical Control Format Indicator CH (PCFICH) and Physical Downlink Control CH (PDCCH) are QPSK modulated. Physical channels for user's data, Physical Uplink Shared CH (PUSCH), Physical Downlink Shared Channel and DL's Physical Multicast Channel (PMCH) can use, depending on channel quality, QPSK, 16QAM and 64QAM. Generally, as less errors channel admits, lower is the order for the modulation.

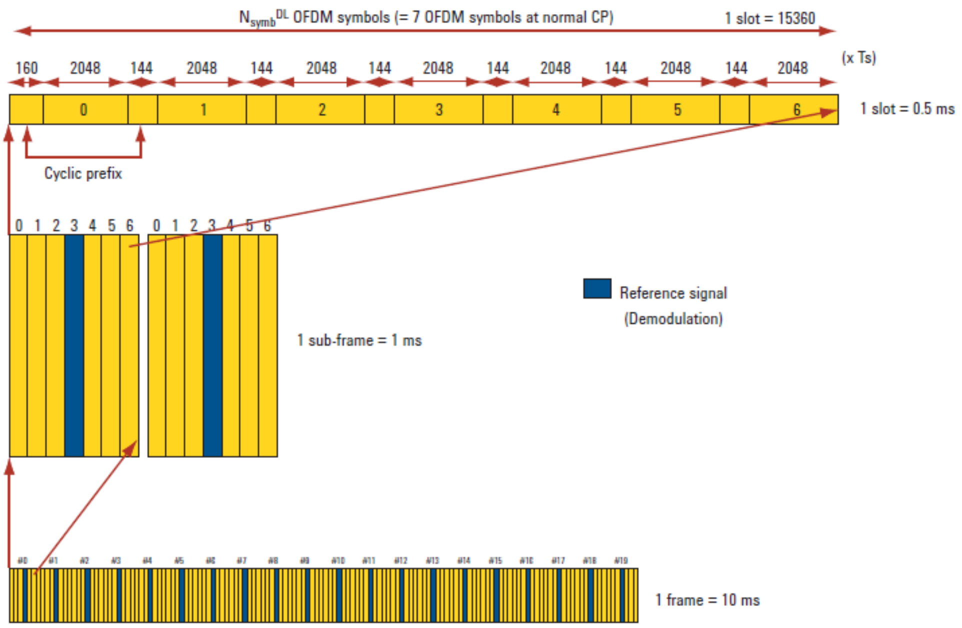

Figure 2.11: UL frame structure and reference signal mapping (extracted from [Agil07]).

2.2.3 Coverage and capacity

The data rate for a particular user depends on the number of resource blocks assigned, modulation applied, channel coding rate, type of cyclic prefix and number of streams (MIMO), beyond the efficiency of the protocol stack. Taking all these aspects into account, based on the physical layer bit rate of each user, by estimation it is possible to get the total number of supported users at the same bit rate, modulation scheme and transmitted power. In this way, the number of resource blocks each user has assigned is equal, and it depends on the transmission bandwidth configuration (N_{RB}), presented in Table 2.2. N_{RB} should be an integer value, and it is obtained by:

$$N_{RB/_U} = \left\lfloor \frac{N_{RB}}{N_U} \right\rfloor \tag{2.13}$$

where:

- N_{RB} is the transmission bandwidth configuration.
- $N_{RB/_U}$ is the number of resource blocks assigned for each user.
- N_U is the total number of users in the system.

The physical layer bit rate for each user is given by:

$$R_{b/_U} = \frac{\left(N_{RB/_U} \times 12\right) \cdot N_{symbols/sub-frame} \cdot \log_2(M) \cdot N_{streams}}{\tau_{\mathrm{TTI}}} \tag{2.14}$$

where:

- $R_{b/U}$ is the physical layer bit rate required for each user.
- $N_{symbols/sub-frame}$ is the number of OFDM symbols per sub-frame (14 for normal CP and 12 for extended CP).
- M is the modulation's order (e.g., $M = 4$ for QPSK, $M = 16$ for 16-QAM).
- R_{coding} is the channel coding rate, which gives the ratio between information and channel coding bits.
- $N_{streams}$ denotes the number of parallel stream, given by MIMO configuration (2x2 MIMO means $N_{streams} = 2$).
- τ_{TTI} is the time transmission interval, equal to 1 ms for LTE.

Replacing (2.13) on (2.14), it is possible to get the estimation of the total number of users served by the system:

$$N_U = \left\lfloor \frac{12 \cdot N_{RB} \cdot N_{symbols/sub-frame} \cdot log_2(M) \cdot N_{streams}}{R_{b/U} \cdot \tau_{TTI}} \right\rfloor \tag{2.15}$$

LTE's coverage evaluation can be performed independently for each sub-carrier. Similarly to UMTS, the coverage area of a cell is obtained by computing the average distance from the BS that keeps the signal-to-noise ratio required by UE above a minimum value, with an acceptable BER, and depends on the modulation scheme and order. The average distance is assessed through the most adaptable propagation model to the scenario where the system is being implemented. The radius of a cell takes a similar expression presented for UMTS and is given by:

$$r_{cell[\mathrm{km}]} = 10^{\frac{P_{TX_{sub-carrier}}[\mathrm{dBm}] + G_{t[\mathrm{dBi}]} - P_{r_{sub-carrier}}[\mathrm{dBm}] + G_{r[\mathrm{dBi}]} - L_{ref[\mathrm{dB}]} - M_{p[\mathrm{dB}]}}{10 \cdot a_{pd}}} \tag{2.16}$$

where:

- $P_{TX_{sub-carrier}}[\mathrm{dBm}]$ represents the transmitting power assigned for each sub-carrier;
- $P_{r_{sub-carrier}}[\mathrm{dBm}]$ is the minimum receiving power required by UE to perform a certain bit rate.

The minimum receiving power required by the UE takes the following expression, again with E_b/N_0 being the signal-to-noise ratio required at UE for the modulation in use:

$$P_{r[\mathrm{dBm}]} = N_{RF[\mathrm{dBm}]} + \left(E_b/N_0\right)_{[\mathrm{dB}]} \tag{2.17}$$

The noise power is taken to the sub-band bandwidth, Δf =15 kHz, and E_b/N_0 required depends on the modulation scheme and order, as well as the channel characteristics, in this case a Rayleigh channel.

2.3 Beamforming

Beamforming comprises the functions performed by a device (usually called as beamformer or generically adaptive antenna) in order to allow the power radiated by an antenna to be focused into a specific direction. In the same way, beamforming consists of receiving a signal from a desired direction, while reducing the interference generated by interferers located in directions that are not the desired one.

A single-element antenna has no evident lobes in its radiation pattern. An array with a number of basic radiators is used to create lobes and nulls in directions of interest. The direction of the main lobe or nulls can be tuned by changing the spacing of the basic radiators in the array. Besides the basic radiators' spacing, also the configuration of the array can change in order to obtain the radiation pattern with more interest to the application, which can be linear, circular, etc. This physical changes made to set up the antenna's radiation pattern are actually performing relative phase shifts between signals captured by each antenna element. Typically, for a desired application, the antenna with the most advantageous radiation pattern is chosen and it remains the same during the operational life of the system.

A Beamforming Network, also referred to as an adaptive antenna array, consists of a number of antenna elements coupled together by a complex shift control, to form a very directive beam able to move the radiation pattern. By creating a directive high gain beam into the direction that the signal preferentially comes from or goes to, the interference generated out of the direction of interest is significantly lower than the signal coming from the direction of the high gain beam. At the same time, when the antenna is transmitting, the extra gain of the antenna (due to the smaller width of the beam) increases the effective isotropic radiated power (EIRP), which leads to an increase of coverage, or keeps the same coverage with less feed power. Also when the antenna is transmitting, a high directive radiation pattern brings reduction of interference to other users in the neighbourhood, and increases at the same time the frequency reuse ratio. The scope of this thesis falls into the energy efficiency improvement by using beamforming in DL.

A basic beamforming network layout is shown in Figure 2.12. The signal arriving at each antenna element is individually weighted to form a beam into the direction of interest. The weighting process is applied in amplitude as well as in phase of the incoming signals. The signals of all elements are then combined in order to create a single signal that will be captured by the receiver. At the same time, a feedback process adjusts the weights of each antenna element. Adaptive antennas are supposed to be reciprocal, and so beamformer network feeds and weights individually each antenna element in order to transmit into a preferential direction.

Despite the high performance of a basic beamforming network, like that one presented in Figure 2.12, the processing is performed at the propagation level and due to this reason, this way of weighting is called as analogue beamforming, which implies that only a limited number of beams can be created at the same time. The solution to create a larger number of beams in the same antenna is the introduction of digital processing between antenna elements and the receiver. Digital beamforming has not the same physical meaning as analogue has. No information is destroyed, at least, until processing begins. Its major advantage relies on the fact that the signal arriving at each antenna element is captured into a digital stream. Figure 2.13 presents the basic layout of a multi-beams beamforming equipment. The signal arriving at each of the N_a antennas is immediately converted into a digital stream. The process of weighting is performed locally at each beamforming unit, according to the radiation pattern desired, and then they are digitally added into a single stream to the receiver. On transmitting, the signal is previously decomposed into N_a components, with each component weighted and then converted to analogue, in order to form the desired beam.

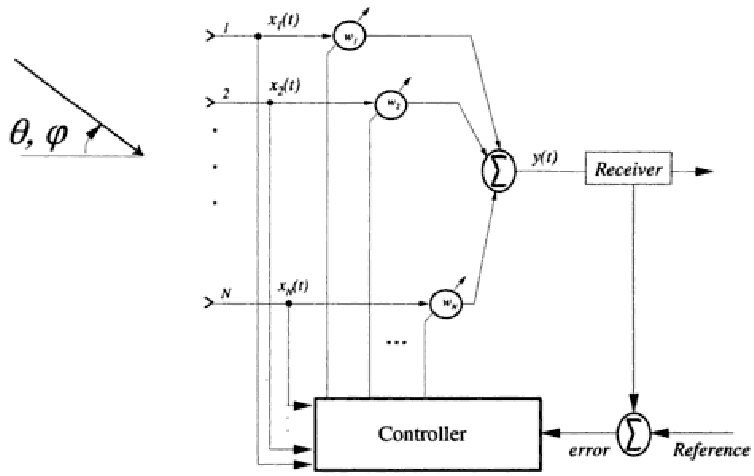

Figure 2.12: Beamforming network basic layout (extracted from [Chan04]).

Beamforming networks can be based on antenna elements or on beams. The basic layout of a digital beamforming network is presented in Figure 2.13 (a) and it is an element-based one. This type of beamformer weights one signal component to each antenna elements. Beam-based beamforming requires a set of beam-space combiners to generate weighted outputs. Instead of consider the signals received by each antenna element, there are several groups of antenna elements that form fixed lobes. Preferentially, all lobes are orthogonal in order to perform an efficient spatial filtering of the incoming and outgoing signals. Figure 2.13 (b) shows the basic structure of a beam-space beamformer. The signals of each antenna element are weighted on a fixed way, to correspond to an orthogonal lobe of the array's radiation pattern.

Regarding adaptive algorithms, they can be grouped into two major methods: Switched Beamforming and Direction Finding Beamforming. Switched Beamforming consists of the less complex operational method for beamformers that measures the power (or SNR) from all the orthogonal beams, and then selects the one with the larger value, or combine the outputs of some beams. The switched method has limited interference suppression and high sensitivity to false beam locking due to interference. Direction finding techniques for beamforming are focused on the perception of the user's behaviour. The idea is to track user's movement to anticipate their future movements, in order to estimate the most advantage configuration for the antenna array, as soon as possible. Tracking requires more computational effort than simple switching methods. Previous beamforming applications were developed for operate in switching method, but computational constraints are nowadays sustainable and the performance improvements are considerable, compared with former solutions. This kind of technique can bring benefits to DL beamforming in FDD systems, where propagation characteristics are not accurately assessed by UL reference signals, but the user's direction remains the same.

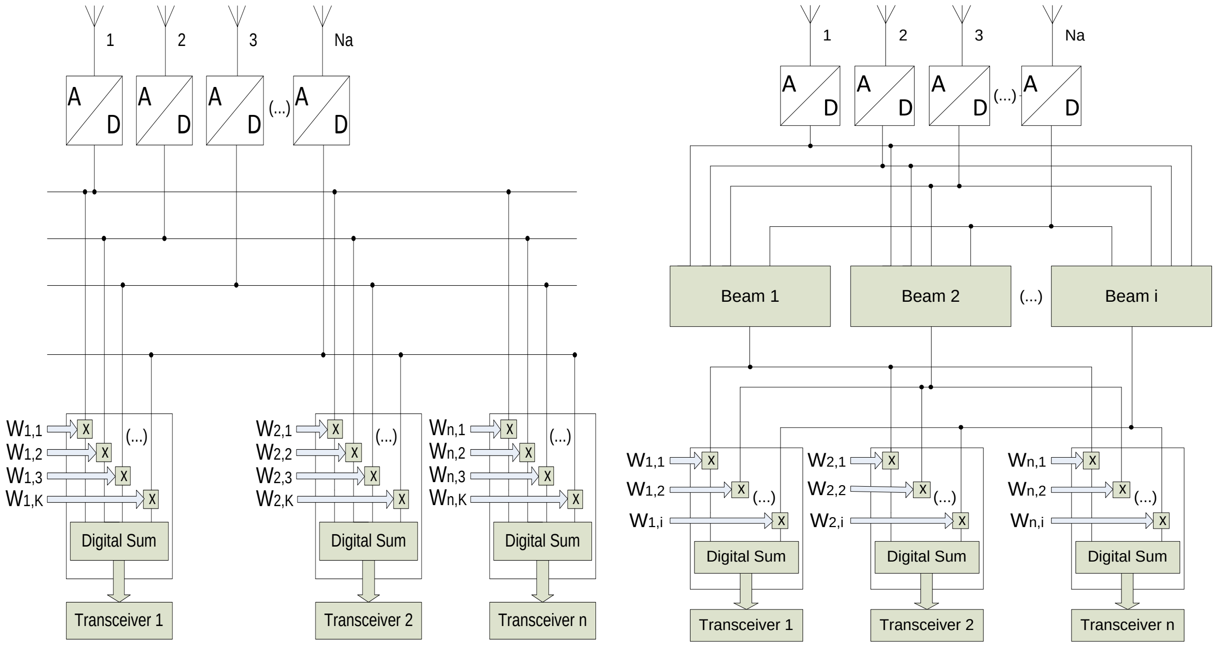

(a): Digital beamformer element-based layout. (b): Basic layout of a beam-based beamformer.

Figure 2.13: Layout of typical digital adaptive antennas.

There are several algorithms able to implement optimal weighting, differing fundamentally on the speed of convergence. The algorithm that is used in work is one that leads to the minimum mean-square error (MMSE).

Consider a uniformly spaced linear array, Figure 2.14, with N_a elements d spaced:

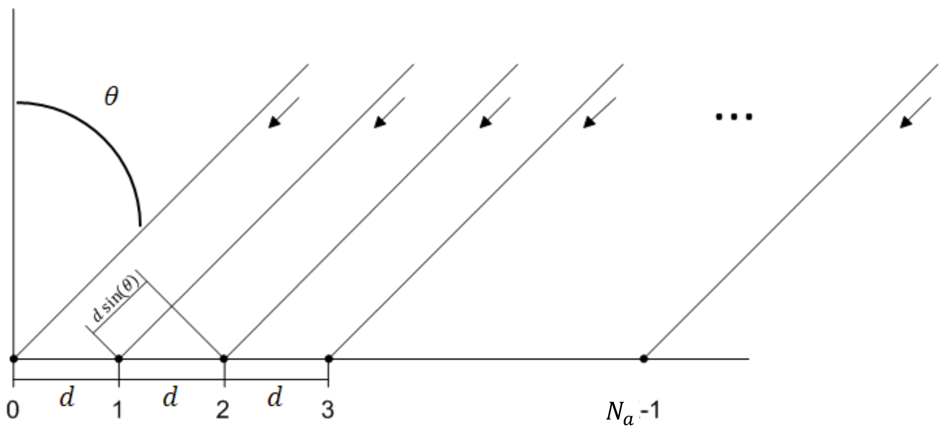

Figure 2.14: Uniformly spaced linear array.

The desire signal, $u_1(t)$, arrives at the array with a spatial angle θ_1. At the same time, there are $N_u - 1$ interfering signals, $\{\boldsymbol{u_i}(t)\}_{i=2}^{N_u}$, each one arrives at the array with a spatial angle θ_i. The output of the array is:

$$\mathbf{x}(t) = \sum_{i=2}^{N_u} u_i(t)\, \boldsymbol{v_i} \tag{2.18}$$

$\boldsymbol{v_i}$ is the array propagation vector for each of the $N_u - 1$ interfering signals and it is represented by:

$$\boldsymbol{v_i} = [1, e^{-jkd\,sin(\theta_i)}, \dots, e^{-jk(K-1)d\,sin(\theta_i)}]^T \tag{2.19}$$

The array's output is then multiplied by the weighting vector $\boldsymbol{w}$, which is choose to minimise the mean-square error between the array's output $\boldsymbol{w}^H\mathbf{x}(t)$ and a reference signal $u^*(t)$, a signal known by both sides of the transmission and used to set the beamformer's weighting vector. The index H above the vector denotes the conjugate transpose and it is used for matrix compatibility. The reference signal can be obtained from some UL control channel. The mean-square error is, in this way, expressed by:

$$\overline{\varepsilon^2(t)} = [u^*(t) - \boldsymbol{w}^H\mathbf{x}(t)]^2 \tag{2.20}$$

The reference signal is expressed in its complex conjugate only for mathematical convenience. Taking the expected value of both sides of (2.20), and using some algebraic manipulations, the expected value for the mean-square error is given by:

$$E\{\varepsilon^2(t)\} = E\{d^2(t)\} - 2\boldsymbol{w}^H E\{u^*(t)\mathbf{x}(t)\} + \boldsymbol{w}^H E\{\mathbf{x}(t)\mathbf{x}^H(t)\}\boldsymbol{w} \tag{2.21}$$

Defining $E\{\mathbf{x}(t)\mathbf{x}^H(t)\}$ as the covariance matrix $\boldsymbol{R}$ and representing $E\{u^*(t)\mathbf{x}(t)\}$ as $\boldsymbol{r}$, the minimum mean-square error between the beamformer's output and the reference signal is given by the null of the gradient vector of (2.21) with respect to $\boldsymbol{w}$, which is show in (2.22):

$$\boldsymbol{\nabla w}\left(E\left\{\overline{\varepsilon^2(t)}\right\}\right) = 0 = -2\boldsymbol{r} + 2\boldsymbol{Rw} \tag{2.22}$$

From (2.22), it is possible to obtain the optimum weighting vector that minimises the MSE:

$$\boldsymbol{w}_{opt} = \boldsymbol{R}^{-1}\boldsymbol{r} = \left(E\{\mathbf{x}(t)\mathbf{x}^H(t)\}\right)^{-1} \cdot E\{u^*(t)\mathbf{x}(t)\} \tag{2.23}$$

For a visual understanding of the minimum mean-square error criterion, Figure 2.15 represents the involved signals over the beamformer's layout.

Although the beamforming technique is applied at the BS on DL, the algorithm for optimum weighting is based on a UL reference signal that is used to track the user's location and set up the weighting vector.

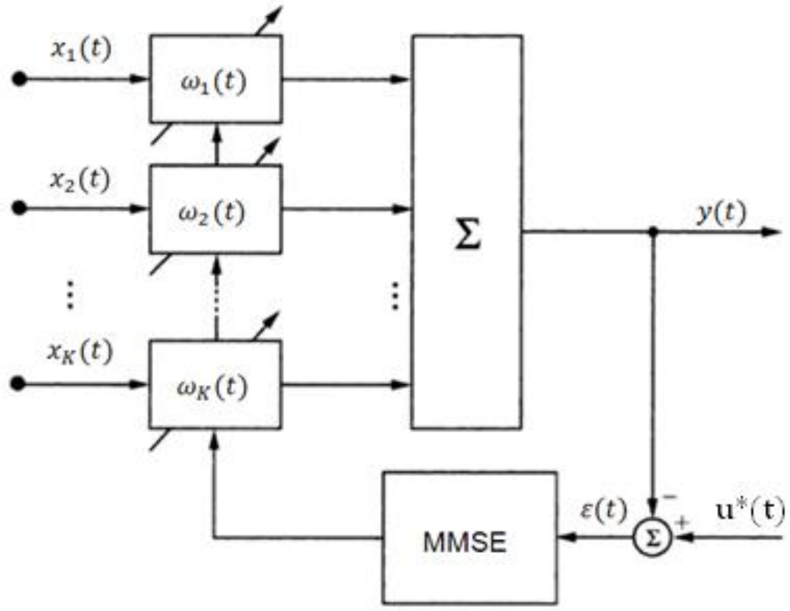

Figure 2.15: MMSE signal flow.

2.4 Energy efficiency and multiple antenna trends.

Early in telecommunication's history, multiple antennas transmission has been a solution for radio communication. However, the high cost always conditioned their usage to critical performance applications, due to its powerful functionality of variable radiation patterns. The high number of reception components need by each element, such as RF amplifiers, D/A and A/D convertors, restricted the implementation of multiple element antennas to the military industry [OhGy00]. With the development of integrated RF components, multi antennas applications became more popular and their price became more affordable to services provided for general public.

Several trends and applications have been developed over the years with special emphasis on throughput improvement to provide high performance wideband services to customers, in an attempt to spectrum efficiency. One of the trends in multi element antenna radio communications is the Spatial Division Multiple Access (SDMA). The idea behind SDMA is the exploitation of users' spatial diversity. Considering a system with multiple access technique based on time, frequency or code multiplexing, by adding a SDMA component, the number of communication channels is maximised over the restriction of time-slots, carriers or codes when users are spatially separated by beamforming [FaNo98]. One of the SDMA based applications is the orthogonal beamforming schedule. Even for limited feedback channel information, orthogonal beamforming for SDMA can achieve twice the capacity of conventional multiple access techniques in terms of users served, for several scenarios [HuAH09].

Another SDMA based technique to improve channel capacity with adaptive antennas is opportunistic beamforming. Opportunistic beamforming can be seen as an intermediate application between static antennas and fully adaptive antennas, where the radiation pattern of the BS antenna is changing in a periodic or even pseudorandom fashion. DL transmission is scheduled in order to serve each user at the moment that his radio channel shows best conditions. By analysing the fading pattern that each user senses, instead of providing best signal strength for the desired user and enhance individual capacity, interference nulling can be also reached in the way that the transmission to an desired user is performed at the moment that his channel is better and the channel of a non-desired user attenuates the desired signal [ViTL02].

The most conventional applications of beamforming to radio communications, where an antenna array has its elements fed individually in order to produce some characteristics into its radiation pattern are used in space communications. In radio links with low margin, as satellite communications are, especially when communicating with mobile satellite devices with low gain antennas, the employment of arrays of antennas at the satellite side provides better quality signals, reduces interference and allows a higher frequency reuse ratio. In these applications, a geographic area is served by a beam in some carrier frequency, in a ground pattern similar to a cellular deployment for mobile communications. Depending on traffic demand, the beam positioning can be changed in order to provide capacity to higher intensity traffic areas. Although the adjustment of the satellite radiation pattern can be considered as a type of beamforming, the time scale in what these adjustments happen, i.e., hours, makes that this type of beamforming cannot be call as dynamic beam steering.

One of the hot seats in what beamforming concerns is the application of adaptive radiation patterns to decentralised antenna elements. In ad hoc networks, without a central controller, distributed beamforming techniques increase system throughput and lower energy consumption by exploiting the diversity where the access points are located. Each access point antenna can be seen as an antenna element that will transmit the same signal than those that are also covering the desired users, however with different power intensity and phases, in order to produce constructive and destructive interference areas where the desired signal is stronger, and regions with low coverage, where the desire signal is seen as interference. The drawback in the application of distributed beamforming to adhoc networks is the absence of a central controller to coordinate the transmission configuration and the improvement that must be done in the reduction of control signals' overhead that confines the throughput severely in this kind of networks [ZKTC11]. Distributed or collaborative beamforming is actually farther way since it requires a new organisation on the networks architectures and a lot of work must be done in order to develop resource allocation for different scenarios. Important results was already done and they show a significant improvement in signal-to-interference ratios experienced by users over distributed broadcast wireless networks (DBWS) in the specific scenario of Manhattan. Redefining the concept of cell with just one BS to several antenna units controlled by a central unit (linked by optical fibre), it is possible to achieved near 4 dB of SIR improvement, when hundreds of users are considered and served by four antenna units [HuGa10]. Figure 2.16 shows the simulated scenario as well as the results for the average SIR improvement.

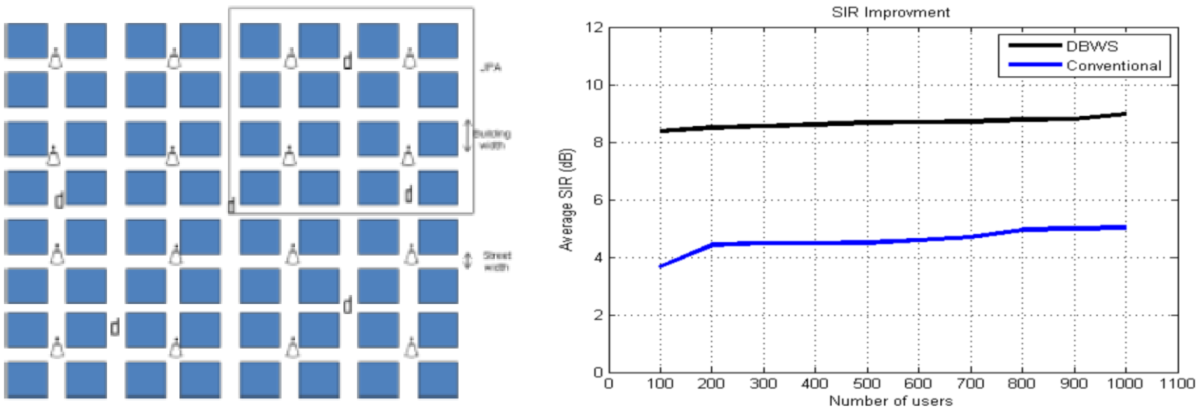

(a): Scenario Layout (b): Average SIR improvement

Figure 2.16: DBWS test scenario and results (extracted from [HuGa10]).

The state of the art in terms of energy efficiency achieved by multiple antenna transmission is what is referred as active antennas. The advantage, compared to distributed beamforming, relies on the fact that active antenna solutions do not required major architecture changes in order to effectively be implemented. An active antenna, like the ones that are under study in this work, is an antenna array that generates radiation patterns on a per-user basis, which focus the radiation into the direction of the desired user in a way that offers the best trade-off in terms of signal improvement and interference suppression. This new BS component can be seen as a combination between a remote radio head and a set of antennas. Figure 2.17 shows the overall logic network architecture after the introduction of adaptive antennas, which is suitable to be applied for actual network architectures.

Some research has been done in order to evaluate the impact of adaptive antennas in actual BSs, mainly in spectral efficiency. Average cell spectral efficiencies near 50% for antennas with four elements, and near 80% for antennas with eight elements, are the reference for future applications operating with active antennas on a per-user way [EarP10]. Table 2.3 summarises the reference results that are supposed to be achievable for spectral efficiency.

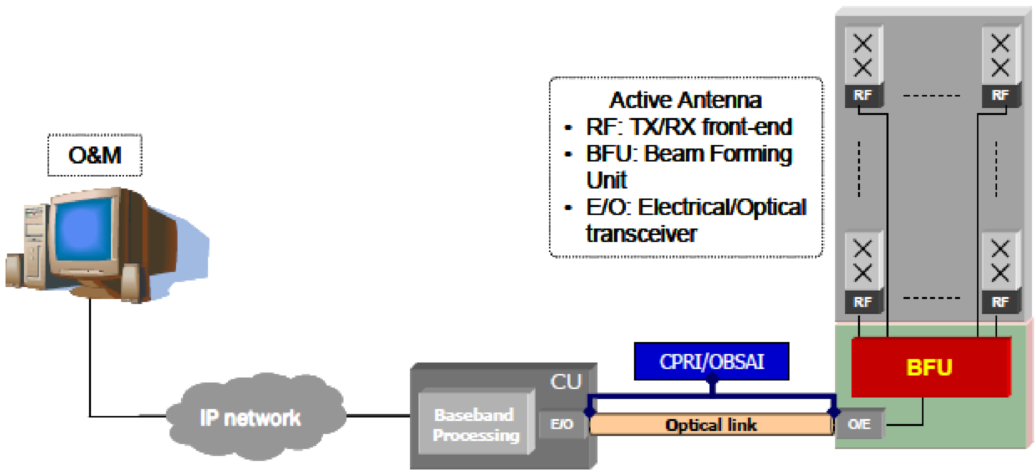

Figure 2.17: Active antenna system overall architecture (extracted from [EarP10]).

Table 2.3: Spectral efficiency reference results for active antenna systems (adapted from [EarP10]).

	Downlink transmission scheme		
Metric	*SIMO 1x2*	*Beamforming 4x2*	*Beamfoming 8x2*
Average cell spectral efficiency [bps/Hz/cell]	0.85	1.28 (+51%)	1.52 (+79%)
User spectral efficiency [bps/Hz]	0.2	0.29 (+43%)	0.33 (+63%)

A higher spectral efficiency allows serving more users or more demanding services with the same transmitted power. The scope of this thesis is the evaluation of the impact on the transmitted power, and consequently in the energy spent by active antennas that are serving the same population of users (or services), under the same conditions that is served by actual static antennas. The objective is a real reduction of the energy spent power, i.e., how much energy is possible to save in some BSs that nowadays serve a certain population. Some interesting results, and the way how it is possible to reach them, is presented in the following sections.

Concerning energy efficiency applied to mobile communications, BS is the most energy demanding element, and for this reason, the focus of the main efforts to reduce the spent energy. Any deployment at this single element that brings energy efficiency is reflected in thousands of BSs all over the world. Power waste is mainly due to power units, (UPS, transformers, etc.) that are operating below their full load capacities. Air conditioning equipment is also a power demanding process that degrades the overall energy efficiency of the system. One option is to investigate alternative thermal removal techniques, like fresh air flowing within BSs and electronic equipment tolerance increase to higher temperatures. A study proved that by increasing the tolerance of a power amplifier from 21ºC to 25ºC, a reduction of the overall BS energy of 10% is achievable [LiK08].

Energy efficiency evaluation can be framed into three main approaches: component, link and network levels. Power amplifiers consume a significant portion of the energy consumed by a BS, between 50 and 80%. Beyond the poor efficiency of power amplifiers near 50%, this efficiency is achieved by high load situations, when amplifiers are near saturation, the efficiency decreases substantially for medium and low load situations. The solution can be obtained by adopting signal-conditioning algorithms to control high peak-to-average power ratios with which WCDMA and OFDMA are characterised, or even special architectures power amplifiers, e.g., Doherty type, which contain one main amplifier always active and an auxiliary one active only when signal peaks occur, showing maximum efficiency below saturation. Concerning link level, it has a lot of potential for energy saving. Reference signals and control channels introduce transmission overheads that have potential to be reduced, and increase spectral efficiency. Discontinuous transmission and BS sleep modes can be the answer for off-peak hours, when virtually all BSs are operating at low load, or they might not even be serving any user, which contributes severely to increase the power consumption per user. Network deployment needs to be flexible in order to allow a heterogeneous site implementation, with consumption scaled as a function of the type of traffic and traffic load [CZBF10].

Chapter 3

Models and Simulation Description

This chapter provides an overview about the procedures to evaluate beamforming performance, in several multi-user scenarios, over an energy efficiency view point. This model can be seen as a tool to estimate the energy reduction achieved in generic scenarios, for typical cell coverage and several numbers of users. Due to the nature of multiple access techniques, UMTS and LTE performance are evaluated differently and separately. Finally, the assessment and some simulation are performed for expected results in order to evaluate the accuracy of the model and the simulator that implements the model.

3.1 Model Overview

The performance achieved by introducing of beamforming is, in a simplistic approach, mainly dependent on users' location. Since the objective of beamforming is the spatial filtering of interfering users, while it tries to focus the main beam into the direction of the desired user, the spatial location of users in the cell area determines how good the filtering can be.

For the same distribution of users in the cell, there are other parameters that can provide better or worst performances. These parameters depend on the system and are not emerging from the randomness of the services, as user's location, mobility, service data rate service, etc. The system's dependent parameters are the number of antenna elements, the operating frequency of the system, and the number of receiving antennas on the MT side, among others.

Users' location is of major importance to achieved performance by adaptive antennas. The spatial filtering provided by several antenna elements and their individual weighting is just possible according to their directions and overlapping effects that some can create on others. Since these effects can really happen on real operation, statistics must be used to ensure a mean value and a standard deviation, to enable the assessment of adaptive antennas' performance within confidence intervals.

Figure 3.1 represents the main steps followed by the model in order to evaluate the energy efficiency that can be achieved when beamforming is applied in mobile networks operating in UMTS and LTE.

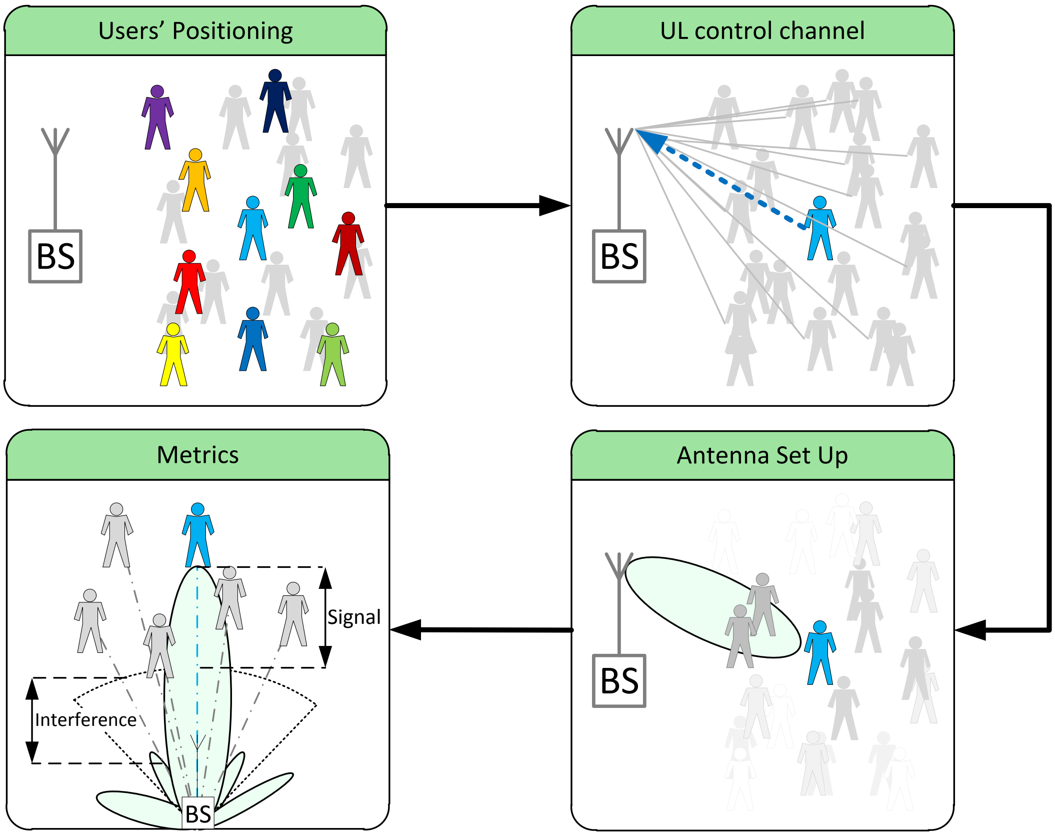

Figure 3.1: Model's steps for performance evaluation of adaptive antennas.

3.2 Multi-user model for UMTS

UMTS code division multiple access operates over the same bandwidth for all users. In this way, it is of the major importance to reduce the interference suffered by one user that is caused by the remaining users in the cell. By reducing the interference, the power of the signal reserved to serve the desired user can be also reduced without any service degradation, which enables the reduction of the overall energy.

3.2.1 Users' generation

In this work, a multi-user model for evaluation of power improvement reached by beamforming is based on users' location. Users' locations is the key factor to evaluate the performance of adaptive antennas, since the direction in which each user's signal comes from determines how good is the spatial filtering that adaptive antennas are able to do. In this way, one has to account for the location of users in the terrain, each one defined by a distance R, and an angle θ, Figure 3.2.

The antennas' weighting (process detailed later) is based on an UL control channel, in which the radio signal of the desired user is recovered, as much as possible, from interference caused by other users. Each user generates a signal that is received at the BS, known *a priori* by both sides. Then, the elements of the BS antenna are individually weighted to recover a replica of the signal sent by the desired user, interference affected by the remaining users. All users' signals are equivalent in energy and power among each other, and their instantaneous values are contained in the same interval. In this way, the signal of the user i is referred to as u_i, with $u_i(t) \in [0, z]\ \forall\, t,$ and their instantaneous values are uniformly distributed in amplitude between 0 and z.

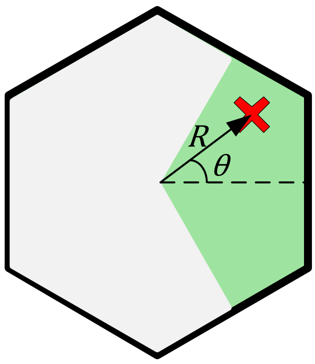

Figure 3.2: Parameters used to locate a user.

The probability of number 1 user's message be equal to number 2 user's message, in the same time instant, is given by $Prob\big(u_1(t_1) = u_2(t_1)\big) = z^{-1}$. The randomness introduced by the generation of symbols leads also to the property that the signal of one user is hardly linearly combined from the signals of some other users:

${}^{u_1}/_{u_2} \neq C,$ with C being a constant.

The signal coming from the desired user is referred to as $u_{du}$from now on.

The path-loss between users and BS is computed according to the model proposed by the EARTH Project [EarP10a]. The EARTH Project provides three scenarios with enough coverage to represent the major percentage of countries. The dense urban scenario comprises the centre and main arteries of a city, with a strong commercial and services traffic, a substantial component of occasional users at the main public transports and streets (tourists, moving professionals, students) and a component of residential load. The dense urban scenario usually has a great concentration of BSs due to the demand for capacity, where cells' areas just assume some hundreds of metres. The suburban scenario is modelled to correspond to typical city's periphery, with major habitation blocks with several floors, that absorbs by night an important fraction of users that were at the city's centre by day. Suburban cells do not need to be as near as at city's centre, since users' location and demand for capacity is usually sparser. The remaining territory corresponds to rural low dense populated scenarios that can be crossed by important highways, and covers areas with a few kilometres radius, where sparsely populated villages are located. Rural BSs usually are far from each other by several kilometres, being responsible for covering more than one village or some kilometres of highways.The path-loss model is the following:

$$L_{p_{LOS}}(R)_{[\mathrm{dB}]} = 97.4 + 20\log_{10}\left(f_{c_{[\mathrm{GHz}]}}\right) + 24.2\log_{10}\left(R_{[\mathrm{km}]}\right)$$
$$L_{p_{NLOS}}(R)_{[\mathrm{dB}]} = 125.1 + 20\log_{10}\left(f_{c_{[\mathrm{GHz}]}}\right) + 42.8\log_{10}\left(R_{[\mathrm{km}]}\right) \quad (3.1)$$

where:

- f_c is the frequency where the system is operating (carrier frequency).
- R is the distance between the user and the BS.
- $L_{p_{LOS}}$ is the path-loss for the Line-of-Sight (LOS) situation.
- $L_{p_{NLOS}}$ is the path-loss for the Non-LOS (NLOS) situation.

The path-loss model is used for three scenarios:

- Scenario 1: Dense urban.
- Scenario 2: Suburban.
- Scenario 3: Rural and high speed.

The difference between scenarios, in terms of path-loss, is set by the probability of occurring LOS ($Prob(LOS)$) and by its standard deviation σ, Table 3.1.

Finally, propagation affects both the amplitude and the phase of signals. In that way, concerning the total randomness that phase can assume, its value is uniformly distributed between 0 and 2π.

Table 3.1: Path-loss models (extracted from [EarP10a])

	Scenario 1	Scenario 2	Scenario 3
$Prob(LOS)$	$\left[\min\left(\frac{0.018}{R},1\right)\cdot\left(1-e^{\left(\frac{R}{0.063}\right)}\right)\right]+e^{\left(\frac{-R}{0.063}\right)}$	$e^{\left(\frac{-(R-0.01)}{0.2}\right)}$	$e^{\left(\frac{-(R-0.01)}{1.0}\right)}$
σ_{LOS}	4 dB	6 dB	6 dB
σ_{NLOS}	6 dB	8 dB	8 dB

3.2.2 Received signals

The output of a linear antenna array is a combination of signals received by each antenna element, according to the direction where signals come from. Taking antenna theory [LiLo96], Figure 2.14, if a signal coming from an angular direction θ reaches an N_a elements antenna array, the steering vector $a(\theta)$ of the array takes the following form:

$$a(\theta) = \sum_{m=1}^{N_a} e^{j\frac{2\pi}{\lambda}d(m-1)\sin(\theta)} \tag{3.2}$$

The output signal of the antenna array $x(t)$ that receives one signal (from user i) from direction θ_i is given by the signal that reaches the antenna array, multiplied by the steering vector:

$$x(t) = u_i(t)\cdot P_{RX_i}\cdot\left(\sum_{m=1}^{N_a} e^{j\frac{2\pi}{\lambda}d(m-1)\sin(\theta_i)}\right) \tag{3.3}$$

where:

- $u_i(t)$ is the message sent by user i, defined in Section 3.2.1.
- P_{RX_i} is power sent by user i that reaches the antenna array.

When there are several signals reaching the array, the output signal of the antenna array is given by a combination of all signals coming from all users, in different locations and with different direction. The output of a linear antenna array that receives signals from N_u users is just the sum of all antennas' outputs:

$$x(t) = \sum_{i=1}^{N_u}\sum_{m=1}^{N_a} u_i(t)\cdot P_{RX_i}\cdot e^{j\frac{2\pi}{\lambda}d(m-1)\sin(\theta_i)} \tag{3.4}$$

The received power from user i at the antenna array depends on the user's location, the propagation scenario and the transmitted power. Since UL control channels have no power control, the radiated power of all users is the same, and it is set to the unitary value. This normalisation does not imply any constraints, because system's performance is assessed through relative metrics. The radiated received power is, in this way, obtained by:

$$P_{RX_i[\mathrm{dBm}]} = P_{TX_i[\mathrm{dBm}]} - L_{p_{i[\mathrm{dB}]}} \tag{3.5}$$

For UMTS, the signal that comes from the desired user is perceived a few dBs stronger than a non-desired signal that suffers the same propagation losses, due to the CDMA's processing gain. The processing gain is the difference between a spread and a non-spread signal, and it is defined according to the bit rate required for the desired user. In this way, the perceived power, after dispreading with desired user's code, denoted as $P_{RX_{du}}$ is given by:

$$P_{RX_{du}[\mathrm{dBm}]} = P_{TX_i[\mathrm{dBm}]} + G_{p[\mathrm{dB}]} - L_{p_{i[\mathrm{dB}]}} \tag{3.6}$$

Replacing (3.5) in (3.4), taking (3.6) and normalising the transmitted power, the output signal of the antenna array that is perceived to serve the desired user is given by:

$$\mathrm{x}(t) = u_{du}(t)\frac{G_p}{L_{p_{du}}}\sum_{m=1}^{N_a} e^{j\frac{2\pi}{\lambda}d(m-1)\sin(\theta_{du})} + \sum_{i=2}^{N_u}\sum_{m=1}^{N_a}\frac{u_i(t)}{L_{p_i}}e^{j\frac{2\pi}{\lambda}d(m-1)\sin(\theta_i)} \tag{3.7}$$

where:

- u_{du} is the desired user's UL control signal.
- $L_{p_{du}}$ is the propagation path loss between the desired user and the BS.
- θ_{du} is the direction of arrival of the signal coming from the desired user.

3.2.3 Weighting and radiation pattern generation

The generation of radiation patterns able to perform spatial filtering among desired and non-desired users is achieved by weighting individually the signal received by each antenna element, to be combined together. Taking (3.7), which is the signal obtained in a unweighted linear antenna array, with N_a elements, when N_u users are active and a desired user is being served, the signal received by an adaptive antenna, y, is just a modification of (3.7):

$$\mathrm{y}(t) = u_{du}(t)\frac{G_p}{L_{p_{du}}}\cdot\sum_{m=1}^{N_a} w_m\cdot e^{j\frac{2\pi}{\lambda}d(m-1)\sin(\theta)} + \sum_{i=2}^{N_u}\sum_{m=1}^{N_a}\frac{u_i(t)}{L_{p_i}}\cdot w_m\cdot e^{j\frac{2\pi}{\lambda}d(m-1)\sin(\theta_i)} \tag{3.8}$$

where w_m is the weight of the N_m^th element of the antenna array.

There are several algorithms to determine the optimum values with which antenna elements are weighted, to privilege the signal coming from the desired user, while the others are suppressed as much as possible. The principle is based on minimising the mean-square error between the recovered signal and a prediction of the signal sent by the desired user. To reach this objective, and since the computational effort is done offline (without timing constraints due to real operation waiting users), the weight vector is derived using the Simple Matrix Inversion (SMI) algorithm. Since, in simulation, channel conditions do not change during estimation and the reference signal is known, SMI is the least square solution of the optimum weighting vector that minimises the MSE, described in Section 2.3.

$$\boldsymbol{w}_{opt} = \boldsymbol{R}^{-1}\boldsymbol{r} = \left(\boldsymbol{y}(t)\boldsymbol{y}^{H}(t)\right)^{-1} \cdot \left({u_{du}}^{*}(t)\boldsymbol{y}(t)\right) \tag{3.9}$$

where:

- ${u_{du}}^{*}$ is the prediction of the signal sent by the desired user, available at the BS

For simulation purposes, ${u_{du}}^{*}$ can be the exact signal sent by the desired user, u_{du}, since the aim of this work is the performance of adaptive antennas and not control channel protocols.

The SMI algorithm gives the weights for the antenna elements and the radiation pattern that serves the desired user. The normalised radiation pattern $g_{norm}(t)$ is defined as:

$$g_{norm}(\theta) = \frac{\sum_{m=1}^{N_a} w_m \cdot e^{j\frac{2\pi}{\lambda}d(m-1)\sin(\theta)}}{\max\limits_{0<\theta<\pi}\left(\sum_{m=1}^{N_a} w_m \cdot e^{j\frac{2\pi}{\lambda}d(m-1)\sin(\theta)}\right)} \tag{3.10}$$

At the BS, one assumes the presence of an ideal reflector that produces an infinite antenna front-to-back ratio, which confines the radiation patterns to 180º. The antenna gain, $g(\theta)$, confined to 180º, is represented by:

$$g(\theta) = \frac{g_{norm}(\theta)}{\frac{1}{2\pi}\int_0^{\pi} g_{norm}(\theta)\, d\theta} \tag{3.11}$$

For each user, the adaptive antenna generates a radiation pattern to serve him. Considering user i, the gain of the radiation pattern, as a function of the direction, is denoted as $g_i(\theta)$.

The reference gain to which the adaptive radiation pattern will be compared to, is the gain of a 120º sector antenna, denoted by $g_{ref}(\theta)$

3.2.4 Metrics

Metrics to evaluate adaptive antenna's performance for UMTS are composed of two components: the first is the signal's power reduction due to the rise of gain into the direction of the desired user; the second emerges from the reduction of interference imposed by the radiation patterns of other users into the direction of the desired user. Considering ΔP_{TX_i} as the variation of radiated power to serve user i, compared to the reference antenna, the power that is radiated by adaptive antennas (**B**eam**f**orming), $P_{TX_i}^{BF}$, is obtained by:

$$P_{TX_i}^{BF} = \frac{1}{\Delta P_{TX_i}} P_{TX_i} \tag{3.12}$$

P_{TX_i} is the radiated power to serve user i with the reference antenna, which means that it is the reference value for the performance achieved by beamforming when just user i is considered.

The variation of the radiated power to serve user i, compared to the reference antenna, ΔP_{TX_i}, is obtained by:

$$\Delta P_{TX_i} = \frac{g_i(\theta_i)}{g_{ref}(\theta_i)} + \frac{1}{P_{TX_i}} \sum_{n \neq i}^{N_u} \left[\frac{g_n(\theta_i)}{g_{ref}(\theta_i)} \cdot \left(\frac{g_n(\theta_n)}{g_{ref}(\theta_n)} \cdot P_{TX_n} \right) \right] \tag{3.13}$$

The first term of (3.13) represents the improvement in signal's power, achieved by the increasing of gain into the direction of the desired user, while the second term is the improvement achieved by interference suppression when power control is considered.

The total power spent for adaptive antennas (and consequently adapted radiation patterns) is given by the sum of all radiated powers to serve all users:

$$P_{TX_{total}}^{BF} = \sum_{i=1}^{N_u} P_{TX_i}^{BF} \tag{3.14}$$

The total performance of adaptive antennas is measured in the volume of radiated power that is reduced, compared to the amount of power spent by the reference antenna:

$$\Delta P_{TX_{total}} = \frac{P_{TX_{total}}^{BF}}{P_{TX_{total}}} \tag{3.15}$$

where $P_{TX_{total}}$ is the total power from the reference antenna, given by:

$$P_{TX_{total}} = \sum_{i=1}^{N_u} P_{TX_n} \tag{3.16}$$

Finally, the performance achieved by adaptive antennas is presented in dB. Just for convenience, when the variation is really a reduction, this metric assumes a positive value, while when the variation represents an increment of the total power transmitted, it assumes a negative one, (3.17).

$$\Delta P_{TX_{total}[\mathrm{dB}]} = 10 \cdot \log_{10}\left(\Delta P_{TX_{total}}{}^{-1}\right) \tag{3.17}$$

Figure 3.3 shows the physical meaning of the metric's parameters when two users are in the cell. The ideal radiation pattern that ordinary static sector antennas present is shown in green.

3.3 Multi user model for LTE

The model developed for LTE is similar to the one for UMTS, differing just on the aspects related to the multiple access technique. First of all, in terms of interference, LTE is more sensitive to interfering users, since the system is based on frequency division, where there is no processing gain to perceive the desired signal stronger than an interfering signal in the same propagation conditions. However, LTE was designed to avoid co-channel interference, allowing just a fraction of interfering power in the total received signal. This awareness for co-channel interference is seen by the absence of users operating in the same sub-carrier frequency within the same cell, at the same time. This means that interference comes from neighbouring cells, where it is allowed for some users to use the same sub-carrier frequency that is being used by the reference user. The adaptive antenna performance is measured in a single cell. The user that is at the cell of interest is the desired user and the users at adjacent cells are interferers, non-desired users for the BS of interest.

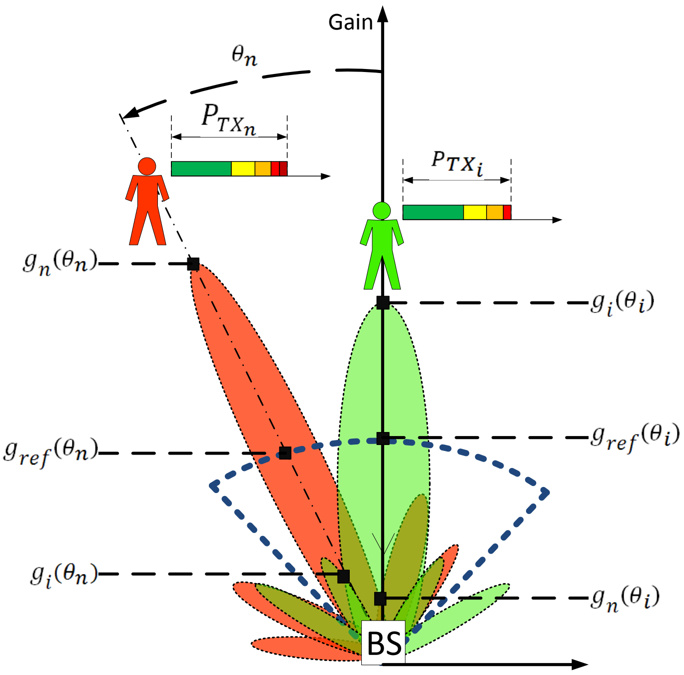

Figure 3.3: Parameters in users' radiation patterns.

The process of antenna weighting is the same that is used for UMTS, being based on an UL control channel. When communication starts, the desired user requests a service to the BS through an UL control channel. u_{du} is the signal sent by the desired user (see Section 3.2.1 for details about u_{du}) and it is used to weight individually each element of the antenna array. At the BS adaptive antenna array, the signal is affected by the signals that are being transmitted by the non-desired users, which are also performing some service in the same sub-carrier frequency. By predicting the content of the desired signal, the algorithm weights individually each antenna element in amplitude and phase, and it tries, as much as possible, to recover a replica of the desired signal from the actual received signal.

From the stage where the location of all intervening users is known, the path loss for all users is determine by (3.1), where R_i is the distance between the BS of interest (cell number 1) and the user in cell i. Once again, the path-loss model is set to dense urban, suburban and rural.

With the prediction of the desired signal, by weighting individually each antenna array element, it is possible to suppress some of the interference introduced by non-desired users. The objective is to focus the main antenna lobe into the direction of the desired user, and to null the direction of interferers. The recovered signal, $y_{LTE}(t)$, is obtained by the Simple Matrix Inverstion algorithm and derives from the UMTS situation by suppressing the processing gain that does not exist in LTE.

$$y_{LTE}(t) = \frac{u_{du}(t)}{L_{p_{du}}} \cdot \sum_{m=1}^{N_a} w_m \cdot e^{j\frac{2\pi}{\lambda}d(m-1)\sin(\theta)} + \sum_{i=2}^{N_u} \sum_{m=1}^{N_a} \frac{u_i(t)}{L_{p_i}} \cdot w_m \cdot e^{j\frac{2\pi}{\lambda}d(m-1)\sin(\theta_i)} \quad (3.18)$$

For the BS of interest, just the desired user is being served, unlike UMTS, where all users are considered as desired and non-desired at a certain moment. In this way, no more users are considered to be desired users in the next steps. The adaptive antenna only needs to generate one radiation pattern, to serve the desired user. After determination of the antenna gain, $g(\theta)$, (3.10) and (3.11), the performance of the adaptive antenna is evaluated through the signal's power improvement, referred to the reference antenna.

LTE uses the same metric of UMTS for the performance achieved by the adaptive antennas. ΔP_{TX_i} is the variation of radiated power to serve the desired user, which is the carrier improvement in comparison to the reference static antenna:

$$\Delta P_{TX_{du}} = \frac{g_{du}(\theta_{du})}{g_{ref}(\theta_{du})} \quad (3.19)$$

where $g_{du}(\theta_{du})$ is the adaptive antenna gain in the direction of the desired user.

Since there is no other user being served at the cell where the measure is taking place, the variation of the radiated power to serve the only desired user is directly the reduction of power:

$$\Delta P_{TX_{total}[\mathrm{dB}]} = 10 \cdot \log_{10}\left(\Delta P_{TX_{du}}{}^{-1}\right) \quad (3.20)$$

Again, when the variation is really a reduction, the metric assumes a positive value, while when the variation represents an increment on the total radiated power, it assumes a negative one.

3.4 Implementation into a simulator

3.4.1 General structure

The model was implemented in two distinct simulators, one to simulate UMTS, and the other LTE. Although there is resemblance between both simulators, different users' arrangement and different multiple access techniques are enough to justify this organisational split of simulators. LTE's implementation is addressed relatively to UMTS' one, with special emphasis in the differences between both systems. All simulators and auxiliary routines were programed into Matworks™ Matlab®.

Following the same structure presented in the model description, the simulator implemented for both UMTS and LTE, follows the general structure that is shown Figure 3.4.

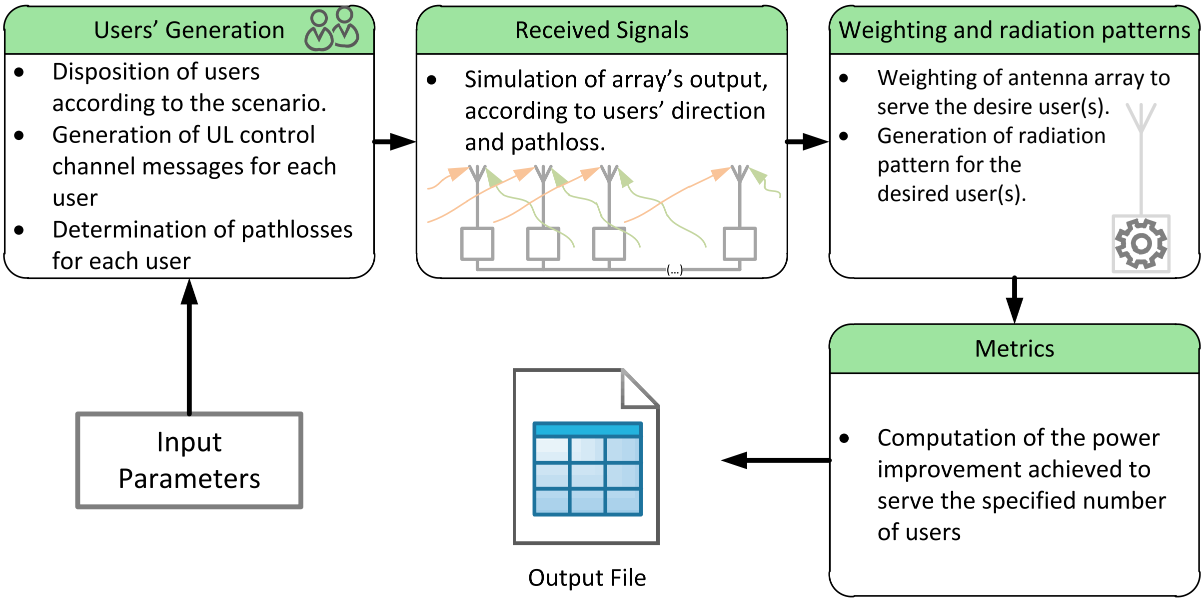

Figure 3.4: General structure of the simulator.

Figure 3.4 represents the main functions that are performed by the simulator. The way those functions are implemented is the subject of the following sections.

The functions to generate users comprise aspects related to their positioning, their UL messages, and the propagation of their signals, namely path-loss. In the Received Signals area, aspects about the reception of signals and the way how an antenna array receives a signal is addressed. Weighting and radiation patterns generation are responsible for correctly set the antenna array according to user's position, as well as for generate the correspondent radiation pattern, to be assessed in Metrics.

3.4.2 UMTS implementation

One of the objectives of this work is to perform simulations with statistical relevance. This means one needs to assume statistical distributions for parameters that are random. When no restrictions on users location are considered (in the situation where a general scenario estimation is wanted), users' positioning is a process that uniformly places each user within the sector covered by the reference antenna. The first step of user's generation is the attribution of an angle, within a sector, which is performed by:

$$\alpha_i = unifrn[0, 120]; \tag{3.21}$$

where $unifrn[0, 120]$ is a function that returns a random value between 0 and 120 according to a uniform distribution. Then, with the user's direction angle, his distance is given between a minimum of 20 m and a maximum of the cell radius:

$$R_{i[\text{km}]} = unifrn\left[0.02, r_{cell[\text{km}]}\right]; \tag{3.22}$$

In the scenario description, several specific scenarios are address in terms of the allowed positions where users are able to be placed. The only difference between the positioning of users in a general scenario and positioning in specific scenarios is the area where users are placed. For general scenarios, users are able to be placed uniformly in the area of the sector reference antenna, while for specific scenarios, users are free to be placed uniformly in the areas that constitute the scenario (a passengers' platform for train stations coverage, for example).

The UL control channel, which is used to weight the antenna elements, has its own pre-set messages, which allows BSs to have some knowledge about users. For simulation purposes, there is no need to implement real UL control messages, since they are closely related to the type of service the user wants to access. The property that the UL control messages needs to have is to be as much as possible uncorrelated to the messages of another user. This property was implemented by generating random discrete signals, with so many samples as those that will be used in the antenna weighting process. So, the simulated UL control channel message of user i, u_i, is generated according to the following random function:

$$u_i(t_n) = \sin\big(unifrn(0, 2\pi, 1, n_{samples})\big)\,; \tag{3.23}$$

Also in users' generation, the propagation path-loss between users and BS is computed through the path-loss model present in Section 3.2.1.

With the response of each antenna element to the signals coming from all users (an element based from the steering vector for each user), the simulator can generate what would be the received signal of each element of the antenna, introducing CDMA's processing gain that makes the signal of the desired user be perceived stronger that non-desired signals, Figure 3.5. The combined signal received by the antenna array, y, is the sum of the signals received by each element of the antenna, Figure 3.6.

Figure 3.7 and figure 3.8 represent, respectively, the algorithm for optimum antenna weighting (for all users) and the generation of individual radiation patterns for all users.

Figure 3.9 represents the flowchart of the functions included into the "user's generation" function. As inputs, just the number of users is mandatory. The system's frequency is assumed to be a parameter set by programmer according to the frequency plan of the country where the system is implemented.

Figure 3.10 represents the flowchart of the processes performed to obtain the total output of the unweighted antenna array, when the contributions of all users' signals that are being served into the cell are considered.

Since one has the signal received by the unweighted antenna array when all users are sending some message, one can apply the algorithm to weight the elements of the antenna and try to recover the original signal that is sent by the desired user. The algorithm to weight the array is the SMI algorithm. Based on (3.9), the algorithm is implemented as described by:

$$\boldsymbol{w}(i) = inv(y^T \cdot y) \cdot y^T \cdot u_i \tag{3.24}$$

where:

- $\boldsymbol{w}(i)$ is the array of the weight for the elements of the antenna, $(1 \times N_a)$, with N_a elements in the array.

$$
\begin{aligned}
&for\ n = 1{:}\,N_u\\
&\quad for\ m = 1{:}\,N_a\\
&\quad\quad for\ i = 1{:}\,N_u\\
&\quad\quad\quad if\ i = n\\
&\quad\quad\quad\quad x(m,i) = x(m,i) + u_i \frac{G_p}{PL_i}\ a(i,m)\\
&\quad\quad\quad else\\
&\quad\quad\quad\quad x(m,i) = x(m,i) + \frac{u_i}{PL_i}\ a(i,m)\\
&\quad\quad\quad end\\
&\quad\quad end\\
&\quad end\\
&end
\end{aligned}
$$

Figure 3.5: Routine for compute the received signal of each element of the antenna.

$$
\begin{aligned}
&for\ m = 1{:}\,N_a\\
&\quad y = y + x(m)\\
&end
\end{aligned}
$$

Figure 3.6: Routine that computes the total array's output, before beamforming.

The algorithm described in (3.9) and implemented by the routine of Figure 3.5 is repeated for every user, in order to generate individual weights for elements that achieve the best signal-to-interference ratio for all users:

$$
\begin{aligned}
&for\ i = 1{:}\,N_u\\
&\quad \boldsymbol{w}(i) = inv(y^T \cdot y) \cdot y^T \cdot u_i\\
&end
\end{aligned}
$$

Figure 3.7: Algorithm for optimum antenna weighting, for all users.

The next step comprises the generation of all radiation patterns, one for each user, confined to 180º, Figure 3.8. With radiation patterns generated for all active users, the proposed metrics are assessed in order to evaluate the performance of the adaptive antenna in the situation of analysis. Due to the resemblance of the simulation assessment to the metric's presented in Section 3.2.4, the implementation was suppressed.

$$
\begin{aligned}
&for\ i = 1{:}\,N_u\\
&\quad for\ \theta = 0{:}\,\pi/180{:}\,\pi(1 - 1/180)\\
&\quad\quad g(i,\theta) = \boldsymbol{w}(i) \cdot \exp(-j\pi \cdot [\mathbf{0}{:}\,\boldsymbol{N_a} - \mathbf{1}]^T * \sin(\theta))\\
&\quad\quad \theta = \theta + 1\\
&\quad end\\
&\quad g(i,\theta) = \frac{g(i,\theta)}{\max(g(i,\theta))}\\
&end
\end{aligned}
$$

Figure 3.8: Generation of individual radiation patterns for all users.

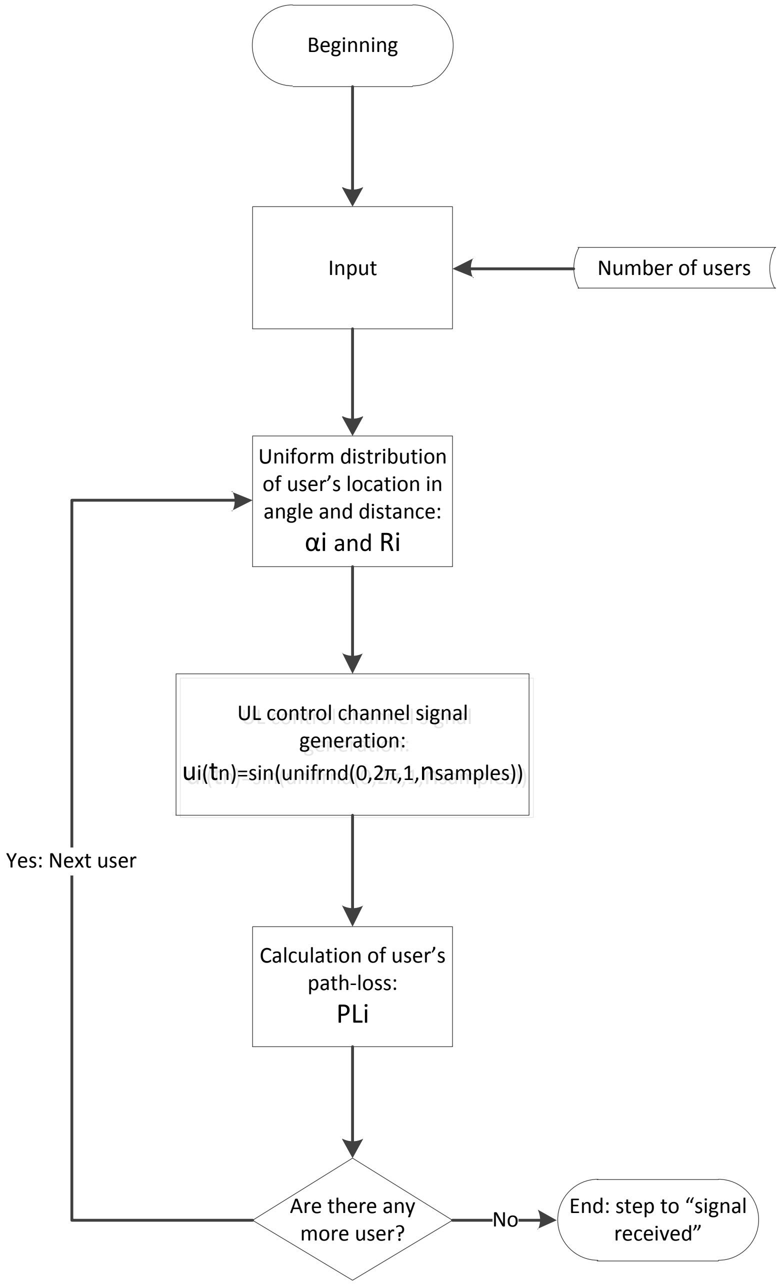

Figure 3.9: Flowchart for users' generation.

3.4.3 LTE implementation

The LTE simulator differs from the UMTS one mainly on the generation of users, and in the CDMA's processing gain that does not exist in LTE. The first main difference between LTE and UMTS simulators is the number of users and the locations where they are allowed to be place. As described in the model, in LTE only one user per cell can be using the same sub-carrier frequency. The way how users' locations are referred in the simulator is the same as in UMTS, with an angle and a distance from the BS generated according to a uniform distribution, hence, not be presented again.

With all users placed, one at each cell, all of them send an UL control channel message that is generated like in UMTS, u_i, (3.23). The determination of the received signal at the antenna array follows the same steps presented in Figure 3.10, which are implemented through the instructions in Figure 3.11.

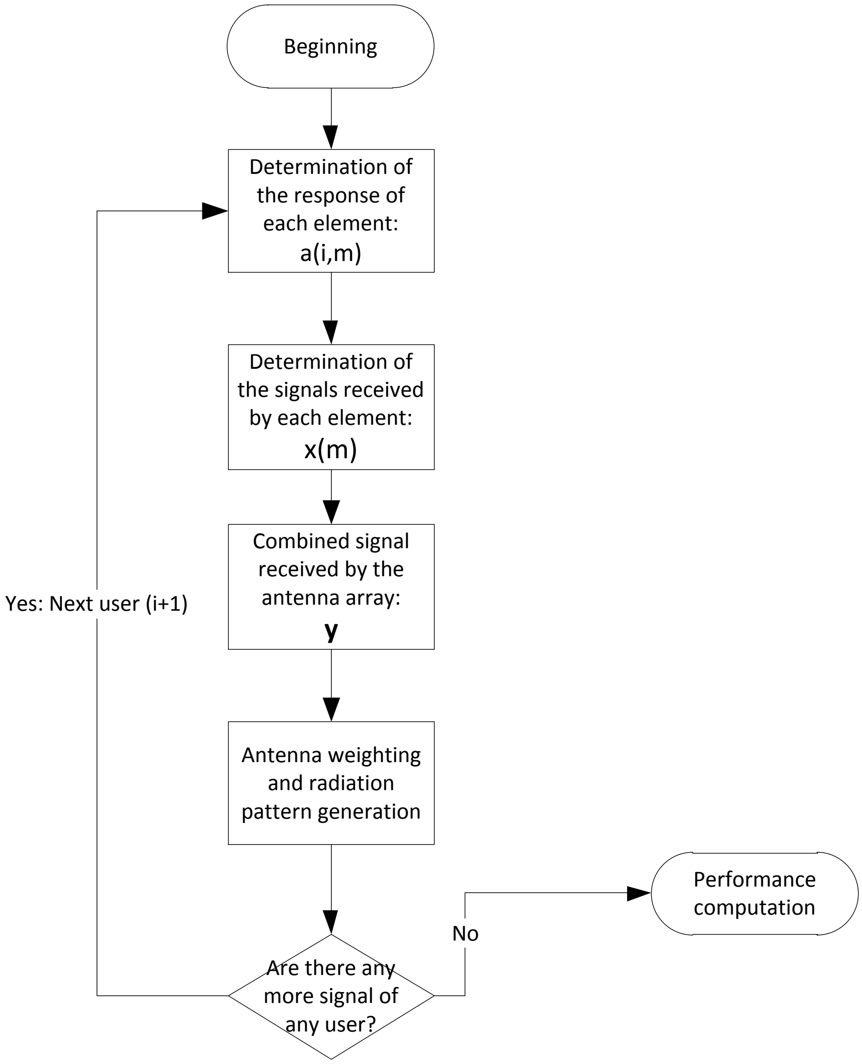

Figure 3.10: Flowchart for determination of combined received signal.

The received signal follows the same process presented in Figure 3.5, while the algorithm for the antenna weighting remains also the same as presented in UMTS, (3.24).

$for\ m = 1{:}\,N_a$

$\quad for\ i = 1{:}\,N_u$

$$x(m,i) = x(m,i) + \frac{u_i}{PL_i}\, a(i,m)$$

$\quad end$

end

Figure 3.11: Routine for determination of the received signal at the antenna array, LTE.

For LTE, the adaptive antenna only generates one radiation pattern to serve the only user placed in the evaluated cell, the desired one. The element weighting processes, as well as the radiation pattern generation, once again, are the same as those used in UMTS that compute the SMI algorithm.

The metrics assessment is similar to UMTS, with performance measured in terms of the amount of power that is possible to reduce by adaptive antennas.

3.5 Input and Output Parameters

The computational routines that were programed to evaluate the performance of adaptive antennas in terms of energy efficiency simulate the radio link between users and BSs. In this way, several parameters can be changed in order to simulate some other system that works with the same radio interface than the ones that were implemented, namely CDMA for UMTS and OFDMA for LTE. No matter what kind of simulation is being performed, the following parameters need always to be specified:

- N_a: number of elements that constitute the adaptive antenna array.
- $d_{[\mathrm{m}]}$: spacing between elements in the antenna array, which is set to half wavelength by default.
- N_u: number of users that will be considered in the actual simulation.
- $f_{[\mathrm{MHz}]}$: frequency where the system is operating, 2100 MHz for UMTS and 1800 MHz for LTE.
- $R_{b_{[\mathrm{Mbps}]}}$: bit rate required by users, with impact on the processing gain for UMTS.
- $Scenario$: scenario where the cell is inserted, which is crucial, since it introduces different propagation effects that are translated through different path-loss models.
- n_sim: number of simulations that will be performed to establish an average value as well as a standard deviation.

For the simulations that do not cover any specific scenario, the amount of users that was specified is placed uniformly across the area of the reference sector antenna. In these situations, also the typical cell radius for the bit rate that is being considered is also asked. Each user is uniquely invoked by his distance to the BS and by the angles from which he is seen at the BS. With all users' position known and referred by its distance and angle, the path-loss that each user's signal suffers in the propagation to the BS is computed according to the scenario, for the distance between the user and the BS.

From this stage, the simulator calculates what would be the output of an antenna array with N_a elements spaced by d and applies an algorithm to compute the optimum weights for each individual antenna element in order to recover the signal sent by the desired user that is affect by the remaining users. Since the optimum weights are available to serve all users, the simulator generates the radiation patterns that comprise the best signal improvement and interference suppression. One radiation pattern is generated for each user, and the power that is possible to be reduced is computed, due to the dedicated radiation pattern. All of these steps are detailed in Sections 3.2.2 and 3.2.3.

As output, the simulator gives the average power improvement that is reached when n_sim simulations are performed for an equivalent number of different users' locations, as well as the standard deviation within the power improvement can floats for the same number of simulations:

$$\Delta P_{TX_{total}[\text{dB}]} = \frac{1}{n\_sim} \sum_{i}^{n\_sim} \Delta P_{TX_{total}[\text{dB}]}{}^{i} \tag{3.25}$$

$$\sigma\left(\Delta P_{TX_{total}[\text{dB}]}\right) = \sqrt{\frac{1}{n\_sim} \sum_{i}^{n\_sim} \left(\Delta P_{TX_{total}[\text{dB}]}{}^{i} - \Delta P_{TX_{total}[\text{dB}]}\right)^{2}} \tag{3.26}$$

3.6 Simulator Assessment

The assessment of the simulator is a crucial step in order to perform simulations with confidence. The model developed and implemented in the simulator has its main function assigned for the antenna array weighting, which provides the best radiation pattern to ensure an improvement in the signal-to-interference ratio. The first assessment is the evaluation of antenna array weighting under some users' locations situation, where the behaviour of the radiation patterns can be expected. Due to the high amount of radiation patterns that are generated at each simulation, one radiation pattern for each user, in Annex A the entire set of radiation patterns can be found for the analysed situations.

The first situation where radiation patterns can be expect is when just one user is placed in the cell. With no constraints about interference, the adaptive antenna should generate a radiation pattern with a high gain lobe into the direction of the desired (and alone) user, Figure 3.12.

As expected, the radiation pattern directs a beam into the direction of the desired user and power reduction is achieved by the extra gain that the high gain beam provides, compared to the gain of the reference antenna.

Another situation where adaptive antennas should provide signal improvement and interference suppressing, as much as users' locations allow, is the situation with more antenna elements than users in the cell. When the desired user has no interferers with similar angles to the BS, the radiation patterns should direct a high gain beam into the desired user's direction and, at the same time, point low gain regions into the direction of interferers. Figure 3.13 shows a simulation run to served four users with adaptive antennas with eight elements.

As noticed before, the radiation pattern of Figure 3.13 presents a high gain lobe into the direction of the desired user, while into the direction of the three remaining interferers, the gain provided by the radiation pattern is very low. A couple of interferes are place into the same direction, seen from the BS and, it can be spotted in the radiation pattern, the gain provided to the direction of both interferers can be considered a null, since from the direction of those two interferers, the interference received is much stronger than any another.

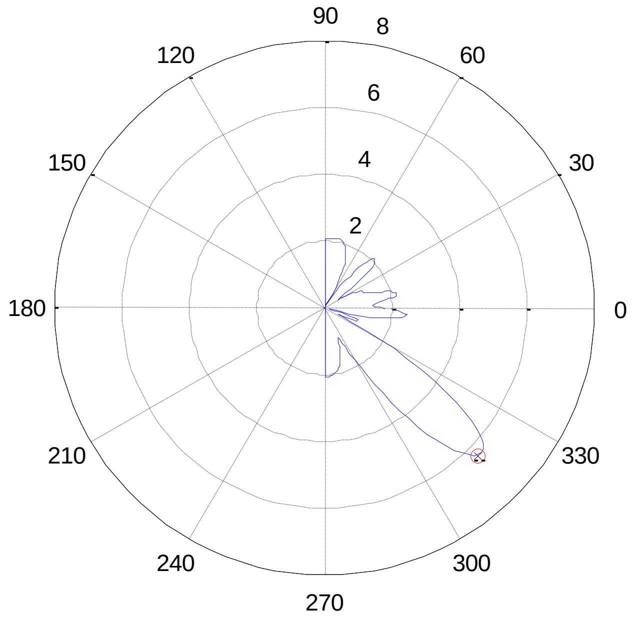

Figure 3.12: Radiation pattern for coverage of a single user in the cell (linear scale).

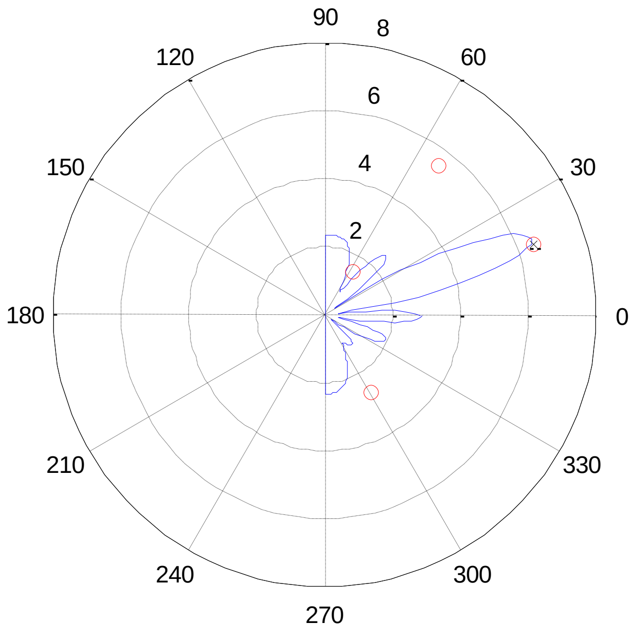

Figure 3.13: Radiation pattern to serve one desired user among three interferers, with antennas with eight elements (linear scale).

Even when there are more users than elements in the antenna, under some certain situations of users' alignment, the radiation patterns that are generated can be predicted. One of these situations is when users do not cause any overlapping effects in between each other, i.e., when there are no users into the same direction seen from the BS. Under this users' alignment, the adaptive antenna is the positions of high gain lobes into the direction of the desired user and, as much as possible, reduces the gain into the directions of all interferers. Figure 3.14 presents the radiation pattern that is generated to serve a desired user that has no interferer on the direction to the BS, when there are eight users to be served with an adaptive antenna with four elements.

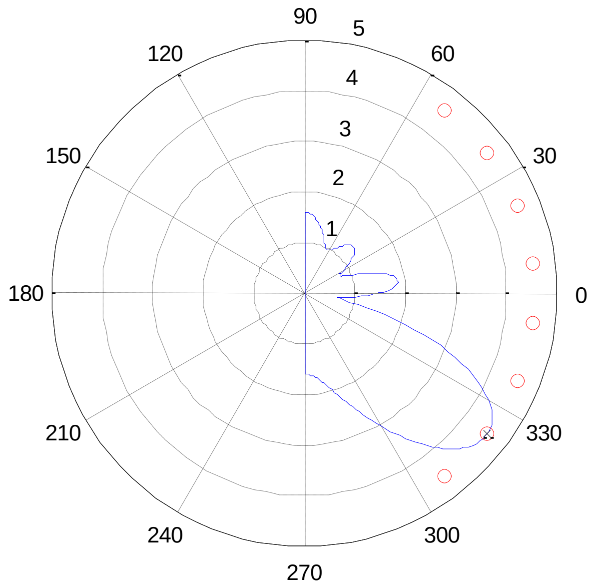

Figure 3.14: Radiation pattern to serve one desired user with antennas with four elements, when eight users are placed in the cell without overlapping.

Figure 3.14 presents the main beam into the direction of the desired user. The secondary lobes are positioned in order to radiate as lower as possible into the direction of the interferers, reducing interference from non-desired users. Due to the limitation on beamwidth reduction that comes from the fact that antennas with just four elements are being used, the gain into near users' directions cannot be reduced as desired, but, for users with enough angular separation, low gain regions of the radiation pattern are steered to reduce interference.

On real operation, users can be almost everywhere within the cell area. Overlapping effects happen producing interference constraints that cannot be solved. If an interfering user is placed in the same direction of the desired user, there is no other option but to focus the main beam into the direction of the desired user. Even in this situation, although it gets extra interference from the non-desired user that is on the same direction of the desired one, power improvement is achieved snce the signal of the desired user is improved by the positioning of the main beam and, at the same time, the remaining non-desired users that are located in outside the direction of the desired user are not covered with such a high gain as they would be if the reference static antenna was used. The final assessment that was made to evaluate the correct operation of the simulator was the simulation of serving random placed users within the cell. Figure 3.15 represents two examples of serving two different users in the same disposition for a total of 16 users in the cell, when antennas with eight elements are used.

Figure 3.15 shows for the desired user, the radiation patterns with their main beams steered to the direction of the desired user, even if in the same direction there are several other non-desired users that will suffer extra interference. Again in the same figure, the awareness for interference suppression for the direction of non-desired users is visible through the location of secondary lobes. Secondary lobes are, as much as possible, steered into the directions where there are not any non-desired users. When there are no free directions from non-desired users, the radiation pattern directs the secondary lobes always outside the direction of major groups of non-desired users or steers the secondary lobes into the direction of the non-desired user that will not suffer so much severely from interference caused by others, usually the farthest.

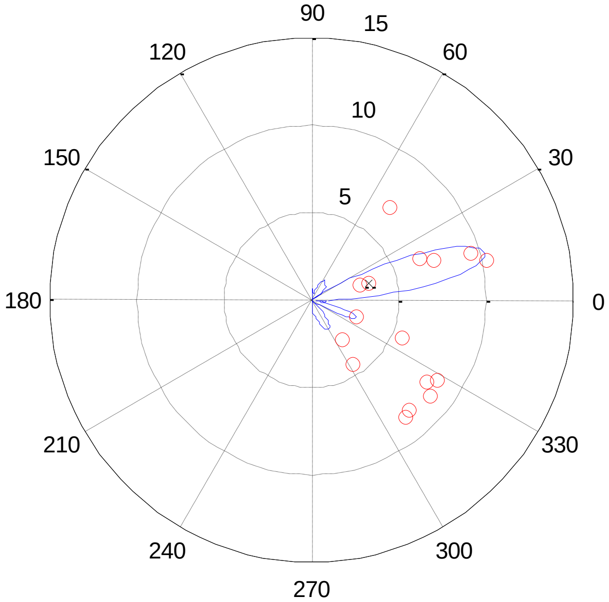

(a): Radiation pattern no. 1.

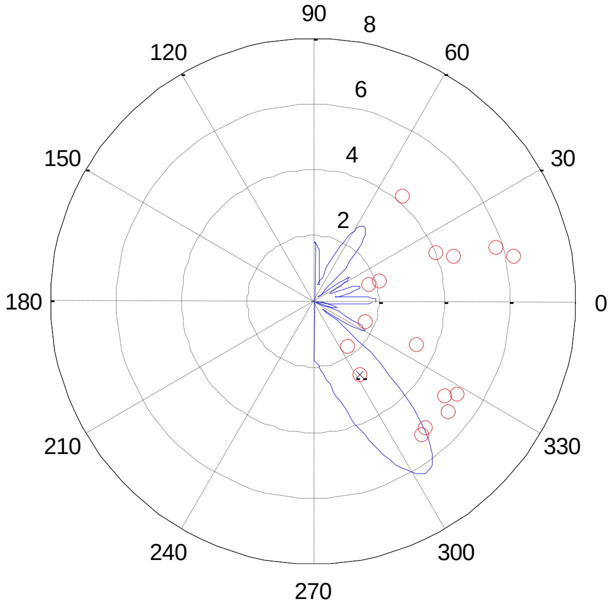

(b): Radiation pattern no. 2.

Figure 3.15: Radiation patterns of 2 users from 16 users in the cell, with antennas with 8 elements.

Chapter 4

Analysis of Results

Along this chapter, the enhancements of adaptive antennas in terms of power saving are evaluated over different perspectives. Once again, the results for UMTS and LTE are presented separately. In both systems, simulations were performed for scenarios where users are place randomly across the cells' area, in order to create a statistical base to validate specific scenarios with users place according to demographic aspects. For UMTS, several specific scenarios were simulated, representing everyday situations where the introduction of adaptive antennas can be advantageous for both users, which keep the same quality of service or benefit with better services, and operators that save energy providing best services for the same cost or providing the same services with less expenses.

4.1 Scenario description

Beamforming energy saving performance is evaluated for several scenarios with different number of users. In order to do this for UMTS, the first set of simulations were performed for general scenarios, where users are placed uniformly within the cell's sector area and there are no constraints on urbanistic or demographic issues, in order to assess the energy gain when the scenario is generically classified as dense urban, suburban or rural/high speed. In this way, it is possible to obtain an average and a standard deviation statistically relevant to represent the best and the worst scenarios that adaptive antennas can face. In Figure 4.1, the green area represents the places where users are allowed to be simultaneously for the generic scenario simulations, which corresponds to the area covered by an actual sector antenna.

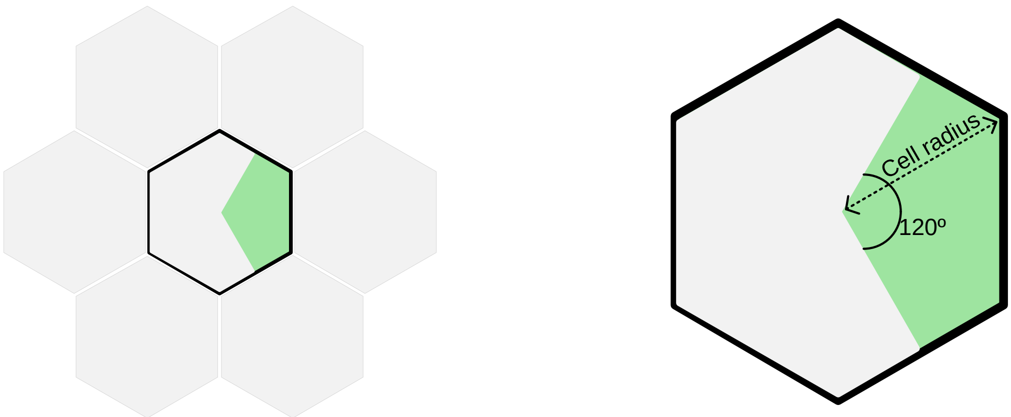

(a): Typical cell deployment. (b): Single cell.

Figure 4.1: Delimitation of the area where users are allowed to be placed to performance evaluation, corresponding to the coverage area of an actual sector, for UMTS.

Simulations for general scenarios are defined to evaluate the behaviour of power improvement when some parameters vary independently, i.e., number of antennas, cell's radius and number of users. Table 4.1 shows the set of simulations that was established; for each antenna configuration (four or eight elements), the three scenarios were simulated, each one tested for four cell's ranges, and each range was simulated from 10 to 70 users. Scenarios' ranges were defined as the most appropriated ones for the environment. Each combination of parameters was simulated in a total of 500 times, and their average and standard deviation were registered. With this simulation set, the objective is to derive a model that correlates power improvement with the parameters that are being changed.

Besides the general scenarios, specific ones were created for users' locations that correspond to everyday situations that can create challenges or provide high energy saving potential to adaptive antennas. These specific scenarios are based on observations of the location and direction of the BSs of one Portuguese mobile operator.

Table 4.1: Simulation set for general scenarios, UMTS.

<table>
<tr><th colspan="2"></th><th colspan="14">Antennas</th></tr>
<tr><th colspan="2"></th><th colspan="7">4 elements</th><th colspan="7">8 elements</th></tr>
<tr><th></th><th>Cell's Radius [km]</th><th colspan="7">Users</th><th colspan="7">Users</th></tr>
<tr><td rowspan="4">Dense urban</td><td>0.2</td><td rowspan="12">10</td><td rowspan="12">20</td><td rowspan="12">30</td><td rowspan="12">40</td><td rowspan="12">50</td><td rowspan="12">60</td><td rowspan="12">70</td><td rowspan="4"></td><td rowspan="4"></td><td rowspan="4"></td><td rowspan="4"></td><td rowspan="4"></td><td rowspan="4"></td><td rowspan="4"></td></tr>
<tr><td>0.4</td></tr>
<tr><td>0.6</td></tr>
<tr><td>0.8</td></tr>
<tr><td rowspan="4">Suburban</td><td>1.0</td><td rowspan="4">10</td><td rowspan="4">20</td><td rowspan="4">30</td><td rowspan="4">40</td><td rowspan="4">50</td><td rowspan="4">60</td><td rowspan="4">70</td></tr>
<tr><td>1.5</td></tr>
<tr><td>2.0</td></tr>
<tr><td>2.5</td></tr>
<tr><td rowspan="4">Rural/High Speed</td><td>3.0</td><td rowspan="4"></td><td rowspan="4"></td><td rowspan="4"></td><td rowspan="4"></td><td rowspan="4"></td><td rowspan="4"></td><td rowspan="4"></td></tr>
<tr><td>4.0</td></tr>
<tr><td>5.0</td></tr>
<tr><td>6.0</td></tr>
</table>

The first specific scenario that was simulated was the coverage of train stations. All train stations of the metropolitan region of Lisbon (Azambuja, Sintra, Cascais and Fertagus lines) were analysed relatively to the length of passengers' boarding platforms and the distance of the operator's nearest BS to the platform [CoPo11]. Fifty observations were done in order to be described by Probability Density Functions (PDF), according to the minimisation of the mean square error. Figure 4.2 represents the observations' distribution and the corresponding PDFs for length of passengers' boarding platforms and distance between the platform and operator's nearest BS.

Concerning the length of passengers' boarding platforms, they are described by a Normal Distribution, with mean value and standard deviation, respectively, of 0.213 km and 0.656 km. The most observed length was registered for values between 0.2 km and 0.25 km. The distance of operator's nearest BS to the passengers' platform is described by a Weibull Distribution, with parameters λ (scale) and k (shape), respectively, of 0.251 km and 0.0013 km. The Weibull Distribution interpolates between the exponential distribution, $k = 1$, and the Rayleigh distribution, $k = 2$.

Scenarios were set to dense urban and suburban. The decision for suburban scenario is made every time the distance is higher than 0.5 km, supported by the absence of train stations in dense urban environment farther than 0.5 km from BSs.

Simulations to train stations' coverage are set to the distance of the train station and its platform's length. For each simulation, a pair distance/length is generated accordingly to the PDFs that describe the observations. The relative position of passenger's platform, in green, is defined in Figure 4.3, which includes the distance to passenger's platform, platform's orientation to antenna (with maximum declination of 15º), angle of platform's head, as well as its length. Except for the distance and platform's length, all remaining orientation parameters are uniformly distributed in their domains.

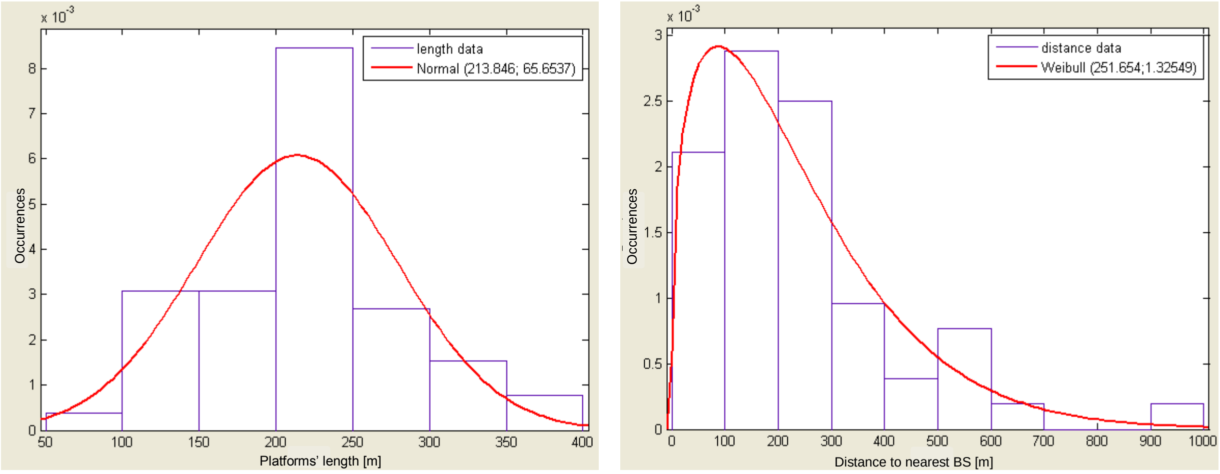

(a):Observations and PDF of length of passengers' boarding platforms.

(b): Observations and PDF of distance of the operator's nearest BS to the platform.

Figure 4.2: Observations' distributions and corresponding PDFs to train stations for the metropolitan region of Lisbon.

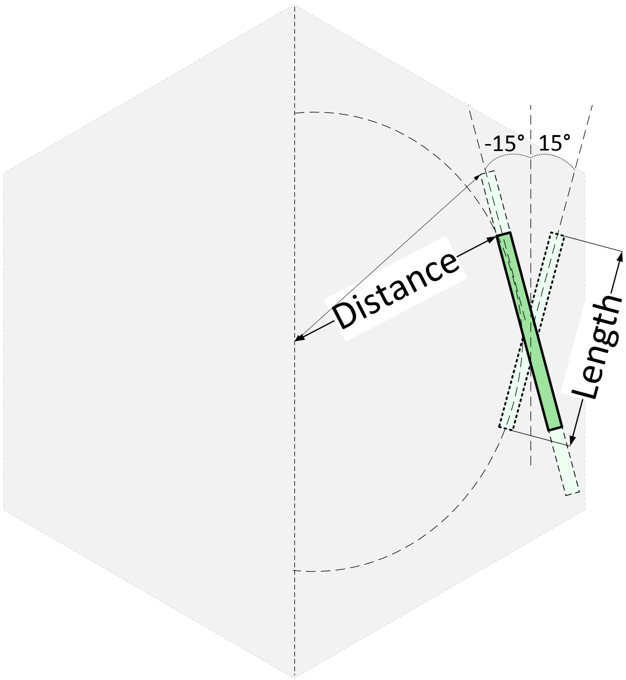

Figure 4.3: Relative position of passengers' platform and orientation parameters at cell, for coverage of train station, UMTS.

Following the same procedure, the coverage of highways represents also a specific scenario where the power improvement of adaptive antennas was simulated. Using the location of several BSs of the same Portuguese operator, fifty BSs located near main Portuguese highways were analysed relatively to their distance to the highway and their radius of coverage. Being in agreement with the traffic relevance of the observations as well as topographic relevance, Portuguese highways (A1) and (A2) are more represented in the observations. The remaining observations were obtained at Algarve's crossing highway (A22), Braga's highway (A3) and Beira Alta's highway (A24) [BrSA11]. The observations include plains (Alentejo), mountains (Beira Alta), and mixed environments. Figure 4.4

shows the observations' distribution and the corresponding PDFs that describe the population.

Concerning the radius of coverage of a BS that typically covers a section of a highway, they are around half the distance between the nearest BS that also covers another section of the highway. The radius can be described by a Weibull Distribution, with parameters λ (scale) and k (shape), respectively, of 2.262 km and 0.0013 km. The distance of the BS to the highway is described as a Lognormal Distribution, with mean value and standard deviation, respectively, of 0.0055 and 0.0014, most part of BSs are at the highway's side.

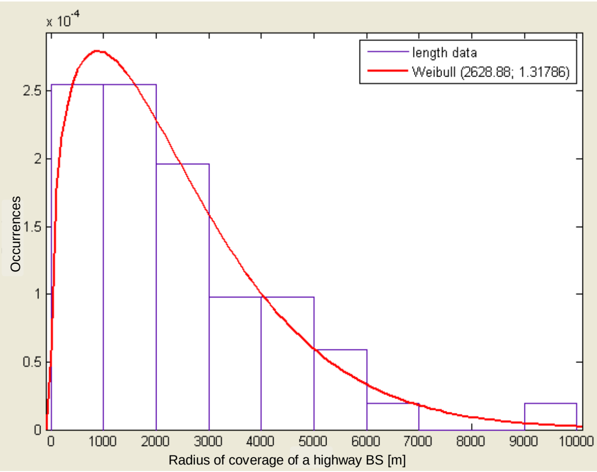

(a): Radius.

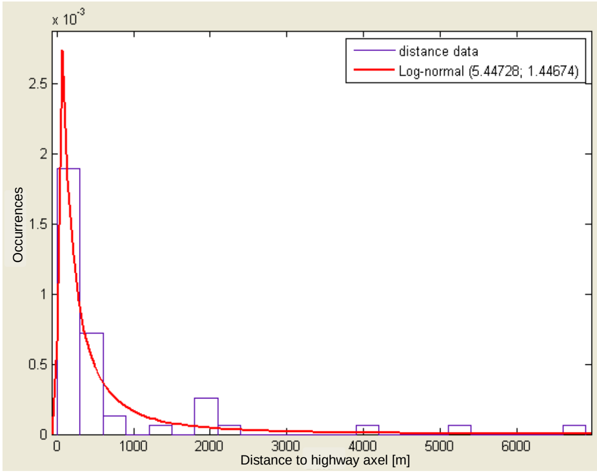

(b): Distance.

Figure 4.4: Observations' distributions and correspondent PDFs to highways' coverage for a representative population of the Portuguese highways, which includes cell's radius and distance of BS to highway.

Again, to allow a comparison with a general scenario, simulations for highways' coverage were performed for 10 to 70 users, with increments of 10. Figure 4.5 represents the orientation and relative position of BS in a highway's layout. To cope with the variations in the orientation that highway's sections can have to antenna's position, also a maximum declination of 15º is considered for the highway section's layout.

A third scenario was taken concerning the coverage of rural areas in UMTS. A rural BS frequently covers more than one village or small city. If a BS covers just one village or small city, the scenario should not be considered as rural, but rather urban BS or suburban, according to the type of buildings and traffic. The number of villages expected to be covered by the same BS was defined within the interval between 2 and 7, with the BS's radius of coverage uniformly distributed between 5 and 7 km, based on observations of the nearest villages of BSs in plain terrain (Alentejo) and mountain terrain (Minho and Trás-Os-Montes). Users are free to be located in any village and they are allowed to be within an area of 1 km^2 centred at the village's centre. The area of 1 km^2 was defined as being convenient to represent the majority of Portuguese rural populations. The number of users varied from 10 to 70, with increments of 10. Figure 4.6 shows the positioning of a hypothetical group of villages in the cell's area. In green, one represents the locations where users are allowed to be, which corresponds to the 1 km^2 typical populated area of rural villages. Usually, rural BSs are placed at the centre of a larger village or in its border, which is why Figure 4.6 presents also an hypothetical village in a BS's near location. For each run, the simulation of rural areas' coverage generates a number of villages to be served (between 2 and 7) and places their centres uniformly within the cell's half covered area (due to the 180º of antenna´s coverage). For the specified number of users, each user is placed in one of the covered villages within the 1 km^2 surrounding area, a process also uniformly distributed.

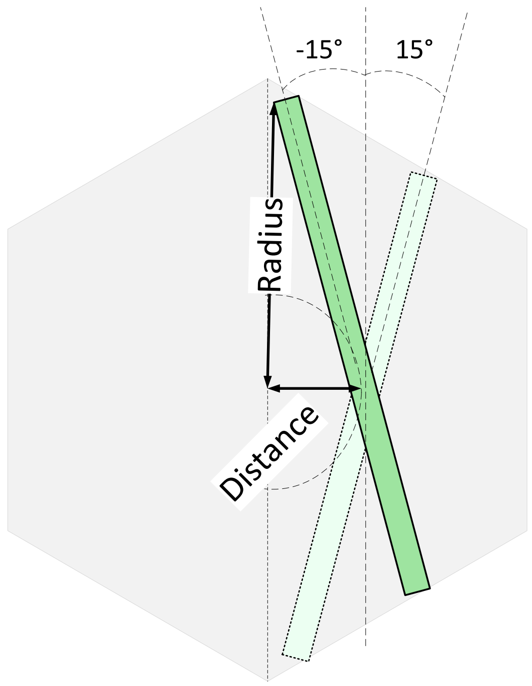

Figure 4.5: Relative position of highway's layout and orientation parameters at cell, for coverage of highway's sections, UMTS.

All the three specific scenarios evaluated for two antenna's configuration. Table 4.2 represents the set of simulations for specific scenarios.

Table 4.2: Set of simulations for specific scenarios' coverage in UMTS.

	Antennas													
	4 elements							8 elements						
	Users							Users						
Train Stations Highways Rural Areas	10	20	30	40	50	60	70	10	20	30	40	50	60	70

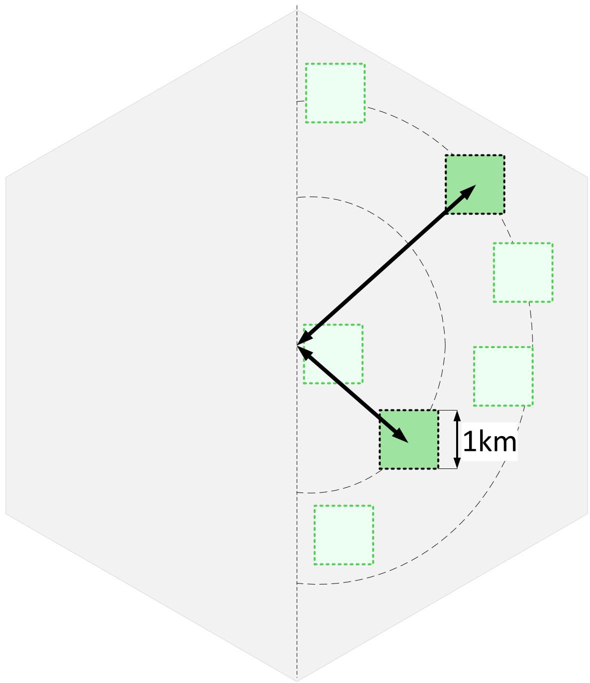

Figure 4.6: Relative position of villages' area where users are allowed to be in simulation for coverage of rural areas, for UMTS.

Concerning LTE, since it is an OFDMA system, where it is not allowed for different users operating at the same frequency at the same time, there is no intra-cell interference and all interference suffered by a user is originated in neighbouring cells. This aspect has impact on the performance in terms of energy efficiency. Within the same cell, just one user operates in some sub-carrier at a certain moment. The evaluation of power improvement when users describe some kind of special positioning (aligned into the train's passenger platform or within a section of highway) does not make sense. In LTE users that use the same sub-carrier frequency are physically apart. For this reason the evaluation of power improvement is presented just for the situations that are called in UMTS as general scenarios. No urbanistic or demographic constraints (like streets, plazas, highways or villages) are taken into account. As interfering cells, one considers those that constitute the first and second rings of a cellular deployment that are in front of the antennas radiating side. In LTE, energy saving comes from improvement of signal, which is obtained through the positioning of high gain lobes into the direction of the desired user. Interference that comes from neighbour BSs (only DL is under study) could have been evaluated, namely the reduction of interference, but the real mapping into energy saving would imply the adoption of adaptive antennas in all BSs, which is why the impact of adaptive antennas is only evaluated at the single cell domain. Figure 4.7 shows the scenario for users' location.

Cell 1 represents the cell where the performance of the adaptive antenna is tested, considering the user placed uniformly in the green area, which corresponds to the area covered by the reference sector antenna. Interferers are place in cells 2 to 9 uniformly, in light red. The maximum number of interferers is 8, but it is not mandatory to be always the maximum number of interferers.

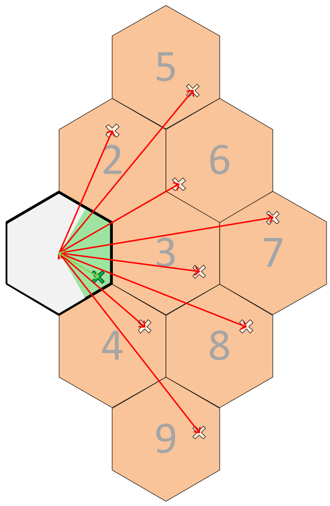

Figure 4.7: Location of desired user and interferes in the cell plan.

The same set of scenarios and cells' radius of UMTS was considered for LTE. Instead of considering a certain number of users, LTE simulations are performed for several numbers of interfering users in neighbouring cells. Table 4.3 presents the set of simulations that were adopted, all combination of ranges and interferers being considered for antennas with four and eight elements.

Table 4.3: Set of simulations for general scenario evaluation in LTE.

<table>
<tr><th></th><th></th><th colspan="18">Antennas</th></tr>
<tr><th></th><th></th><th colspan="9">4 elements</th><th colspan="9">8 elements</th></tr>
<tr><th></th><th>Cell's Radius [km]</th><th colspan="9">Interferers</th><th colspan="9">Interferers</th></tr>
<tr><td rowspan="4">Dense urban</td><td>0.2</td><td rowspan="12">0</td><td rowspan="12">1</td><td rowspan="12">2</td><td rowspan="12">3</td><td rowspan="12">4</td><td rowspan="12">5</td><td rowspan="12">6</td><td rowspan="12">7</td><td rowspan="12">8</td><td rowspan="12">0</td><td rowspan="12">1</td><td rowspan="12">2</td><td rowspan="12">3</td><td rowspan="12">4</td><td rowspan="12">5</td><td rowspan="12">6</td><td rowspan="12">7</td><td rowspan="12">8</td></tr>
<tr><td>0.4</td></tr>
<tr><td>0.6</td></tr>
<tr><td>0.8</td></tr>
<tr><td rowspan="4">Suburban</td><td>1.0</td></tr>
<tr><td>1.5</td></tr>
<tr><td>2.0</td></tr>
<tr><td>2.5</td></tr>
<tr><td rowspan="4">Rural/High Speed</td><td>3.0</td></tr>
<tr><td>4.0</td></tr>
<tr><td>5.0</td></tr>
<tr><td>6.0</td></tr>
</table>

4.2 UMTS

The first step to evaluate the performance of adaptive antennas in UMTS is the general scenario simulation. No urbanistic or demographic constraints (like streets, plazas, highways or villages) are taken into account, and it is allowed for users to be at any location. With this approach, the objective is to create general performance estimation when the classification of the area where the adaptive antennas will be installed is not possible, or when the BS is not designed to serve just one type of traffic (for example, offices' coverage by day and shopping centre's by night). Several scenarios have traffic enough to justify a dedicated BS. Major transport stations or main roads to city centres create enough traffic to be assigned a dedicated BS. For this reason, a second approach on the adaptive antennas takes place within specific scenarios, in order to have a better idea of the general scenario performance.

4.2.1 Performance for general scenarios

The first analysis was done on the evolution of adaptive antennas' performance as a function of cell's radius. The increment of the cell's radius should not assume a key role in the performances' evolution, since UMTS has power control, which brings the same quality of service for all users, no matter if they are at the cell centre or at its edge. In Figure 4.8, one presents the evolution of the power improvement, according to Section 3.2.4, (3.17), as a function of the cell's radius. The number of served serve is kept constant.

As Figure 4.8 shows, the variation of average power improvement is accommodated into an interval of 1 dB. In the transitions between scenarios (dense urban to suburban, and then to rural/high speed), the variation is more visible, mainly due to the change of LoS probability. With less users in LoS, the BS needs to radiate more power, which introduces a slightly increase of interference and originates the decrease of beamforming's power improvement. The behaviour that is seen for 20 and 30 users, either with four or eight elements in antennas, is noted for all number of users that were simulated, hence not being presented here. The evolution of power improvement as a function of cell's radius can be seen in the Annex B. Attention must be given to the value of the standard deviation. The resemblance of standard deviations in between all cell's radius, around 2 dB, supports the idea that the power improvement of adaptive antennas is constant as a function of cell's radius. With similar averages and standard deviations for different cells' radius, the variation of the cells' radius does not impact significantly in the performance of adaptive antennas.

Generally, the telecommunication industry resists to changes unless they effectively create added value for their business. It is not common to see an operator introducing a new component in its network with, for example, 10% of efficiency compared with the former version, unless the component that is being replaced is damaged. The threshold for new technology is set to at least 50% of efficiency. Analysing Figure 4.8, even in the worst case of performance for four elements in the antennas, the amount of power that is predicted to be save is above 4 dB, which corresponds to 60% of energy saved at all antenna elements, therefore, adaptive antennas have enough energy saving potential to be considered as an effective improvement to be added in operators' networks.

The interference suffered by a user depends on the number of other users that are active within the same cell. To overcome the increment of interference caused by the increment of users, with static antennas (the same radiation pattern for all users) the solution is to increase the signal's power of each user to keep the Signal-to-Interference ratio untouched.

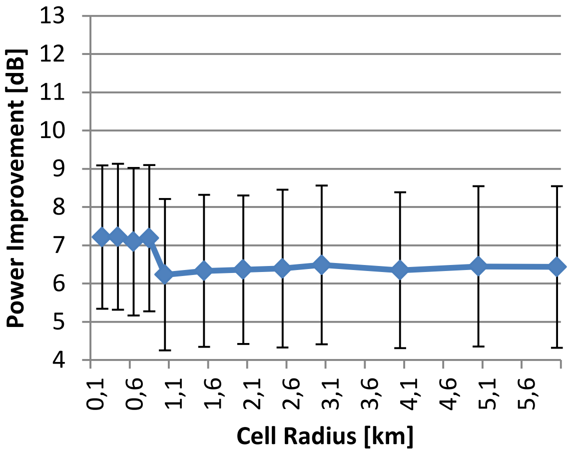

(a): 20 users, antenna with 4 elements.

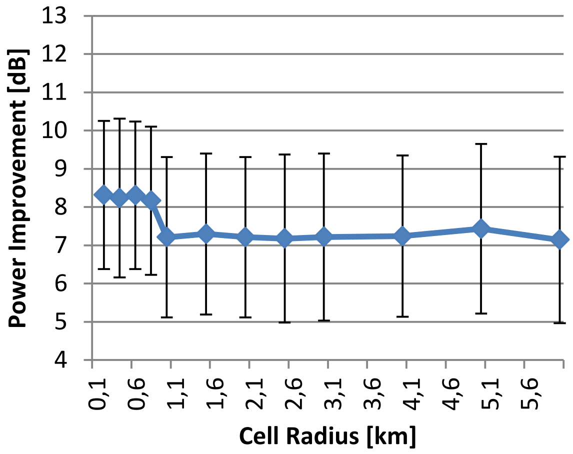

(b): 30 users, antenna with 4 elements.

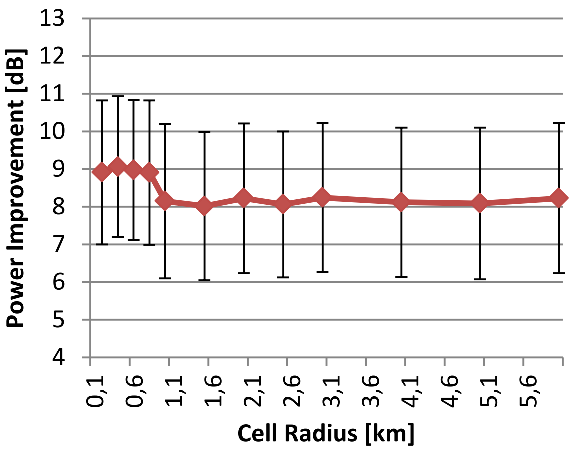

(c): 20 users, antenna with 8 elements.

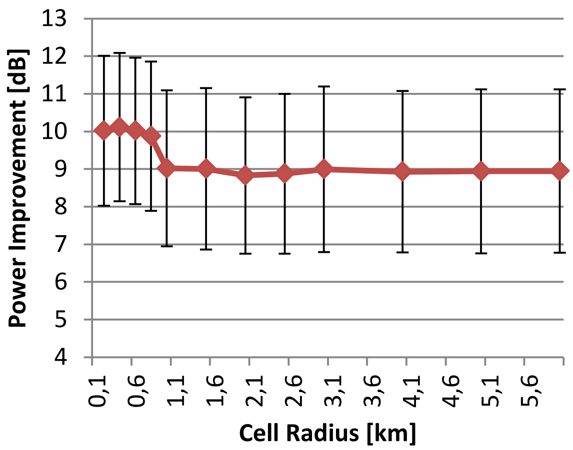

(d): 30 users, antenna with 8 elements.

Figure 4.8: Variation of power improvement when cell's radius vary, for UMTS.

Adaptive antennas generate radiation patterns that try to focus the signal mainly into the direction of the desired user, contributing to reduce as much as possible its radiation into the direction of non-desired users. Reducing the interference, signal's radiated power can be reduced without Signal-to-Interference ratio degradation. With the increment of users within the same cell, potential harmful interference also rises, which becomes the perspective for energy saving higher. To evaluate the impact of the variation of users in the performance of adaptive antennas, Figure 4.9 shows the evolution of the power improvement when the number of users changes, for antennas with 4 and 8 elements.

The expected increase of power improvement as a function of the number of users within the same cell is seen in Figure 4.9. For all scenarios, when more users are active within the cell, more power the adaptive antenna is able to save, while the Signal-to-Interference ratio is kept. An interesting fact is the logarithmic behaviour of the power improvement as a function of the number of users. The coefficient correlation, R^2, rounds 100%, showing a very good fit of the power improvement to the model. Figure 4.10 combines the performance of adaptive antennas with four and eight elements to the logarithm fit, based on average values.

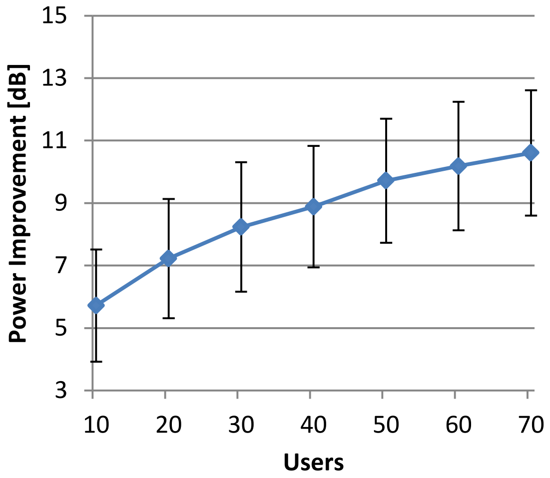

(a): Dense Urban (0.4 km radius), 4 elements.

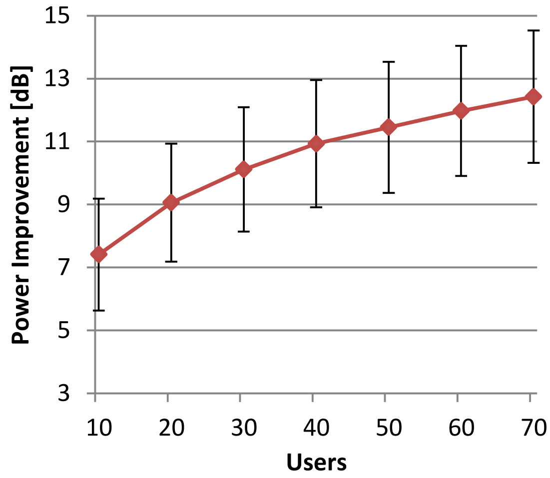

(b): Dense Urban (0.4 km radius), 8 elements.

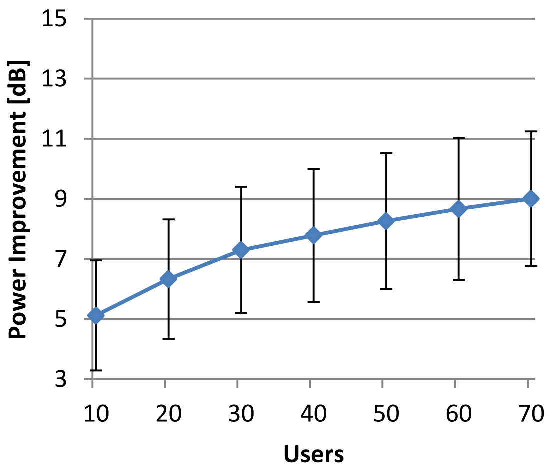

(c): Suburban (1.5 km radius), 4 elements.

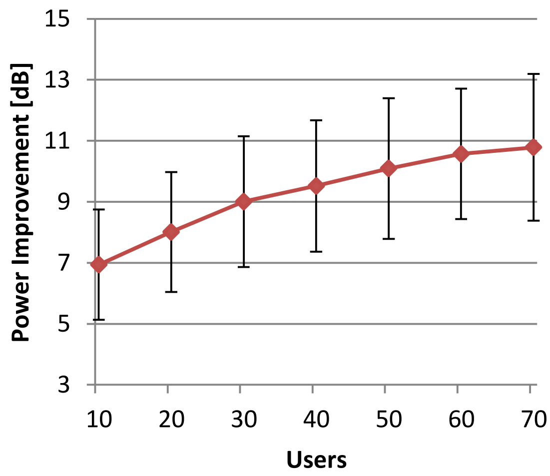

(d): Suburban (1.5 km radius), 8 elements.

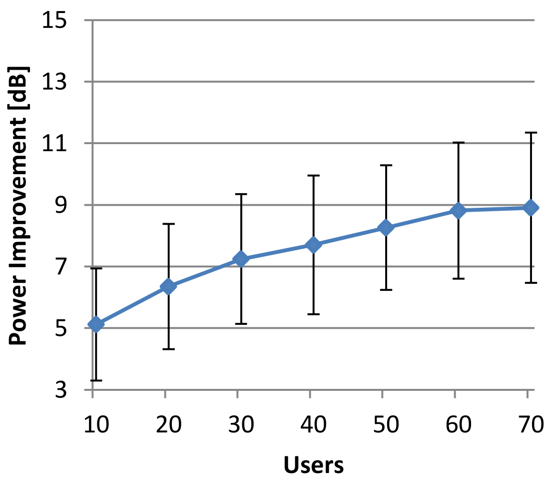

(e): Rural/High Speed (4 km radius), 4 elements.

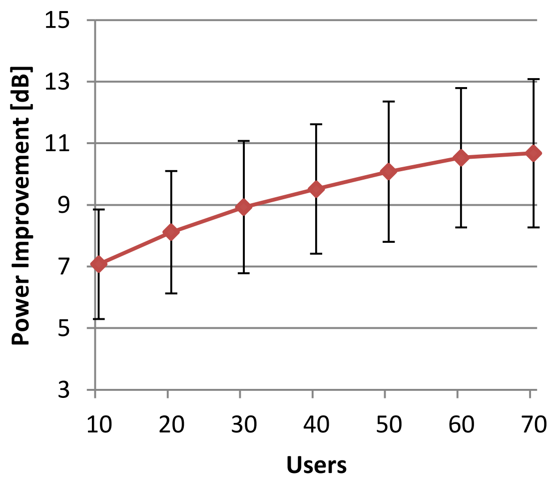

(f): Rural/High Speed (4 km radius), 8 elements.

Figure 4.9: Variation of power improvement when the number of users vary, for UMTS.

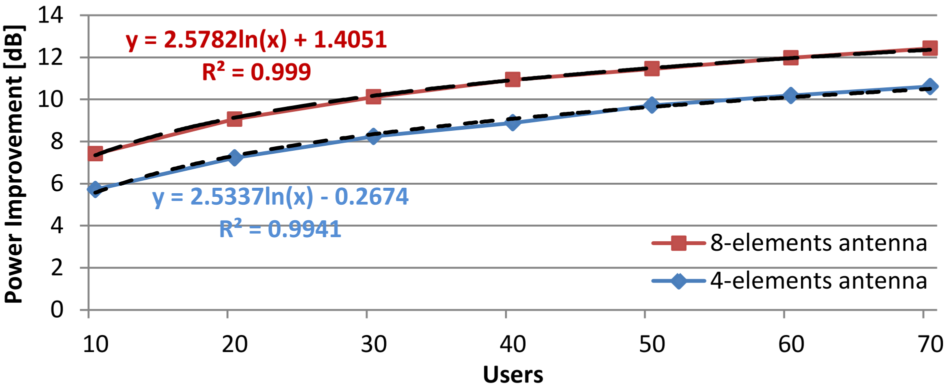

(a): Dense Urban scenario (0.4 km radius).

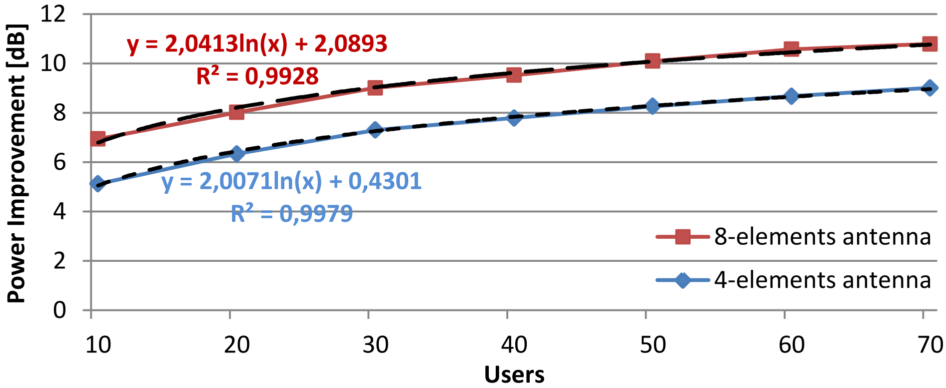

(b): Suburban scenario (1.5 km radius).

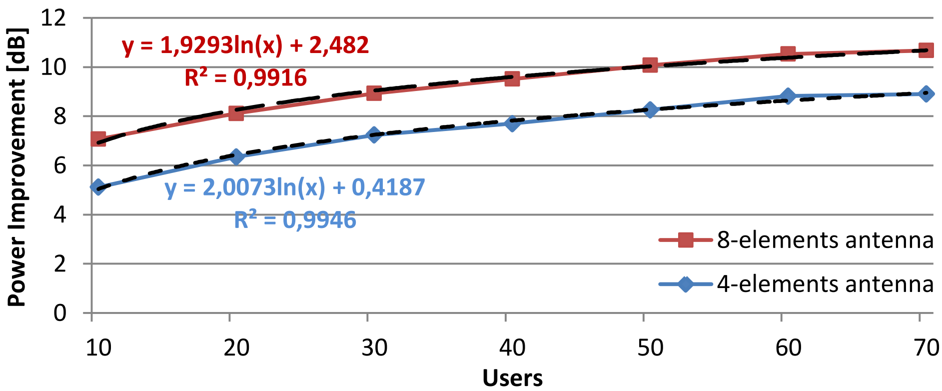

(c): Rural/High Speed scenario (4 km radius).

Figure 4.10: Power improvement and logarithmic fit, as a function of users' variation for UMTS.

Using the trend lines for all ranges within all scenarios (presented in Annex B), it is possible to derive a general logarithmic model, per scenario, by defining also a standard variation where the power improvement can float. Considering just the antennas with four elements, the general expression for the power improvement, $\Delta P_{TX_{total}}{}^{4\ elements}$, is given by:

$$\begin{aligned} \Delta P_{TX_{total}}{}^{4\ elements}{}_{[\mathrm{dB}]}(N_u) &= 2.20 \log_e(N_u) + 0.25 \\ \sigma^{4\ elements}{}_{[\mathrm{dB}]}(N_u) &= 0.25 \log_e(N_u) + 2.85 \end{aligned} \tag{4.1}$$

To confine the standard deviation, the logarithm model for power improvement can be derived by sections, each section representing one scenario::

$$\Delta P_{TX_{total}}{}^{4\ elements}{}_{[\mathrm{dB}]}(N_u) = \begin{cases} 2.50 \log_e(N_u) + 0.15 \text{ (dense urban)} \\ 2.05 \log_e(N_u) + 0.35 \text{ (suburban)} \\ 2.00 \log_e(N_u) + 0.55 \text{ (rural / high Speed)} \end{cases}$$

$$\sigma^{4\ elements}{}_{[\mathrm{dB}]}(N_u) = \begin{cases} \sigma_{[\mathrm{dB}]} = 0.20 \log_e(N_u) + 2.85 \text{ (dense urban)} \\ \sigma_{[\mathrm{dB}]} = 0.05 \log_e(N_u) + 2.55 \text{ (suburban)} \\ \sigma_{[\mathrm{dB}]} = 0.10 \log_e(N_u) + 2.65 \text{ (rural / high Speed)} \end{cases} \tag{4.2}$$

The same procedure was taken for antennas with eight elements:

$$\Delta P_{TX_{total}}{}^{8\ elements}{}_{[\mathrm{dB}]}(N_u) = 2.20 \log_e(N_u) + 2.00$$

$$\sigma^{8\ elements}{}_{[\mathrm{dB}]} = 0.30 \log_e(N_u) + 2.95 \tag{4.3}$$

$$\Delta P_{TX_{total}}{}^{8\ elements}{}_{[\mathrm{dB}]}(N_u) = \begin{cases} 2.65 \log_e(N_u) + 1.25 \text{ (dense urban)} \\ 2.00 \log_e(N_u) + 2.25 \text{ (suburban)} \\ 2.00 \log_e(N_u) + 2.35 \text{ (rural / high Speed)} \end{cases}$$

$$\sigma^{8\ elements}{}_{[\mathrm{dB}]}(N_u) = \begin{cases} 0.05 \log_e(N_u) + 2.25 \text{ (dense urban)} \\ 0.05 \log_e(N_u) + 2.60 \text{ (suburban)} \\ 0.05 \log_e(N_u) + 2.70 \text{ (rural / high Speed)} \end{cases} \tag{4.4}$$

Through (4.1) and (4.3), it is visible that the variation of power improvement between adaptive antennas with four and eight elements is constant, which enables the derivation of a general expression for power improvement as a function of the number of users, N_u, and number of elements of the antenna, N_a, with the standard deviation being given by the higher standard deviation observed in simulations, in between the four and eight elements situations:

$$\Delta P_{TX_{total[\mathrm{dB}]}}(N_u, N_a) = 2.20 \log_e(N_u) + 0.44 N_a - 1.75, (N_a \geq 4)$$

$$\sigma_{[\mathrm{dB}]}(N_u) = 0.30 \log_e(N_u) + 2.95 \tag{4.5}$$

4.2.2 Performance for specific scenarios

Concerning the train stations scenario, Figure 4.11 shows the power improvement, for antennas with four and eight elements.

The first aspect that stands out is the agreement with the logarithmic behaviour that is found for the general scenarios. Power improvement for both numbers of elements follows the same trend and, as expected, the antenna with eight elements comprises more power improvement than the one with four. The absolute value of the power improvement achieved on train stations' coverage is also higher than the general scenario, showing that the special alignment of users stations' platforms provides better angular separation.

Using the general scenario and the model derived in (4.5), the results for train stations are compared in order to determine if the standard deviation obtained for the general scenario estimation covers the magnitude of power improvement achieved for train stations, Figure 4.12.

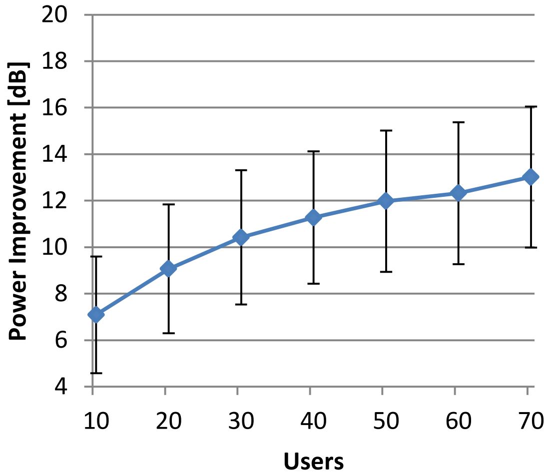

(a): 4 elements.

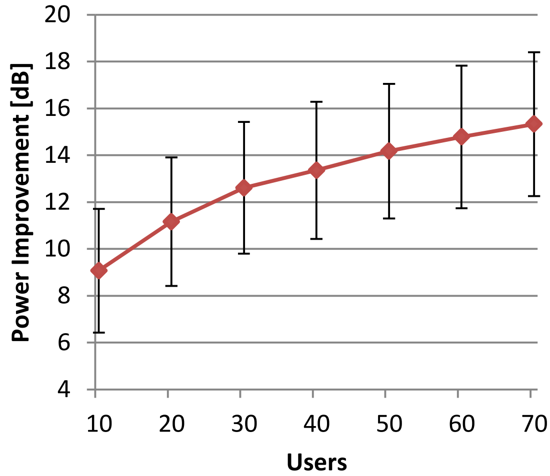

(b): 8 elements.

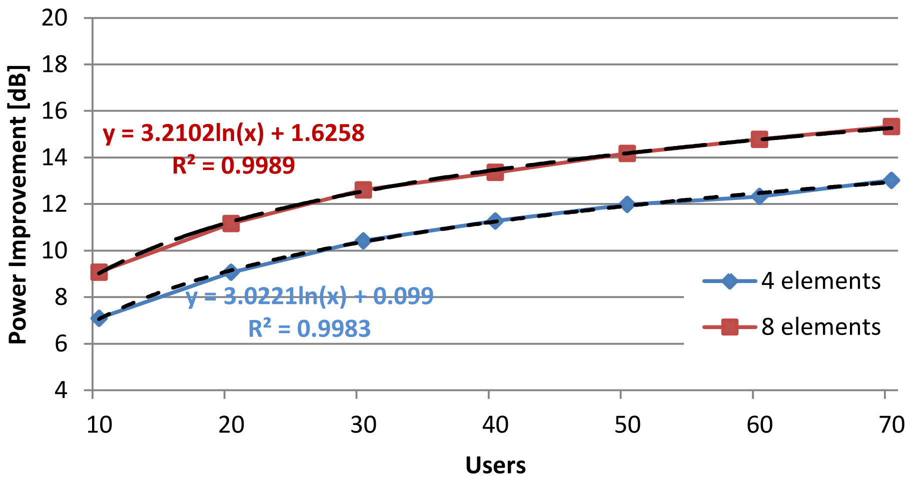

(c): Comparison and trend lines for 4 and 8 elements.

Figure 4.11: Power improvement for coverage of train stations and flag stops for UMTS

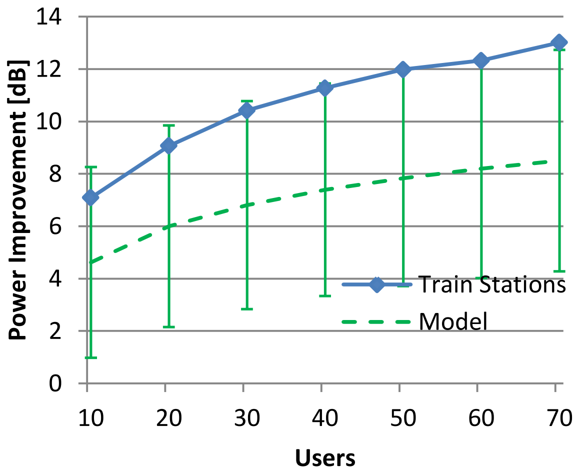

(a): 4 elements.

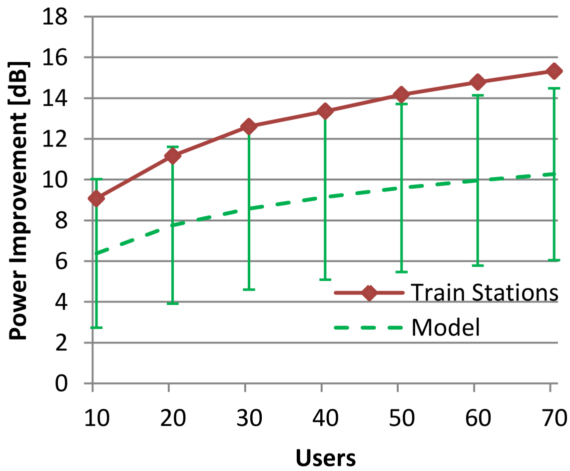

(b): 8 elements.

Figure 4.12: Comparison between simulated results and proposed model, for coverage of train stations for UMTS configuration

For both antenna configurations, the power improvement achieved in simulations of train stations' coverage is at the upper limit of the performance assumed by (4.5). At the higher numbers of users, the power improvement that is achieved for the coverage of train stations is slightly out of the model's standard deviation, however, always less than 1 dB. This way, the coverage of train stations can be considered as being in the group of specific scenarios where adaptive antennas enable higher power improvements, confirming the prediction of higher performance due to the high angular separation of users that are at the passengers' platform.

Figure 4.13 shows the power improvement when users vary, for antennas with four and eight elements, for the scenario of highway's coverage.

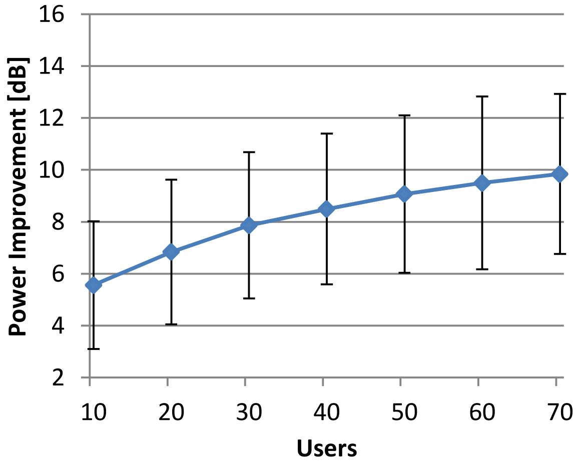

(a): 4 elements.

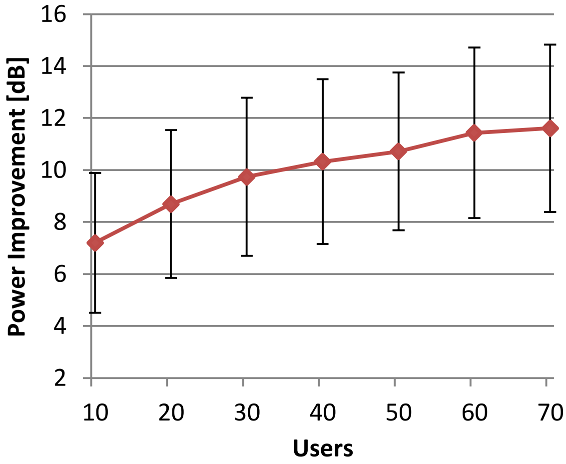

(b): 8 elements.

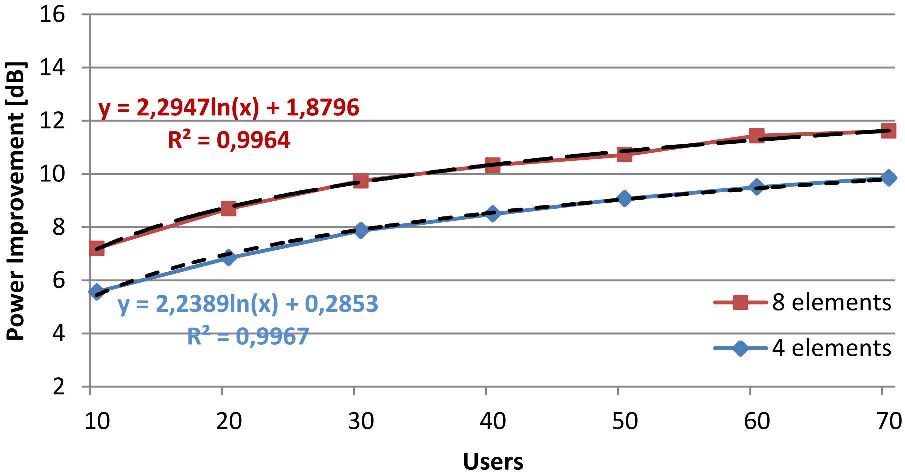

(c): Comparison and trend lines for four and eigth elements.

Figure 4.13: Power improvement for coverage of highways for UMTS.

Like the train's station situation, the behaviour of the power improvement follows the logarithmic behaviour. The absolute values for power improvement, for both four and eight elements at the antennas, are covered by the interval of accepted values of (4.5). Figure 4.14 presents the comparison between highways' coverage and the model (4.5).

Although the large axis where users can be placed is much higher than the distance of the BS to the highway (usually placed sideward), the absolute value of the involved distances between BS and users makes angular separation between each users' directions short, when users are several tens of metres apart. Compared with train stations, the power improvement achieved in the coverage of highways is more modest, at least 1 dB less, but it is higher compared with the one from (4.5). For this reason, the coverage of highways can be also considered as part of the specific scenarios where adaptive antennas reach good performance.

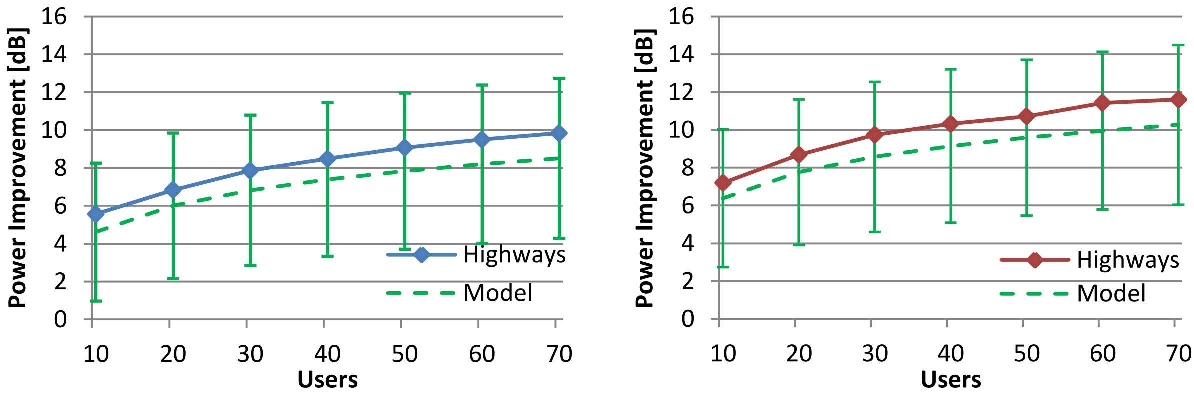

(a): 4 elements. (b): 8 elements.

Figure 4.14: Comparison between simulated results and proposed model for coverage of highways.

Figure 4.15 shows the results for rural villages.

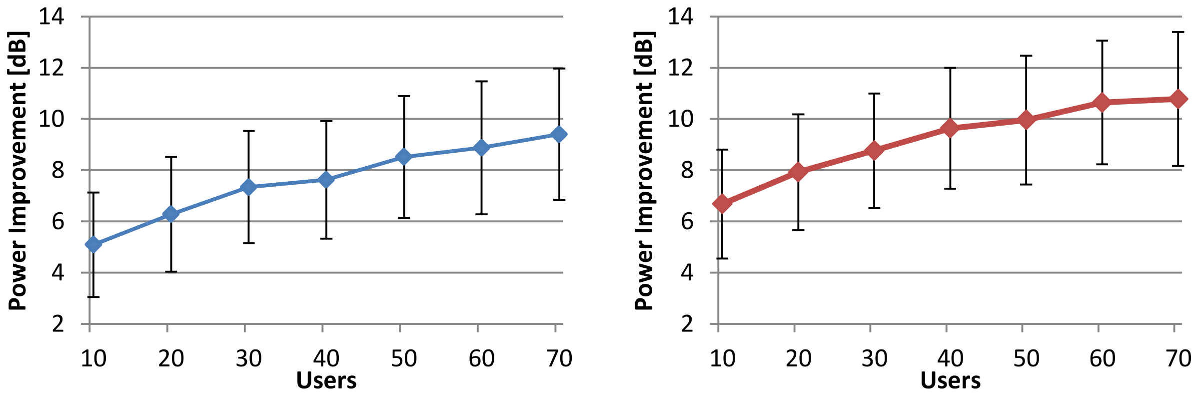

(a): 4 elements. (b): 8 elements.

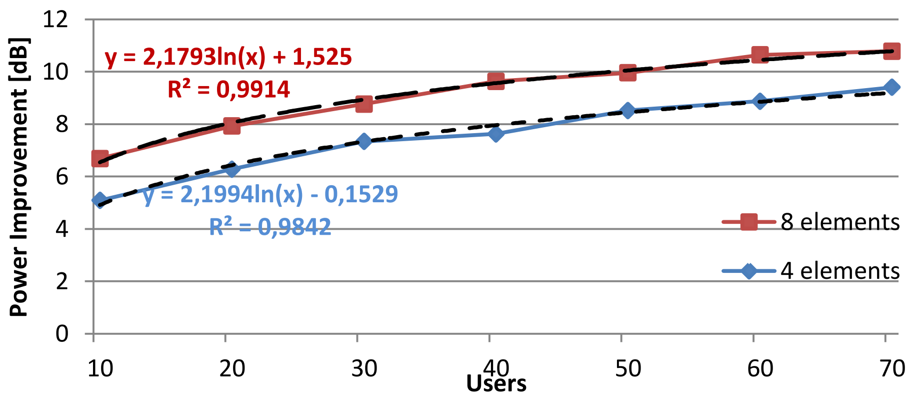

(c): Comparison and trend lines for 4 and 8 elements.

Figure 4.15: Power improvement for coverage of rural villages.

For the coverage of rural villages, again the behaviour of power improvement when the number of users vary does not present any new evolution, compared with the previous scenarios. The behaviour of the power improvement follows a logarithmic evolution and the saved absolute power is larger for the antennas with eight elements. The rural scenario covers areas between 5 and 7 km, but the majority of users are placed mainly within the small areas corresponding to the populated area of the villages, with users concentrate in small areas, compared with the total covered area. For this reason, the resemblance between the angles in which users' signals come from makes that adaptive antennas do not have the capacity to focus the main beam into the desired user's direction without radiate also non desired users, which reduces the performance of this kind of adaptive antennas in terms of power saving. Figure 4.16 shows the comparison between rural villages and the model proposed in (4.5).

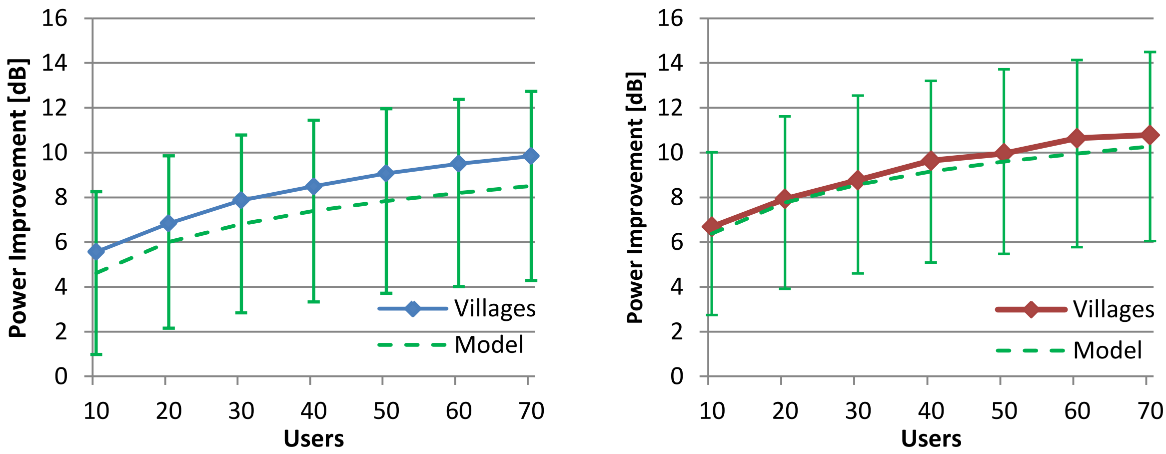

(a): 4 elements. (b): 8 elements.

Figure 4.16: Comparison between simulated results and proposed model for coverage of rural villages for UMTS.

Comparing the results obtained for rural villages' coverage with the model proposed in (4.5), the performance achieved is within the range of expected values for the model. For four elements in the antenna, the power improvement obtained is above the average value of the model (less than 1 dB). At the same time, the power improvement for rural villages is similar to the one obtained for highways' coverage (although slightly below, less than 1 dB), which can be justified with the similitude of scenarios, where users are placed in relatively small areas, compared with the entire covered area of a BS. In the particular situation of rural villages with antennas with eight elements, the results for power improvement meet the average power improvement of (4.5) with less than 0.7 dB of deviation.

The analysed specific scenarios also, besides the comparison with the general scenario estimation, serve to assess the model for power improvement, which was derived based on simulations for general scenarios (dense urban, suburban and rural). Due to timing constraints, the three specific scenarios were chosen to correspond to traffic mainly produced and served within the three general scenarios that are the base for the logarithmic model. The absence of specific scenarios where the average power improvement is below the average power improvement of the logarithmic model is explained by the objective to perform simulations where the power improvement was *a priori* expected as being larger than the average performance. The standard deviation that propagation models introduce into the results must not be forgotten, since it has the same order of magnitude of the one from the logarithmic model.

A final mark concerns UMTS services' bit rate. Since, the processing gain depends on the bit rate of the user, it corresponds to the fraction of power with which the desired user's signal is perceived above another signal of a non-desired user that is with the same propagation conditions, namely path-loss. The results presented in this analysis were performed for voice bit rates. However, simulations were done for specific scenarios to evaluate the impact of users' bit rates in the final power improvement. It is seen that, even for 2 Mbps, the processing gain guarantees the lock of the main direction of the radiation patterns into the direction of the desired user. The power improvement obtained for 2 Mbps presents variations below 0.01 dB, which is why the results for high bit rates are not presented in this work.

Concerning computer effort, the entire set of simulations for UMTS general scenarios took a week to be finished. However, such large period of time comes from the fact that statistical relevance was the aim for this set of simulations. Running just a single simulation for 70 users, top capacity, takes around 25 s to be finished, with figures of radiation patterns accounted. The processor used for the set of simulations was an Intel Pentium M 760, 2.0 GHz, and 1 GB of RAM.

4.3 LTE

The simulations for LTE were done for the same general scenarios as in UMTS. Three scenarios were tested with four cell's radius ranges each, which were tested from 0 to 8 interferers in neighbouring cells. Eight interferers correspond to the eight nearest neighbour cells in front of the antenna, forming the so called first and second rings of cells of a cellular deployment. For each combination of scenario/interferers, 500 simulations were run in order to establish a mean value and a standard deviation. In terms of users' positioning, they are allowed to be in any location of their cells, except for the user placed into the cell where the adaptive antennas are being assessed, which can be at the 120º covered by the reference sector antennas. The limitation of 120º for the desired user is justified by the reference antenna under analysis.

Concerning the variation of the radius of cells, the previous three scenarios were taken: dense urban, suburban and rural or high speed scenario. The metric from Section 3.3, by (3.20), was used. Figure 4.17 shows the power improvement when cells' radius vary for the same number of interferers in neighbouring cells.

The first aspect is the constant behaviour (with in an one dB interval) of power improvement when the radius of cells changes, which can be explained with the attempt by adaptive antenna in positioning the main lobe into the direction of the desired user. When the distance of the desired user changes, the adaptive antenna also locks the main beam of the radiation pattern in the direction of the desired user and the power improvement is given by the extra gain of the main lobe, compared with the reference antenna. The gain of the main lobe of the antenna does not depend on the cells radius, hence the constant power improvement behaviour.

Another aspect that must be notice is the change in standard deviation with the variation of cells' radius. For the situation where no interferers are present, the standard deviation remains controlled, since it is just conditioned by the capacity of the adaptive antenna in positioning the main lobe in the direction of the desired user. When more interferer users are placed in neighbouring cells, besides the ability to direct the main beam to the desired user's direction, there are radiation constraints on the direction of non-desired users, not being possible to position of high gain beams to serve the desired user. In this way, the standard deviation grows (up to 2 dB), which can make the operation of adaptive antennas even more expensive in energy than ordinary sector antennas, for four elements.

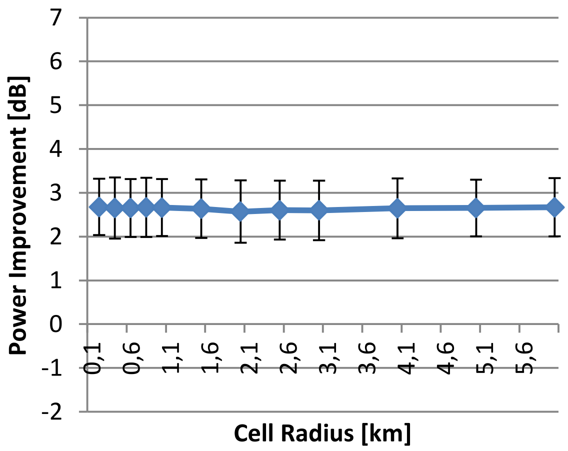

(a): 0 interferers, antenna with 4 elements.

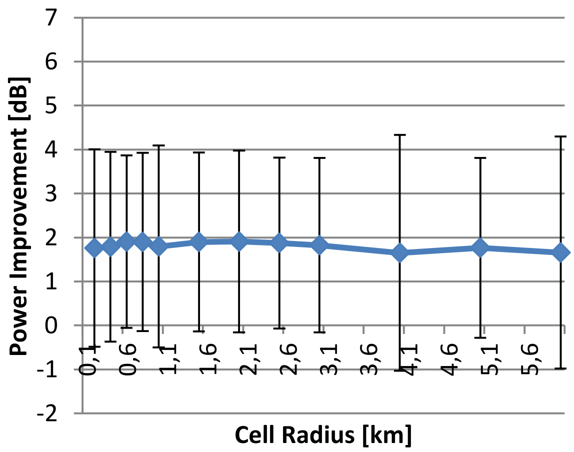

(b): 4 interferers, antenna with 4 elements.

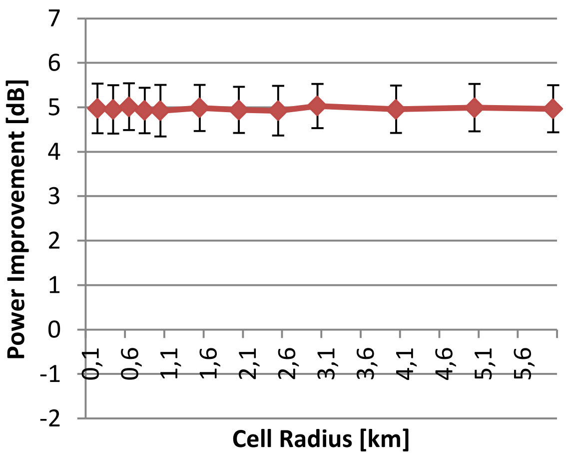

(c): 0 interferers, antenna with 8 elements.

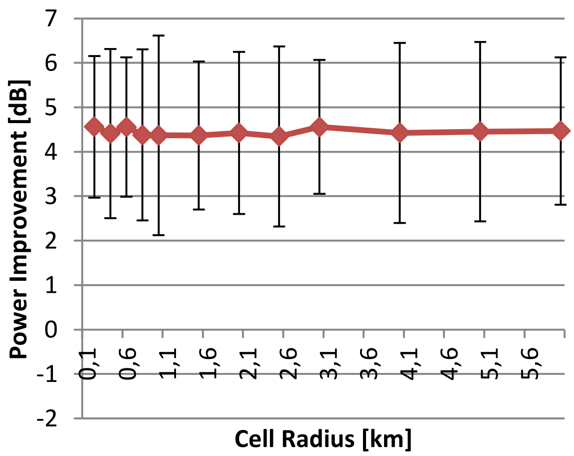

(d): 4 interferers, antenna with 8 elements.

Figure 4.17: Variation of power improvement as a function of cells' radius for LTE.

Figure 4.18 shows the variation of power improvement when interferers in neighbouring cells vary. The entire set of results is presented in Annex B.

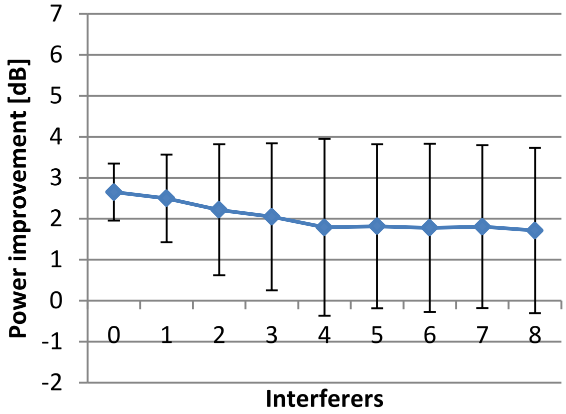

(a): Dense Urban scenario (0.4km radius), antennas with 4 elements.

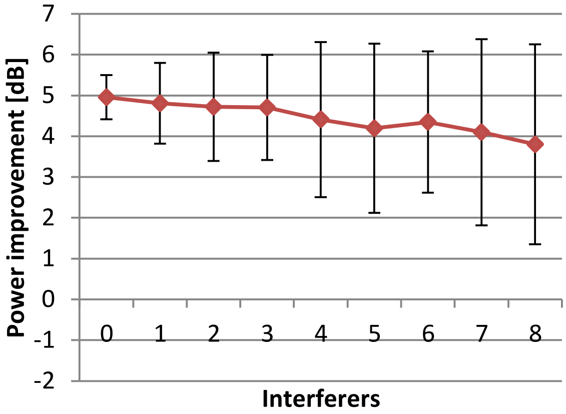

(b): Dense Urban scenario (0.4km radius), antennas with 8 elements.

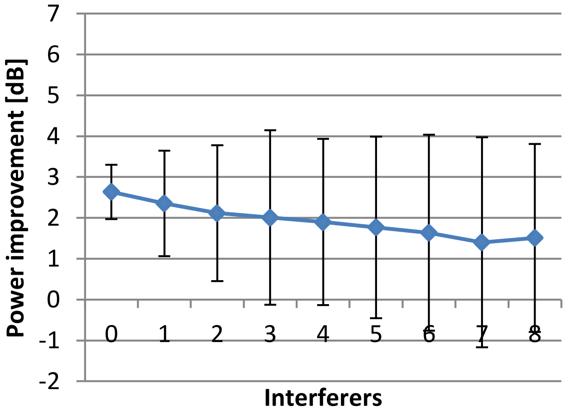

(c): Suburban scenario (1.5km radius), antennas with 4 elements.

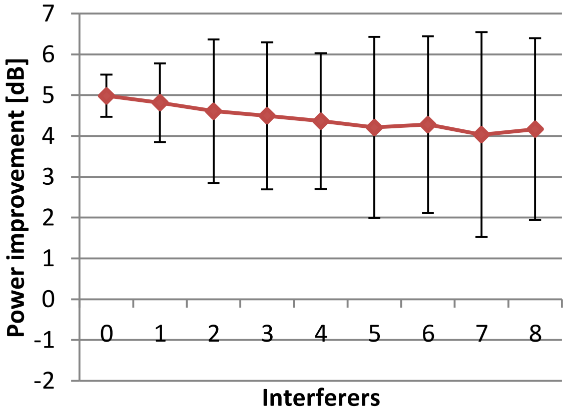

(d): Suburban scenario (1.5km radius), antennas with 8 elements.

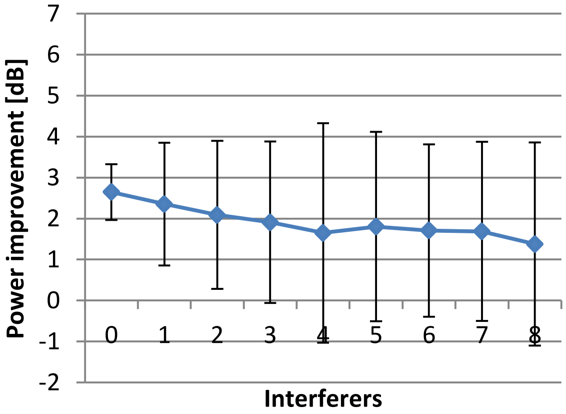

(e): Rural/High Speed scenario (4km radius), antennas with 4 elements.

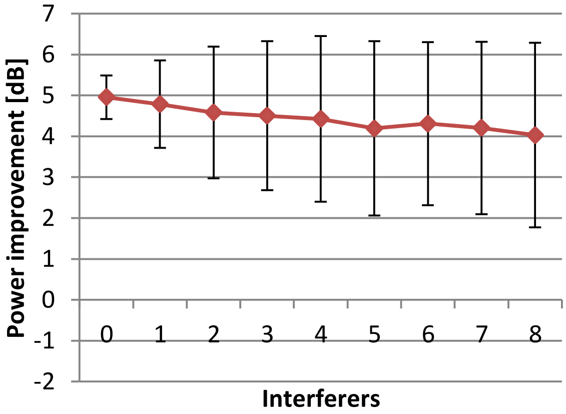

(f): Rural/High Speed scenario (4 km radius), antennas with 8 elements.

Figure 4.18: Variation of power improvement as a function of number of users for LTE.

With the increment of interfering users, the power improvement of adaptive antennas decreases. However the difference between the maximum and the minimum improvement rounds only 1 dB, for all analysed scenarios and ranges and the trend for improvement decreasing is always present. When the number of interferers grows, also the constraints in interference limitation assumes more relevance, since the radiation pattern must be able to direct a high gain beam in the direction of the desired users, and at the same time to limit as much as possible the gain in the direction of the interferers. With more interferers, the requirements for interference limitation can imply that the gain of the desired user's beam becomes lower than it would be if no interferers were present.

Another aspect is the increment of the standard deviation with the rise of interferers. When no interferers are active, power improvement does not float considerably. However, caused again by the growth of interference constraints, when the number of interference grows the standard deviation also becomes larger, and the capacity to predict power improvement of a certain scenario is reduced. In fact, the absolute value of the standard deviation does not constitute a problem, but its value, compared with the average one, is so high that can caused a situation where it is not possible to predict if adaptive antennas will save or waste energy, as seen in Figure 4.18 for antennas with four elements.

Focusing the attention on the antennas with four elements and their power improvement as a function of interfering users, the magnitude of the standard deviation, compared with the average value, makes it hard to derive a model to describe the behaviour, or leads to a model where the average value has the same magnitude of the standard deviation. For this reason, and due to the low variation of average power improvement with interferers, instead of deriving a model, one presents the analysis of the absolute value for the power improvement.

Adaptive antennas with four elements are able to improve the propagation's efficiency on average between 1.5 and 2.5 dB. Under certain conditions of users' alignment, when there is possible to focus the main high gain beam in the direction of the desired user without creating extra interference in the non-desired ones, power improvements can reach up to 4.5 dB, corresponding to a power saving of 65%. Concerning antennas with eight elements, on average they achieve 2.5 dB, more than the one with just four elements. Due to their narrower lobes, antennas with eight elements are able to direct the high gain main lobe into the direction of the desired user, and they are able to handle more severe interference constraints that happen with the increase of interferers, which is why the improvement for antennas with eight elements reachs at least (and at the worst case) near 1.5 dB, corresponding to 30% of energy saved. The average power improvement reached by antenna with eight elements 4.5 dB, which is the maximum for antennas with four elements under the best conditions. Antennas with eight elements can reach a maximum of 6.5 dB, under certain conditions of users' alignment, which corresponds to 77% of energy saved. It must be remembered that for LTE, power control in DL is not implemented, and any fraction of power that is reduced to serve a user can make a difference between serving or not extra users due to insufficient signal-to-noise plus interference ratio.

Chapter 5

Conclusions

In this chapter, the main conclusions from this work are pointed out and criticised. Future research is discussed, as well as features that can be added to the present work, in order to valorise it from the viewpoint of application to mobile communications.

The start for this work was the motivation for energy efficiency based on beamforming for mobile communications. Chapter 1 gives an overview about the commercial reasons that motivates the introduction of green systems. The challenge for energy efficiency is framed by the economical perspective that a major reduction on the energy expense can create in the overall mobile communication business.

Chapter 2 introduces the basic aspects that are related to the systems under analysis. For both UMTS and LTE, architecture, radio interface, coverage and capacity aspects are visited.

From the conceptual viewpoint, the introduction of adaptive antennas can be done at the BS, since some timing constraints related with the radio interface are respected. Timing is crucial to obtain good performance. UMTS and LTE have well defined temporal structures, in which all type of channels are transported. Since an UL control channel is used, the periodicity on which UE sends information cannot be too long, in order to be possible to correct update of users' radiation patterns. UMTS defines TTIs from 10 to 80 ms for R99 and 2 ms to HSPA, while for LTE, it is defined to 1 ms. 10 ms between radiation pattern update would not be a problem for pedestrians, which move less than 1 m in this period, at a maximum of 30 km/h. However, considering a fast train traveling at 300 km/h, in 10 ms it is able to move more than 80 m, which can be a problem at short distances from the BS due to highly directive radiation patterns. The choice of the update period for the adaptive antennas must be, first of all, a routine that already is implemented into the radio interface, to avoid extra complexity. Other aspect that should be measured into the choice of the update period is the type of traffic. For high dense populated areas, with traffic generated mainly by pedestrian, there is no need to implement short update periods if people only move some metres in between updates, and cell cover several hundreds of metres.

Also in Chapter 2, the basic structure of an adaptive antenna is presented, followed by the propagation aspects that are relevant to study the behaviour of the signals that arrive to an antenna array. Finishing Chapter 2, several works performed in energy efficiency and multiple antenna applications are addressed, their main results being presented.

Based on the specificities of the radio interfaces of UMTS and LTE, two models, one for each system, were developed and implemented into a simulator, programmed in Matlab, in order to measure, by simulating, the power improvement that adaptive antennas offer, compared with the current static sector antennas. The models are similar between each other, and they were developed in order to represent the radio interface of each system, specially related to the radio link and the multiple access technique. Protocols and radio interface procedures that are not the focus of this thesis were simplified as much as possible.

The first step for the evaluation of the power improvement reached by beamforming was done by simulating general scenarios, where several arrangements of users were located uniformly in a sector. For each arrangement of users, several cell radius were used and simulated. In this simulation type, where no urbanistic or demographic issues were taken into account, the objective was to create a statistical base to derive a model of the power improvement with range to describe the majority of situations that can be considered for that particular scenario, namely dense urban, suburban or rural. The set of simulations was run 500 times in order to derive the average value as well as a standard deviation, which was considered enough, since results converged.

For UMTS, the simulations for general scenarios' show a logarithmic behaviour of power improvement with the number of users. Two configurations of antennas elements were considered, one with four elements and another with eight, in a linear array with half wavelength of separation in between each element. The variation on power improvement, for the same number of users in the cell, when the cell radius changes does not vary significantly and its value is within 1 dB interval for all the cell radii that were simulated. Also the standard deviation is consistent, with similar values. The scenario where adaptive antennas show a lower performance for 10 users is served by an antenna with four elements. Even for this worst case performance, adaptive antennas are able to save, on average, near 5 dB of radiated power, which corresponds to a percentage of power saved near 70%. When the lowest limit for the standard deviation is considered, the situation with 10 users and 4 elements at the antenna are able to save near 50%, 3 dB of radiated power. When the worst situation of 10 users in the cell is considered to be covered with antennas with eight elements, the power improvement that is reached is near 7 dB, which corresponds to a total power saved of 80%.

In UMTS, when the number of active users grows, also the amount of interference grows, which increases the potential for saving power by suppressing interference as much as possible. A logarithmic model was derived to represent the power improvement that is achieved by adaptive antennas as a function of the number of users and the number of elements at the antenna array. When cells are near its top capacity, which was simulated with 70 users within the same cell, the average radiated power that is saved with antennas with four elements is near 10 dB, which means that 90% of the power that is radiated by static sector antennas can be saved if adaptive antennas are used, and for antenna arrays with eight elements, the average power improvement rounds 12 dB, more than 93% of radiated power saving.

The number of active users within the same cell is the factor that more influence has in the power performance of the adaptive antennas. When the number of users grows, the amount of interference that is generated in between users is so high that adaptive antennas, by suppressing a major percentage of interference, can reduce the desired signal's power with no Signal-to-Interference degradation. If the improvement on radiated power is reached by focusing the radiation mainly in the direction of the desire user, also an important power efficiency comes from the interference that is suppressed, which is why the total saved power can reach more than 90% with no service degradation.

In LTE, no intra-cell interference is present, since the system is much more critically affected by non-desired signals at the same carrier frequency. For this reason, within the same cell, the same carrier frequency is not assigned to different users, which means that all the interference that is suffered by a user comes from neighbouring cell. The power improvement that is achieved by adaptive antennas comes from the signal's improvement introduced by focusing the desired radiation in the direction of the desired user, which is the only one at that specific carrier frequency within the cell. Co-channel inter-cell interference sources are seen by beamformers as constraints, which imposes that no high gain lobes can be steered in the direction of neighbouring cell's interfering sources.

LTE power improvement, compared with current static sector antennas, does not change with the variation on the cell's radius, for the same number of interferers in neighbouring cells. When the number of interferers in neighbouring cells varies, the radiated power that is possible to save does not vary substantially, with the average improvementbeing near 2 dB for antennas with four elements and 4.5 dB for eight elements, which corresponds to an average power saved of 35% and 65%, respectively. The variation on the number of neighbour interferes affects mainly the standard deviation, which rises with the increment of interferers. This behaviour is explained by the fact that the interferers are active in neighbour cells, more interference constraints adaptive antennas faces, which may imply that the main beam of the radiation pattern cannot be steered in the direction of the desired user due to the increment of interference that the radiation pattern creates.

Even being less attractive than in UMTS, adaptive antennas in LTE have significant power efficiency, especially for arrays with eight elements where power saving of 65% is achieved on average. The power efficiency that is achieved for arrays with eight elements is appealing, for example, to increase the coverage of a cell without spending extra power, since the gain that is introduced in the link between BS and users can make the difference between being covered or not, with positive consequences that new covered customers' profits can bring for operators.

Although the power efficiency that was studied in this thesis has a significant impact on the amount of energy that is spent for radiators, the efficiency gains that were presented are gross ones. This first approach to the energy efficiency had the aim to evaluate the potential for power saving that adaptive antennas introduce in today's and tomorrow's mobile communication systems. Of course, if the model that simulates the radio interface and the antenna's weighting is implemented into commercial products, the computational effort that is need to be spent in order to serve the studied amount of users, may not compensate the energy gains that are achievable by adaptive antennas. Some work is being performed in the domain of real time light algorithms for antennas weighting that reduces the computational effort that was spent in this thesis to assess the achievable power efficiency. The order of magnitude that was seen to be feasible for adaptive antennas in UMTS and LTE has a margin to be considered in the development of new hardware BS components, even if the actual power improvement is less than the one verified in this work.

The spatial domain where the study of beamforming was considered was only the azimuthal plane. For future work, fully directional beamforming, with adaptive vertical and azimuthal radiation patterns, has a high interest to be studied. Cities with massive population concentrations, like Singapore, Hong Kong, New York, among others, where massive skyscrapers take the scenery, would have enough potential to exploit vertical diversity of users, combined with the azimuthal beamforming that was studied in this thesis.

Annex A

Validation of Algorithm for Antenna Weighting

This Annex presents the validation and assessment for the algorithm used to weight each element of an adaptive antenna array, used to eliminate interference caused by non-desired users into the signal of a desired user. For this validation, several situations with predicted results are analysed to show the algorithm reacting as expected.

The first situation where the algorithm was tested was when just one user is placed into the cell. The adaptive antenna array should direct a high gain lobe into the direction of the only user (also the desired one) once no constraints about interference are presented in the scenario.

Antenna Gain with reference to the isotropic antenna

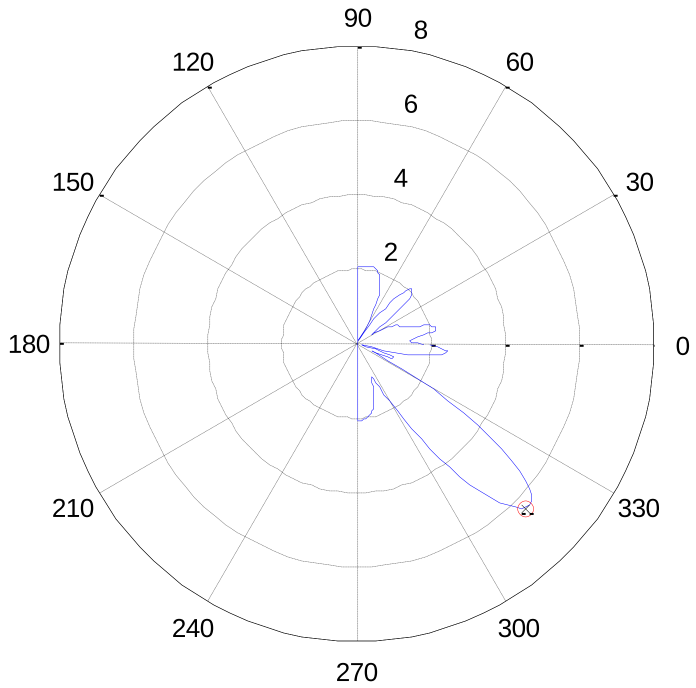

Figure A.1: Simulation of single user scenario (linear scale).

As Figure A.1 shows, the algorithm does exactly what it is supposed to do and directs a high gain lobe into the direction of the user.

The adaptive antenna array should present good performance in presence of lower number of users than number of antenna elements. In this way, when the number of users is lower than the number of antenna elements, the antenna array should be able to direct a lobe to the direction of each desired user, and suppress as much as possible the interference created by non-desired users, reducing the antenna's gain into the direction of the non-desired users. In

Figure A.2, a scenario where is presented an adaptive antenna with 8 elements and 4 users to serve was tested. The simulation proves the spatial separation of the users by the antenna array, being generated individual lobes to serve each user, with obvious care on secondary lobes' direction in order to suppress interference. Always when there are no non-desired users into the near directions of the desired user that is being served, the radiation pattern focus the main beam into the direction of the desired user, and tries to direct nulls into the direction of the non-desired users. When the desired user and some non-desired user has similar angles to the antenna array, there is no option unless focus the main beam into the direction of the desired user.

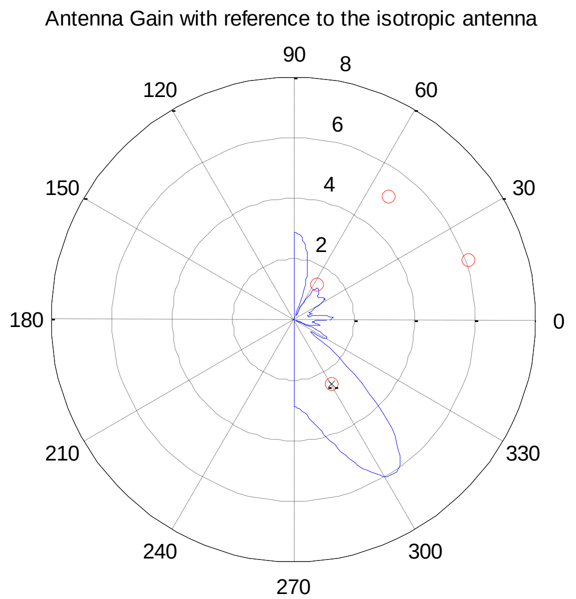

(a): User no.1

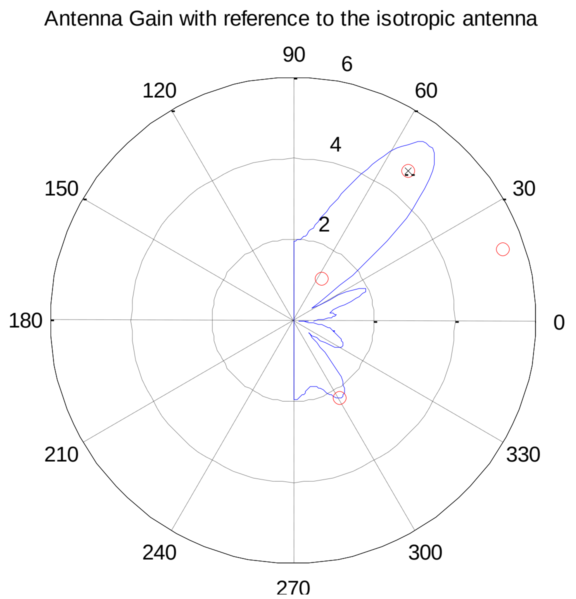

(b): User no.2

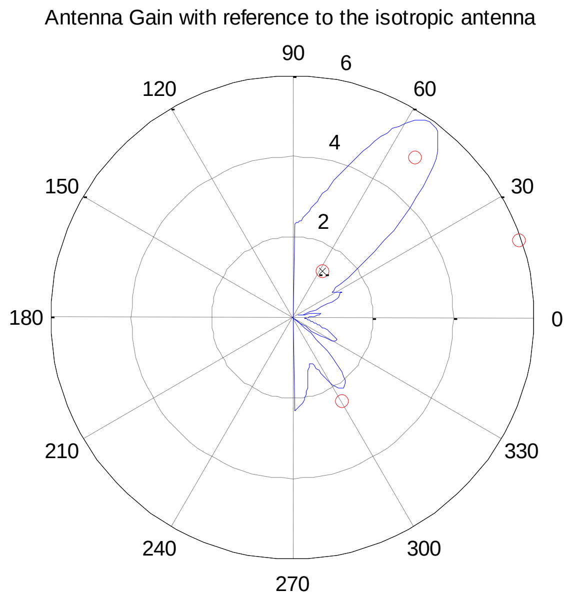

(c): User no.3

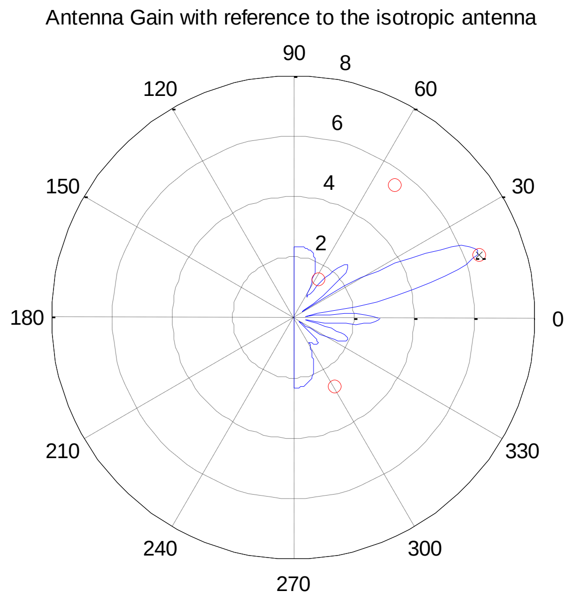

(d): User no.4

Figure A.2: Radiation patterns for scenario simulation with adaptive antennas with 8 elements and 4 users (linear scale)

When there are more users than antenna elements, the result of the algorithm to weight the elements is unpredictable. The reduction of radiated power is achieved by improving carrier and reducing interference. When there are more users than elements of the antenna, the interference cannot be all suppress, once the ability to introduced nulls into the direction of interferes is limited by the number of elements available at the antenna array. The propagation conditions that each user has in his radio link to BS depend on his distance, the absence or not of line-of-sight, fading effects, etc. In these conditions, the algorithm for antenna weighting should be able, at least, to direct the main lobe into the direction of the desired user. To evaluate the situation with more users than antenna elements and see if the algorithm for antenna weighting is working as it is supposed, it was tested the situation where 16 users are being served by an 8-element antenna array,

Figure A.3.

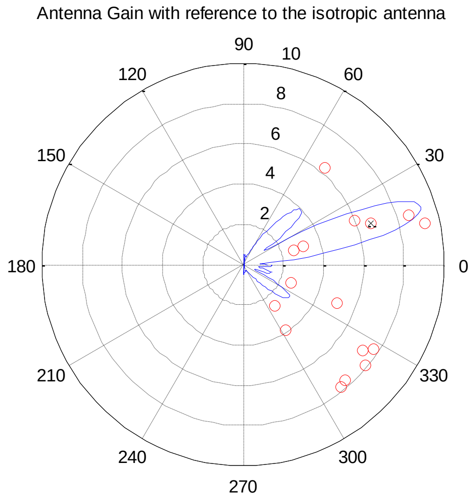

(a): User no.1.

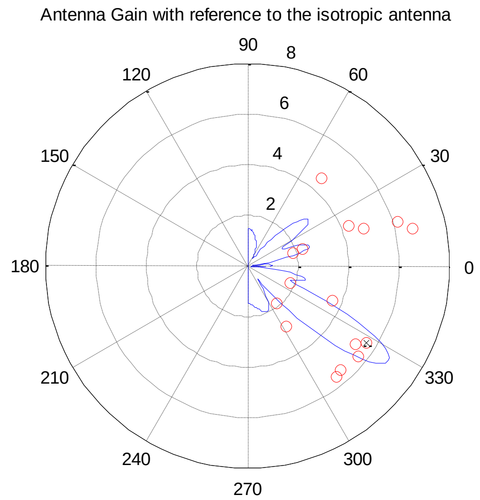

(b): User no.2.

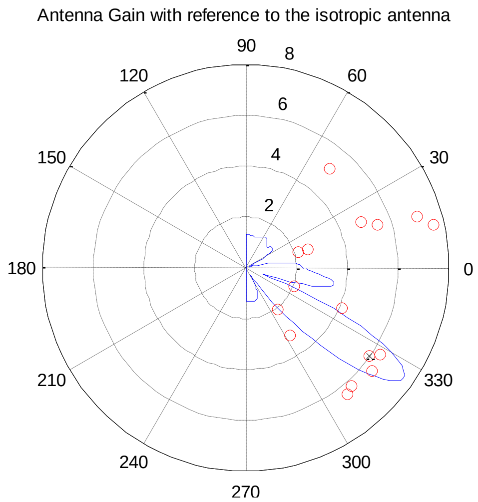

(c): User no.3.

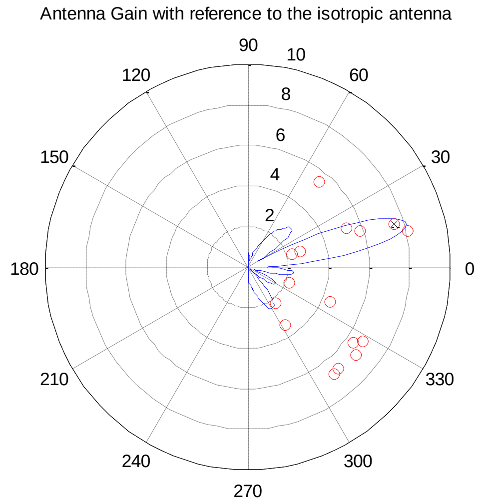

(d): User no.4.

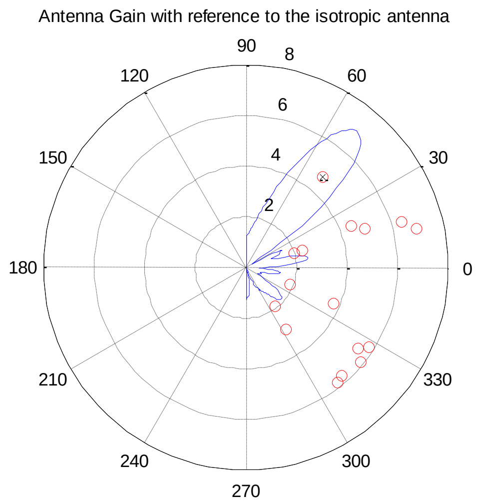

(e): User no.5.

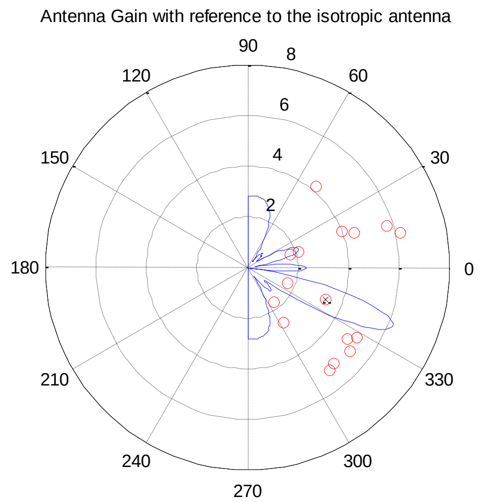

(f): User no.6.

Figure A.3: Radiation patterns created to serve 16 users by an 8-element antenna array

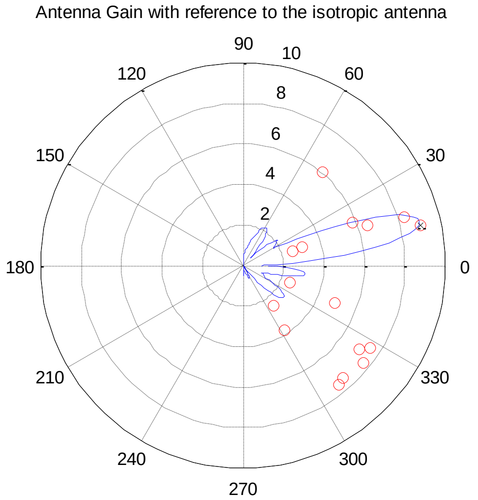

(g): User no.7.

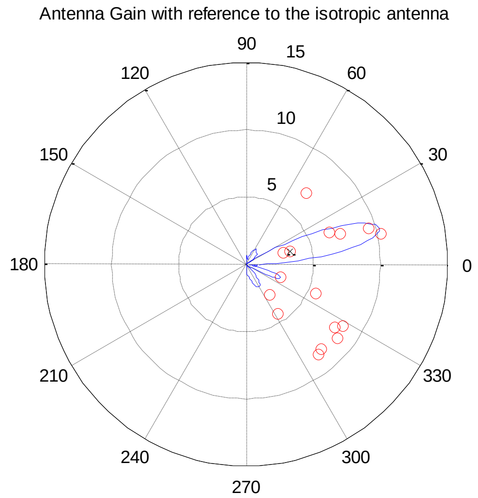

(h): User no.8.

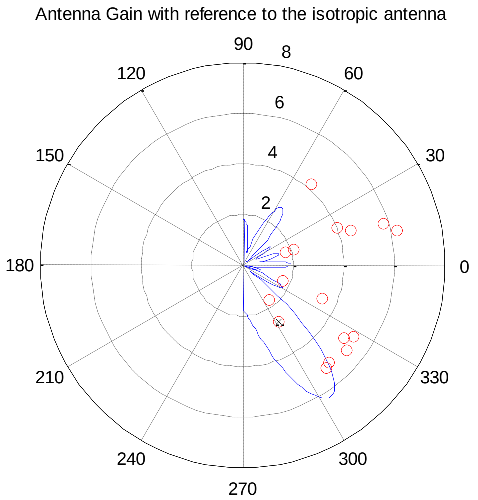

(i): User no.9.

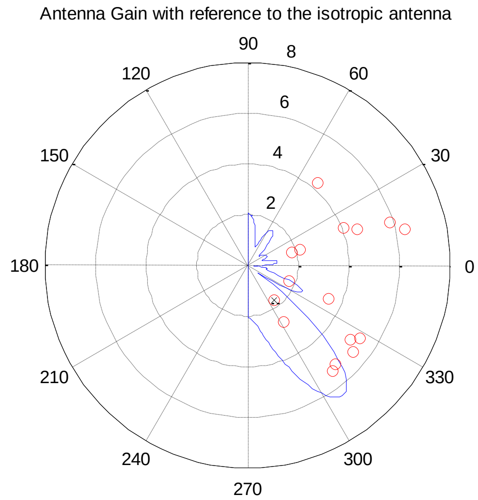

(j): User no.10.

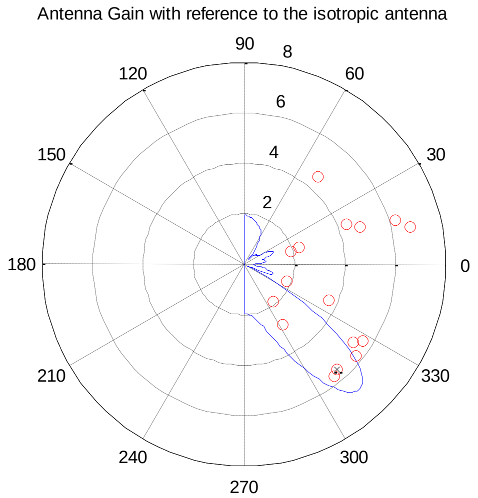

(k): User no.11.

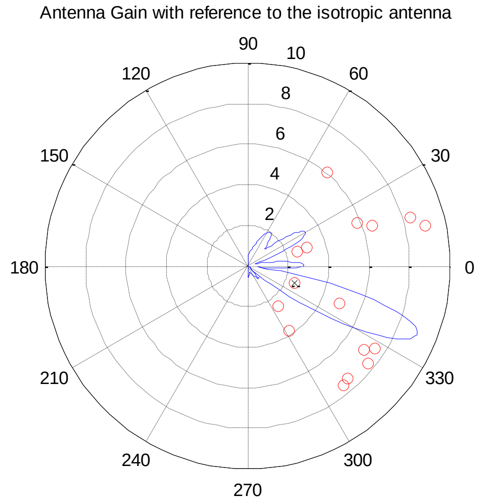

(l): User no.12.

Figure A.3 (continuation): Radiation patterns created to serve 16 users by an 8-element antenna array

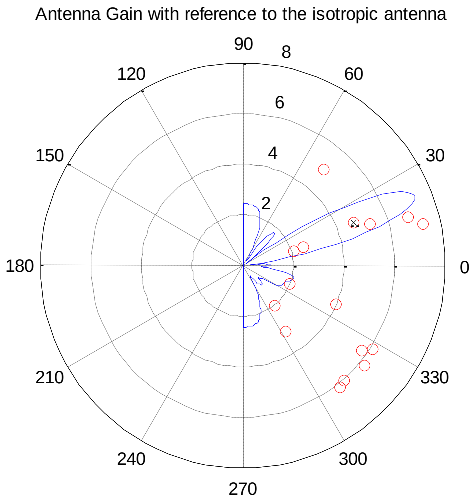

(m): User no.13.

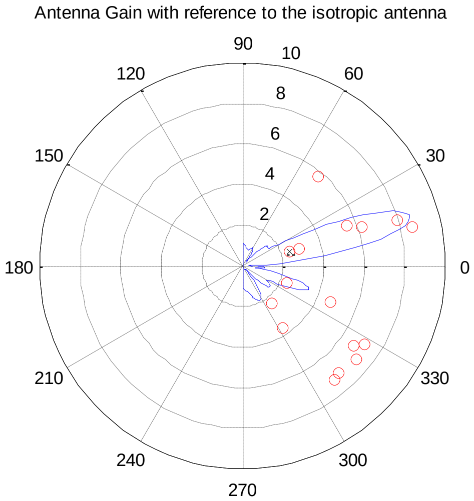

(n): User no.14.

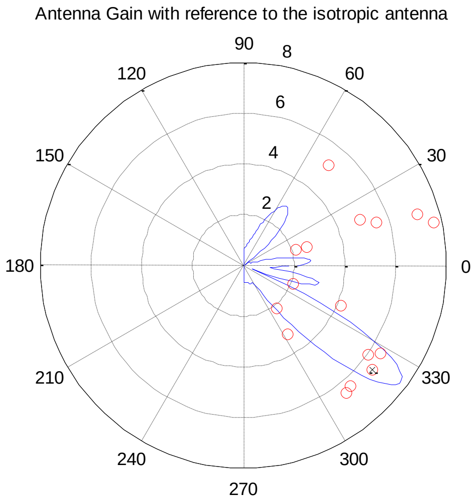

(o): User no.15.

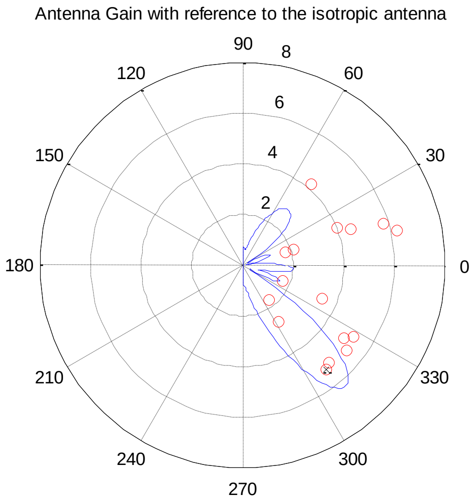

(p): User no.16.

Figure A.3 (continuation): Radiation patterns created to serve 16 users by an 8-element antenna array.

Attention must be done to the directions where the side lobes of the radiation patterns are located. In almost all users' radiation patterns, the side lobes are pointed to direction where there are no users, in order to not introduce extra interference on serving other users. This feature of the algorithm, visible at the radiation patterns, is more evident when all users have similar propagation conditions, namely similar path losses, making interference constrains more relevant once the radiated powers are also similar in between users. Figure A.4 represents the simulation of serving 8 users with a 4-element antenna array, where the users all at the same distance from the BS and there are not co-located in between each other. In all radiation patterns of Figure A.4, the side lobes are pointed to directions where there are not any users, while always that it is possible, there are nulls pointed into the direction of non-desired users.

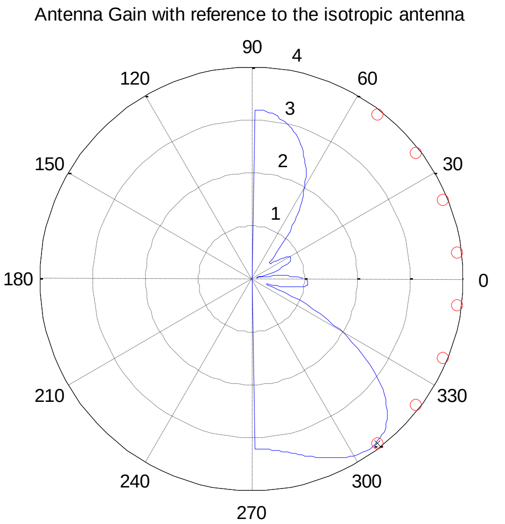

(a): User no.1.

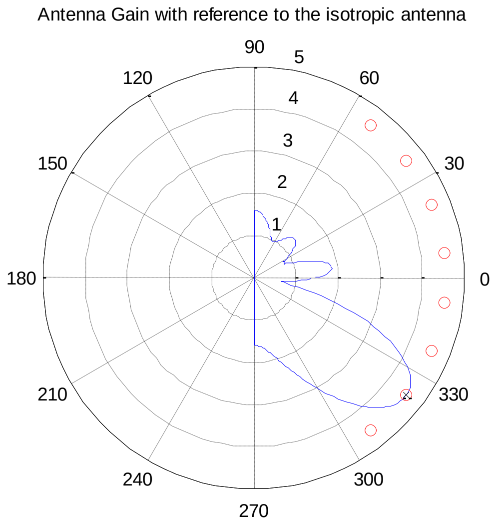

(b): User no.2.

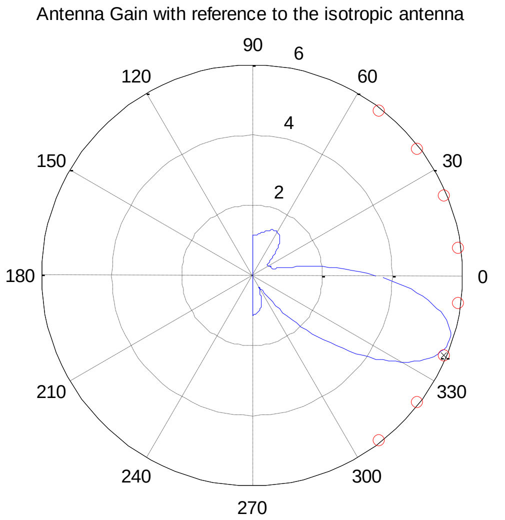

(c): User no.3.

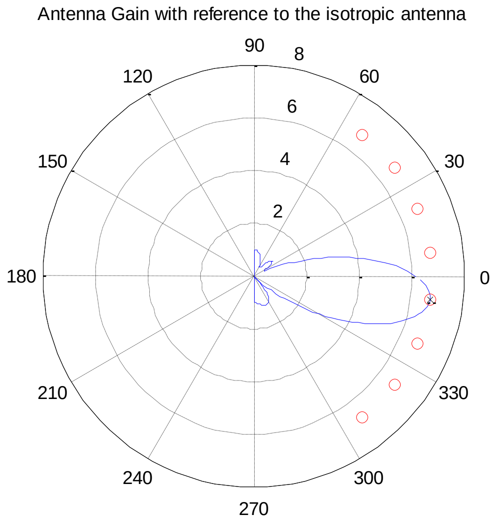

(d): User no.4.

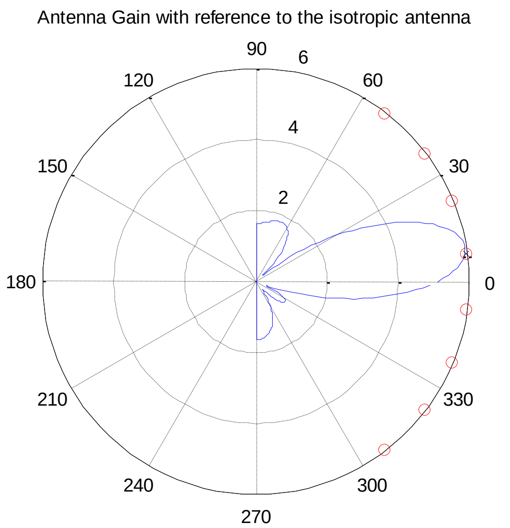

(e): User no.5.

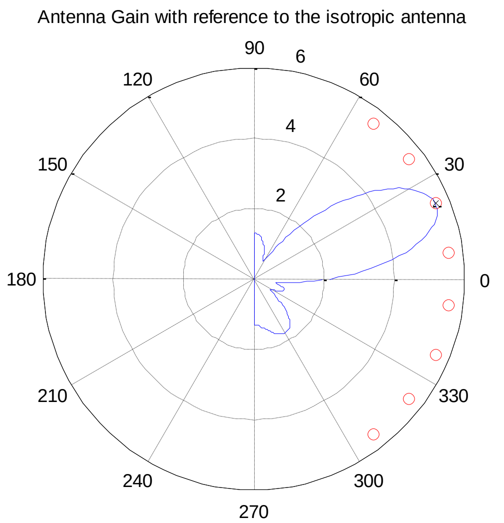

(f) User no.6.

Figure A.4: Radiation patterns to serve 8 users with a 4-element antenna array, where the users all at the same distance from the BS.

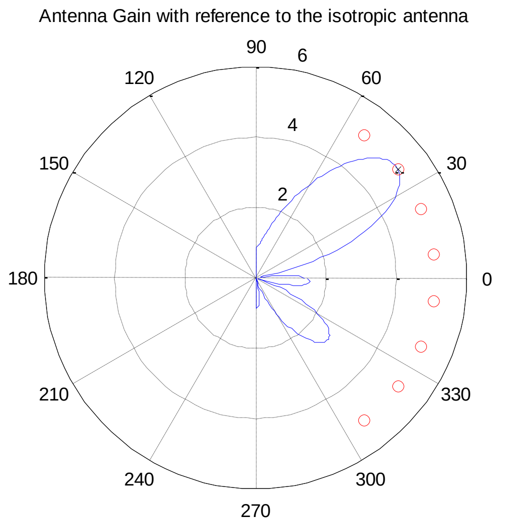

(g): User no.7.

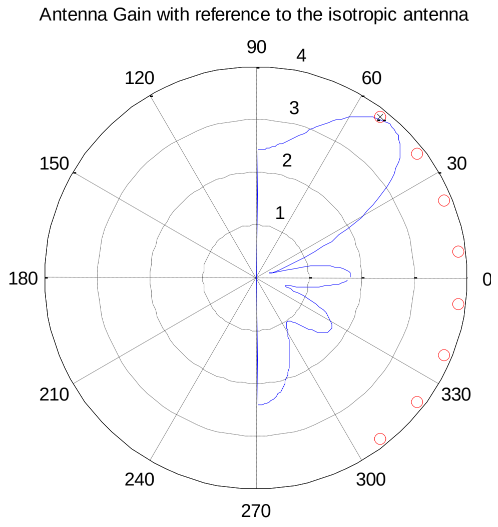

(h): User no.8.

Figure A.4 (continuation): Radiation patterns to serve 8 users with a 4-element antenna array, where the users all at the same distance from the BS.

Annex B

Additional Results

This annex presents the entire set of results obtained by simulations. Results for all scenarios, all cells' radius and several numbers of users were combined in order to analyse all the relevant aspects about the power improvement achieved by adaptive antennas. For convenience, and not to repeat similar information, the entire set of simulations is no presented in the chapter of Result analysis.

Following the same sequence with which results were shown in result analysis, the first variation to be shown is the variation of power improvement when cells' radius vary, for UMTS, Figure B..

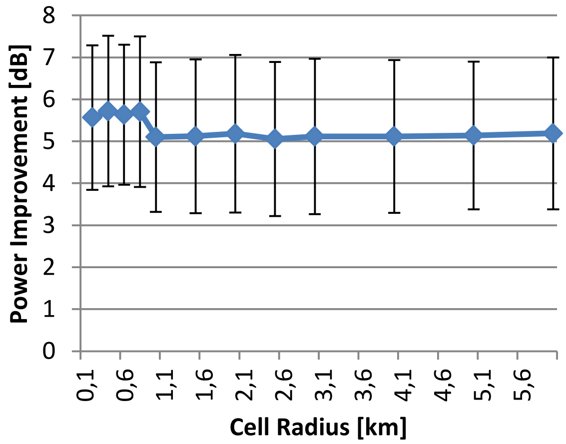

(a): 4 elements, 10 users.

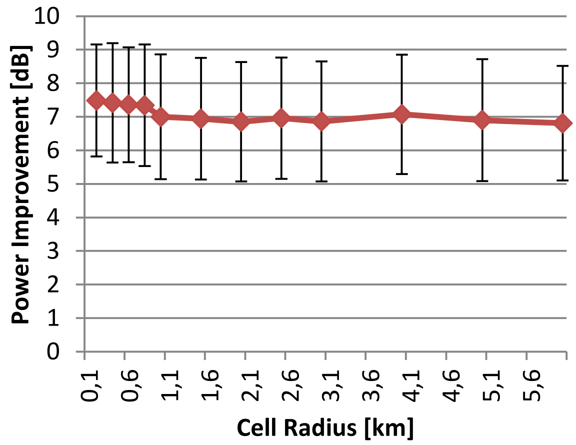

(b): 8 elements, 10 users.

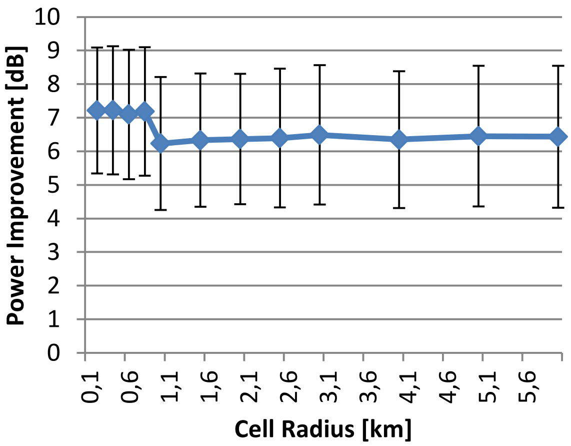

(c): 4 elements, 20 users.

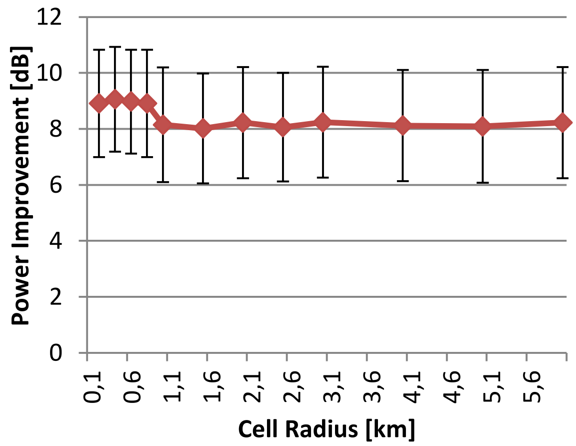

(d): 8 elements, 20 users.

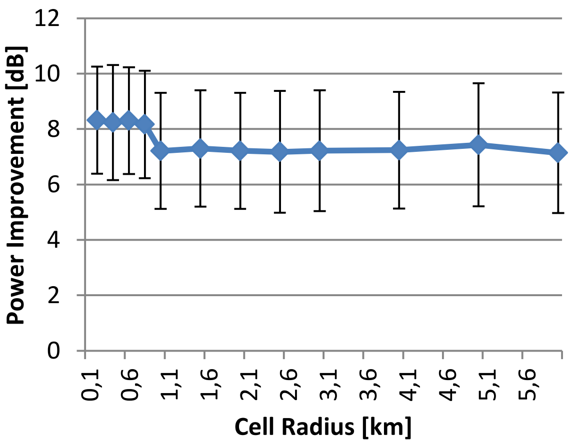

(e): 4 elements, 30 users.

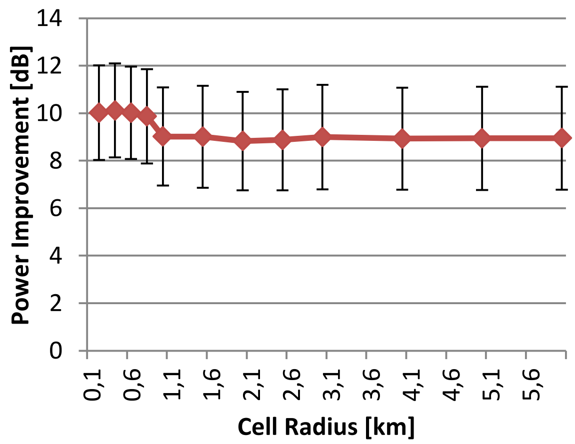

(f): 8 elements, 30 users.

Figure B.1: Variation of power improvement as a function of variation of cells' radius for UMTS

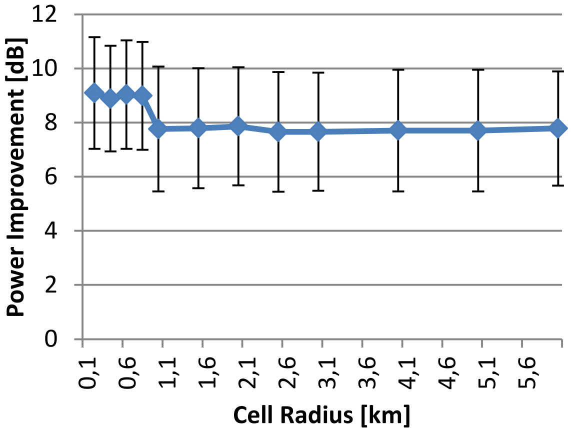

(g): 4 elements, 40 users.

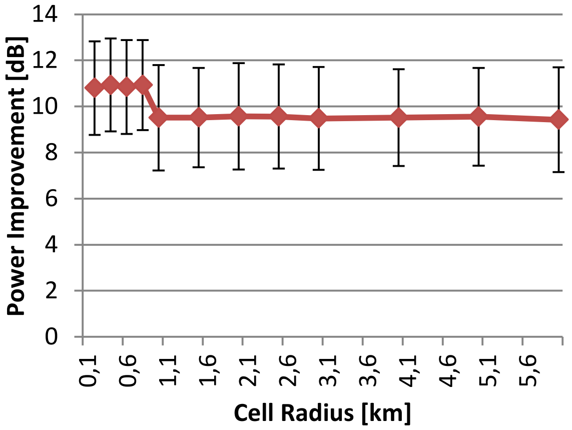

(h): 8 elements, 40 users.

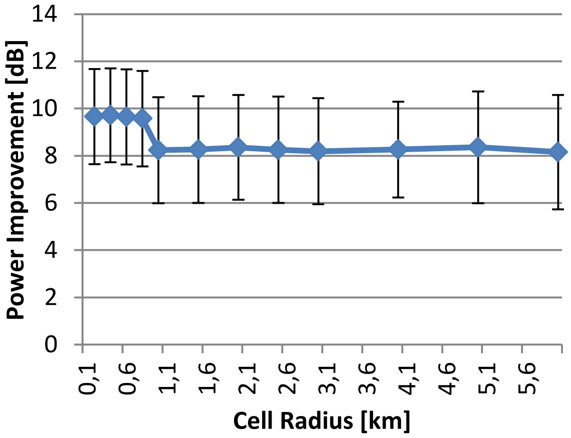

(i): 4 elements, 50 users.

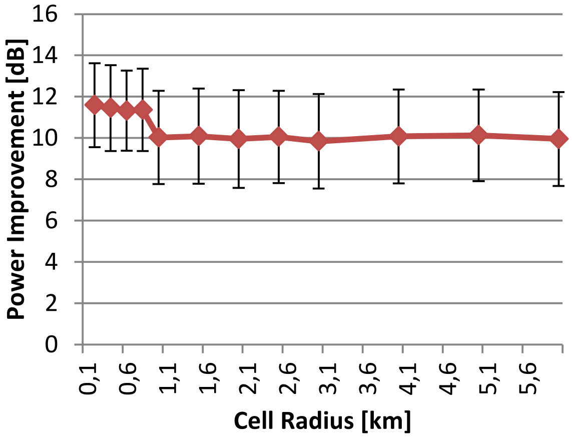

(j): 8 elements, 50 users.

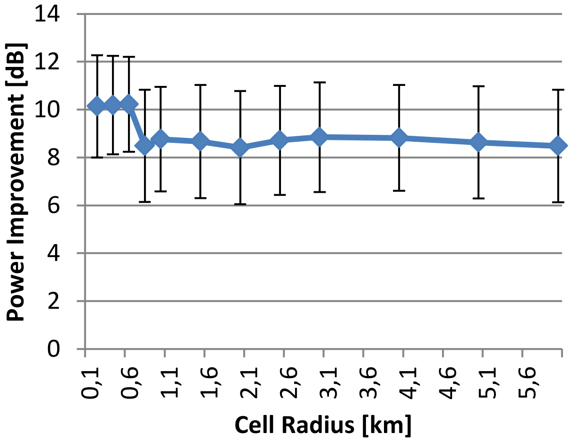

(k): 4 elements, 60 users.

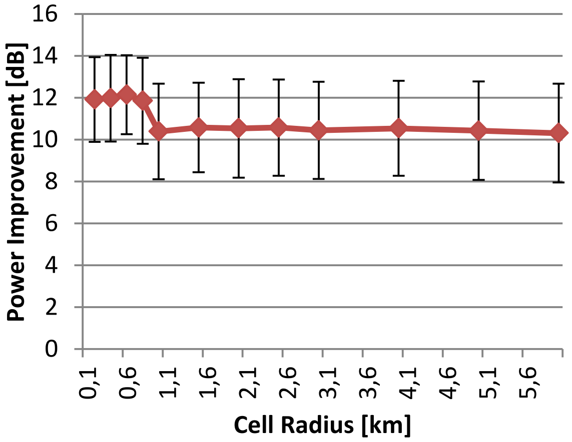

(l): 8 elements, 60 users.

Figure B.1 (continuation): Variation of power improvement as a function of variation of cells' radius for UMTS

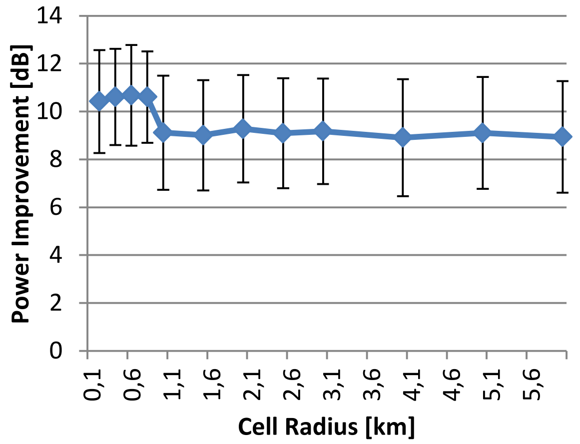

(m): 4 elements, 70 users.

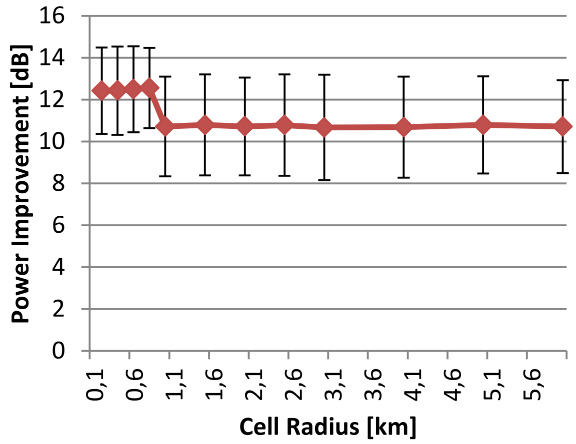

(n): 8 elements, 70 users.

Figure B.1 (continuation): Variation of power improvement as a function of variation radius for UMTS.

Power improvement of adaptive antennas in UMTS is strongly dependent on the number of users being served at the same moment within the cell, fact that derived into a proposed model, (4.5) and the entire set of power performance and the trend lines for all scenarios are shown in Figure B.2.

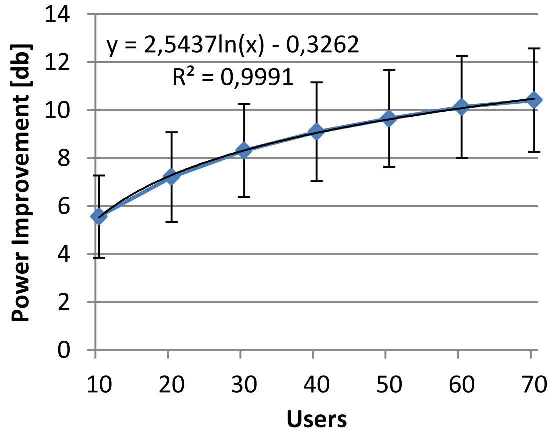

(a): Dense urban (0.2km), 4 elements

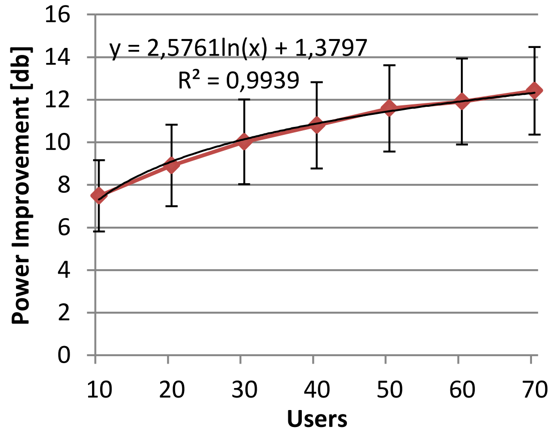

(b): Dense urban (0.2km), 8 elements

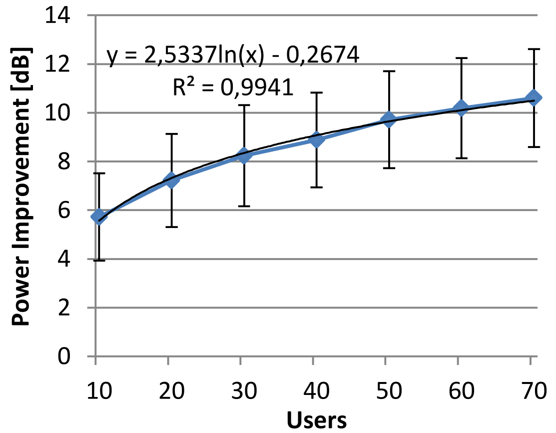

(c): Dense urban (0.4km), 4 elements

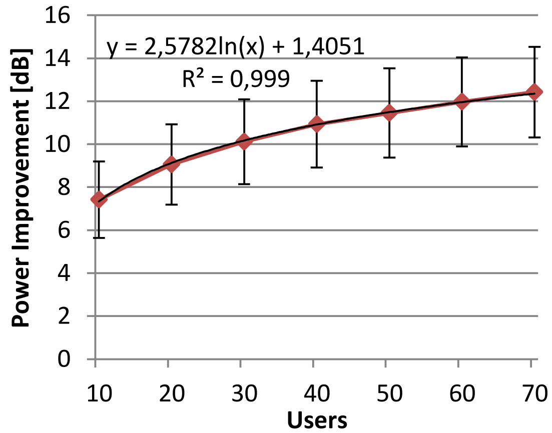

(d): Dense urban (0.4km), 8 elements

Figure B.2: Variation of power improvement as a function of users' variation for UMTS.

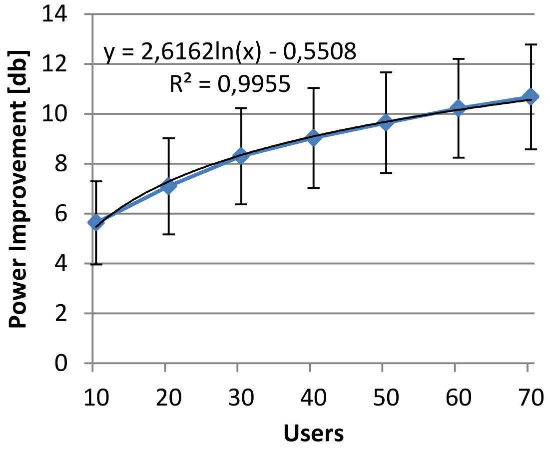

(e): Dense urban (0.6km), 4 elements

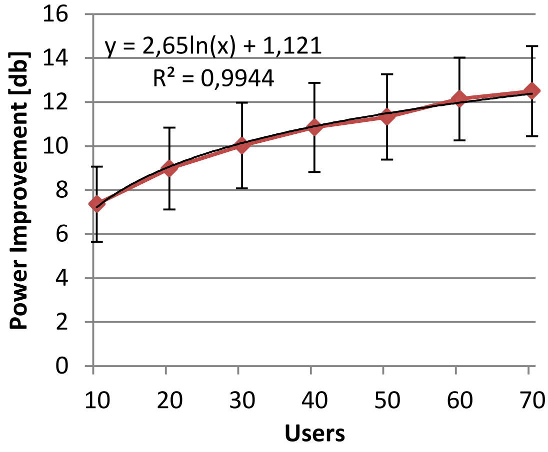

(f): Dense urban (0.6km), 8 elements

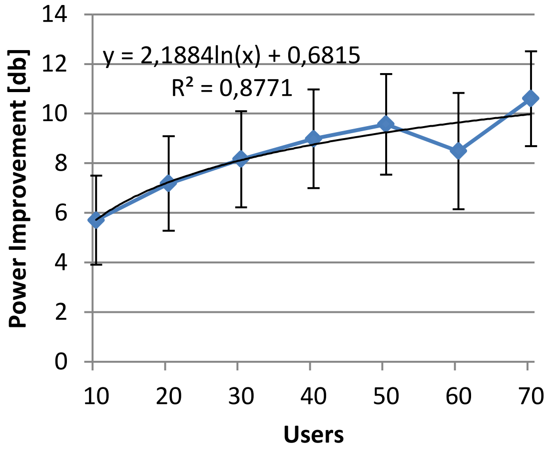

(g): Dense urban (0.8km), 4 elements

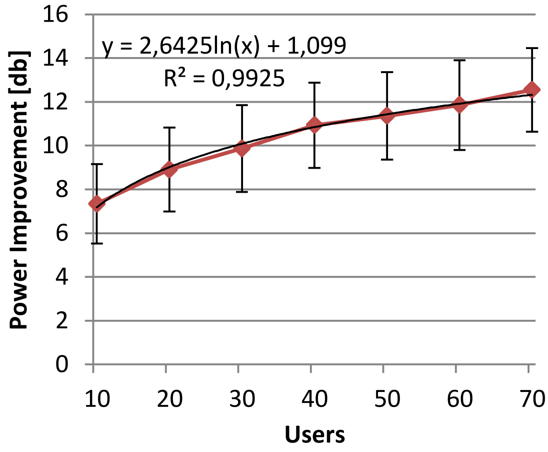

(h): Dense urban (0.8km), 8 elements

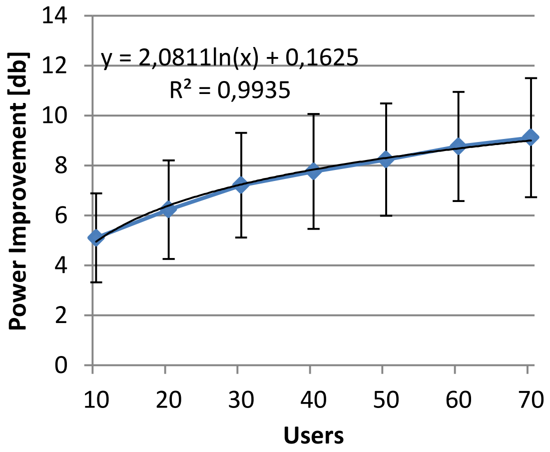

(i): Suburban (1km), 4 elements

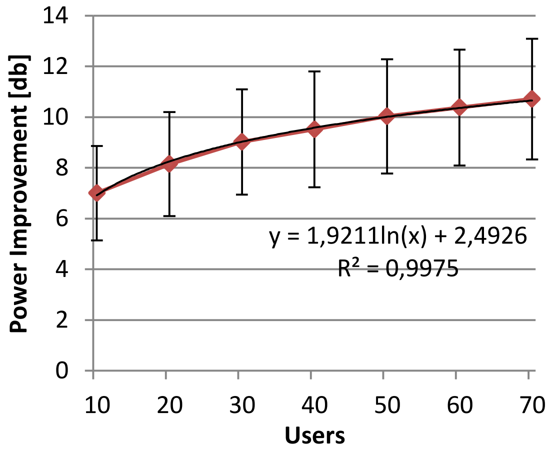

(j): Suburban (1km), 8 elements

Figure B.2 (continuation): Variation of power improvement as a function of users' variation for UMTS.

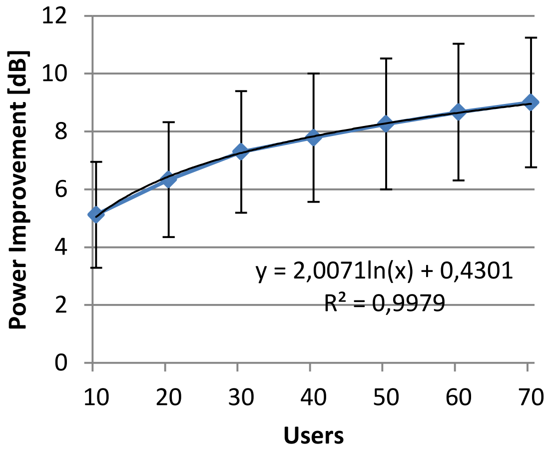

(k): Suburban (1.5km), 4 elements

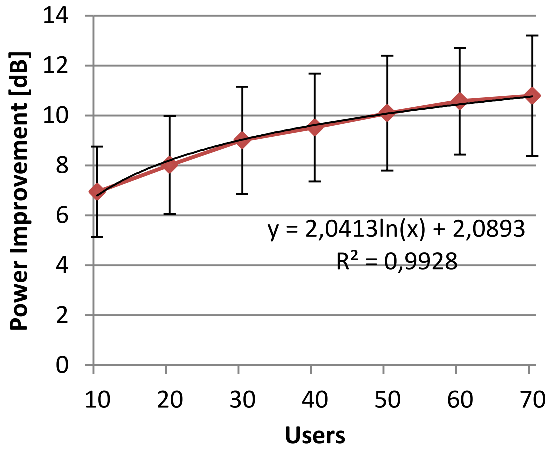

(l): Suburban (1.5km), 8 elements

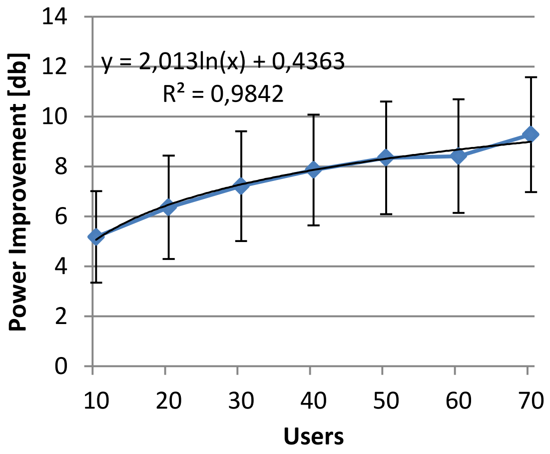

(m): Suburban (2km), 4 elements

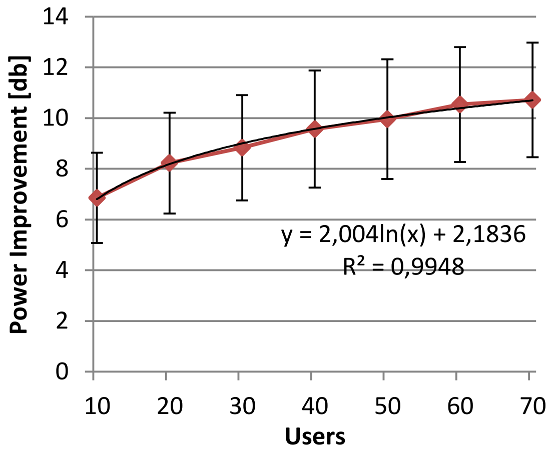

(n): Suburban (2km), 8 elements

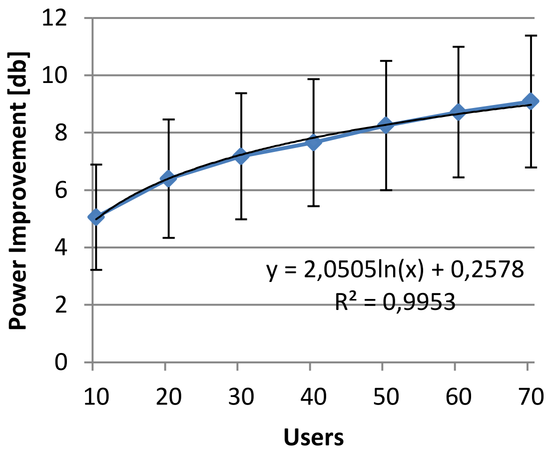

(o): Suburban (2,5km), 4 elements

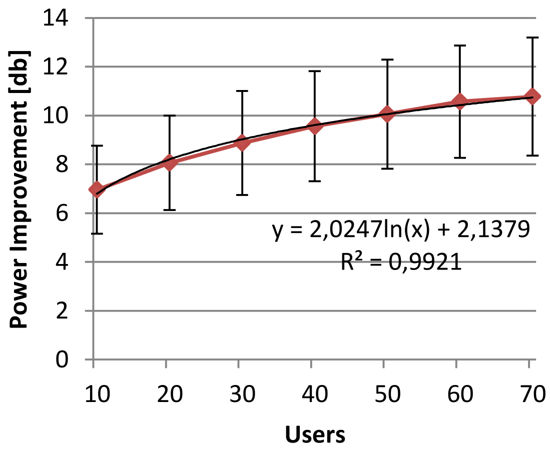

(p): Suburban (2,5km), 8 elements

Figure B.2 (continuation): Variation of power improvement as a function of users' variation for UMTS.

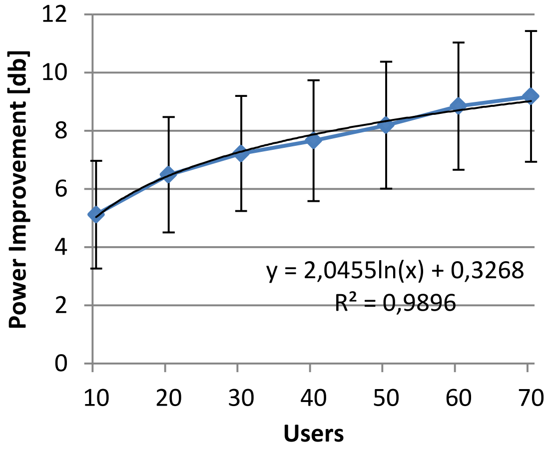

(q): Rural/High Speed (3km), 4 elements

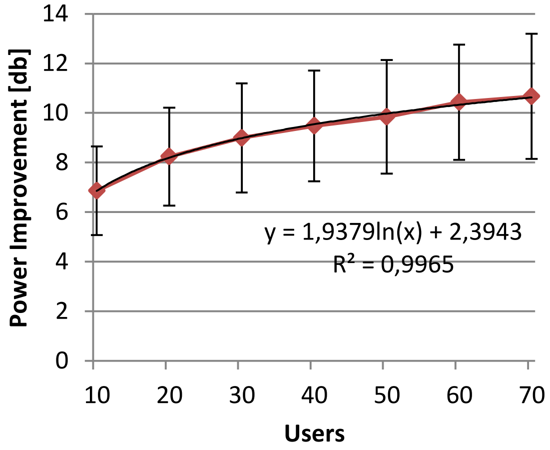

(r): Rural/High Speed (3km), 8 elements

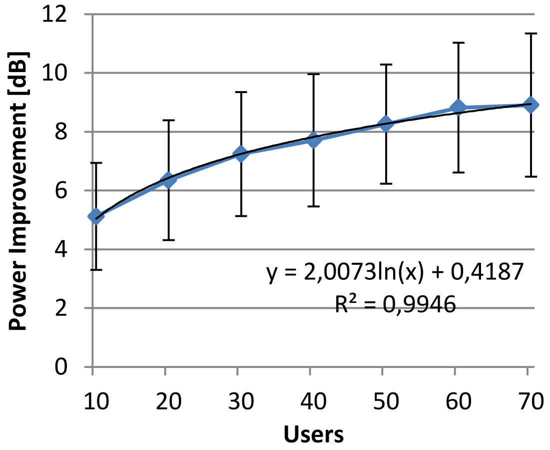

(s): Rural/High Speed (4km), 4 elements

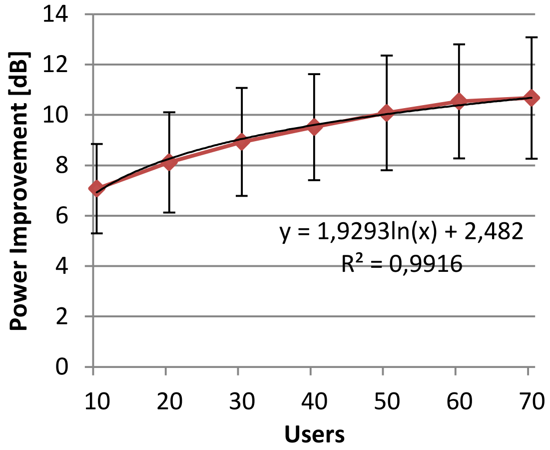

(t): Rural/High Speed (4km), 8 elements

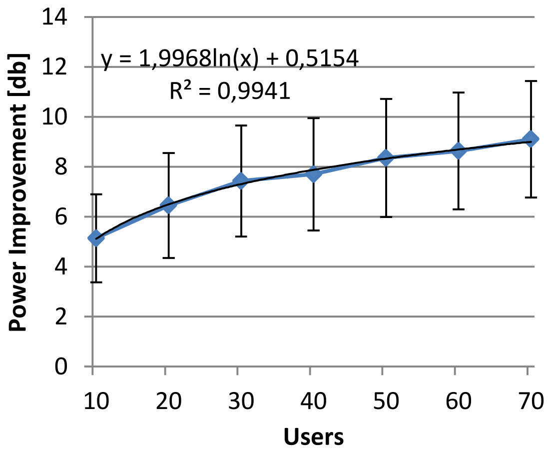

(u): Rural/High Speed (5km), 4 elements

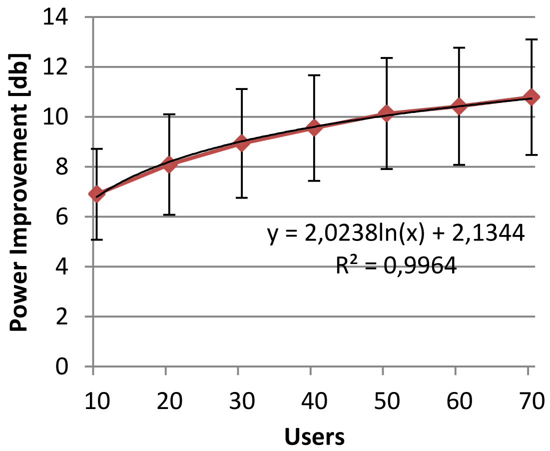

(v): Rural/High Speed (5km), 8 elements

Figure B.2 (continuation): Variation of power improvement as a function of users' variation for UMTS.

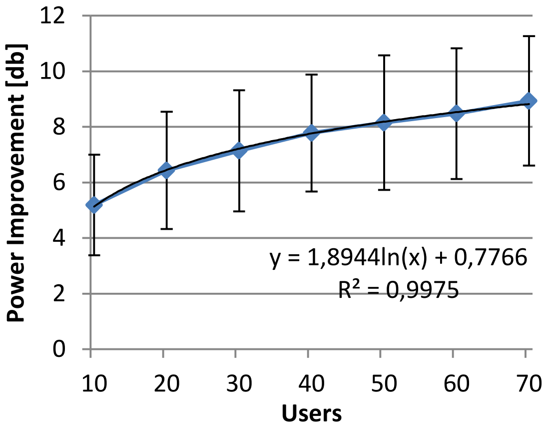

(w): Rural/High Speed (6km), 4 elements

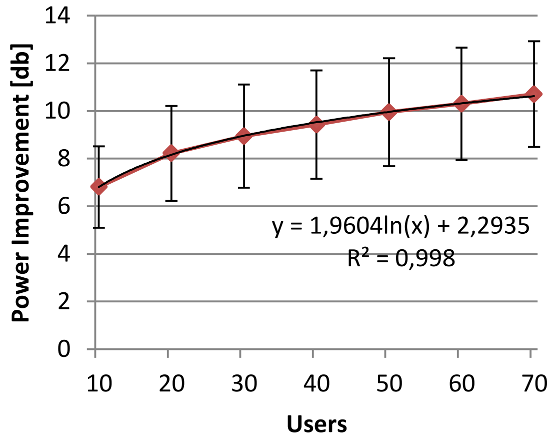

(y): Rural/High Speed (6km), 8 elements

Figure B.2 (continuation): Variation of power improvement as a function of users' variation for UMTS.

A similar set of results was created to LTE. Instead of users, the variation of power improvement is compared with the variation of the number of interferers at neighbour cell, while the variation as afunction of cells' radius remains equal to the UMTS case. Figure B.3 represents the power improvement when cell's radius varies for all the number of interferers that were taken into account.

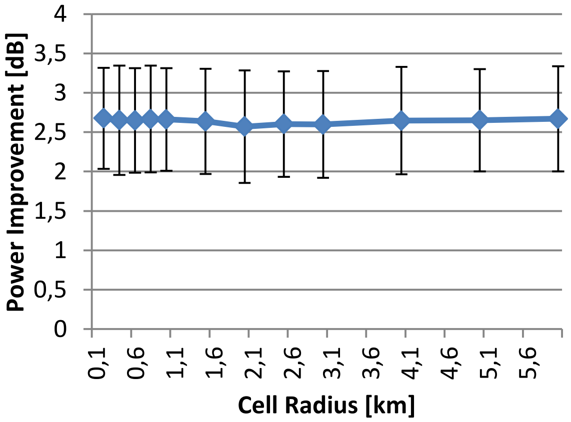

(a): 4 elements, 0 interferers

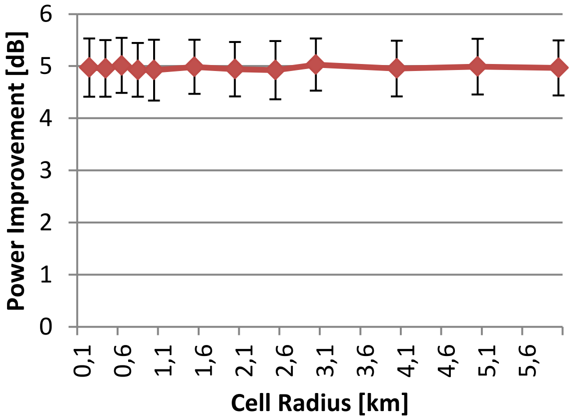

(b): 8 elements, 0 interferers

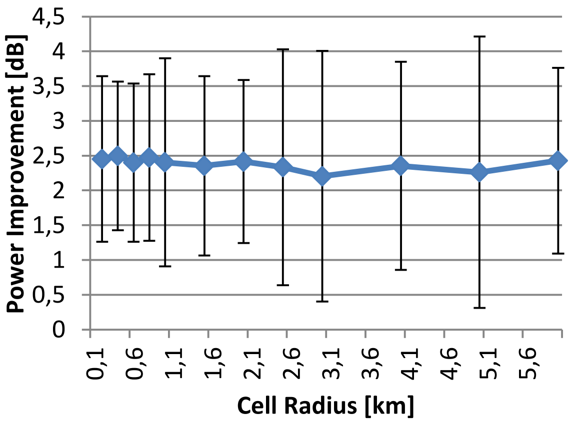

(c): 4 elements, 1 interferers

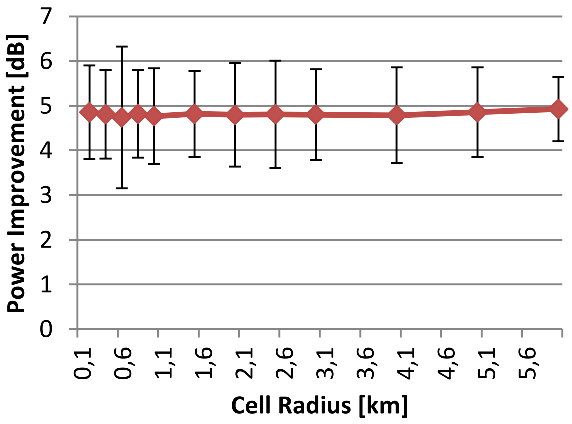

(d): 8 elements, 1 interferers

Figure B.3: Variation of power improvement as a function of variation of cells' radius for LTE.

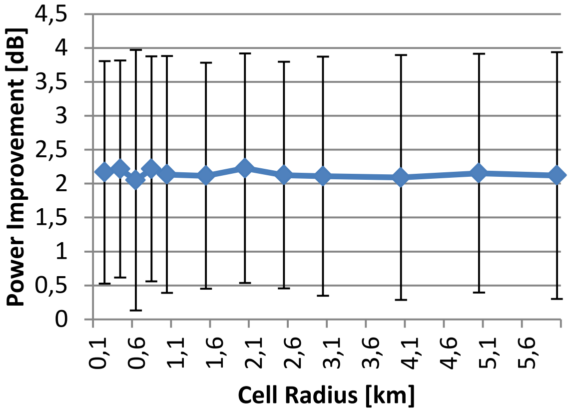

(e): 4 elements, 2 interferers

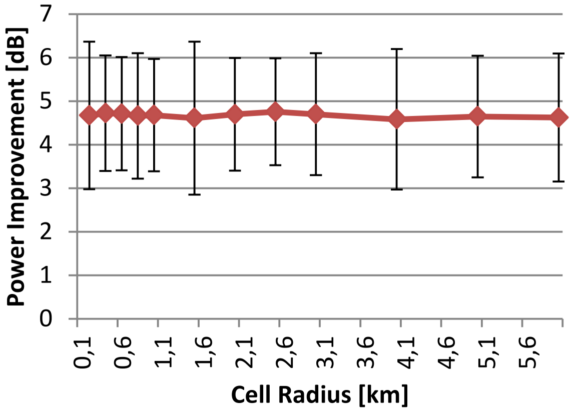

(f): 8 elements, 2 interferers

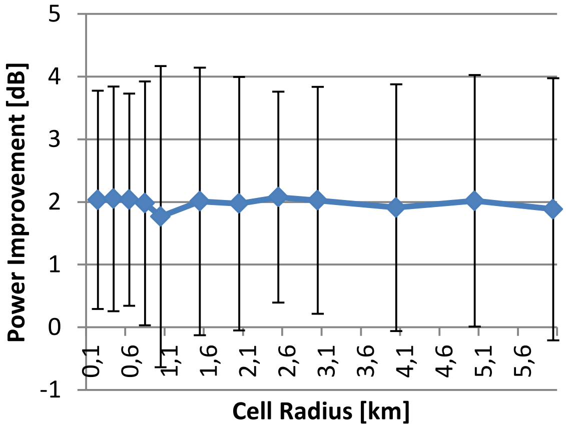

(g): 4 elements, 3 interferers

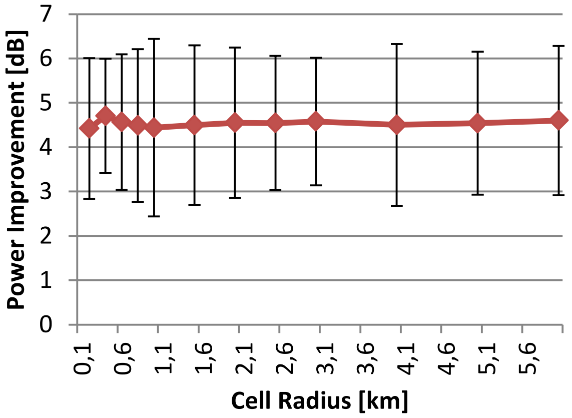

(h): 8 elements, 3 interferers

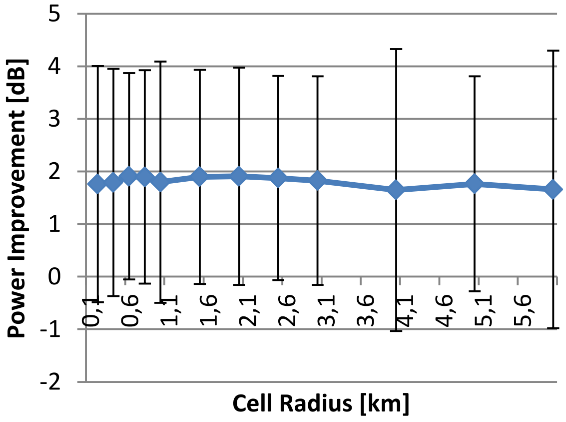

(i): 4 elements, 4 interferers

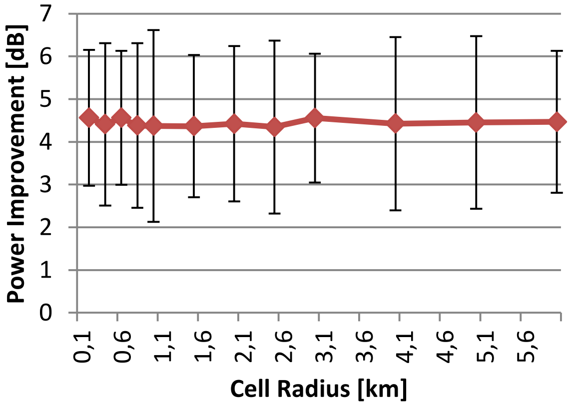

(j): 8 elements, 4 interferers

Figure B.3 (continuation): Variation of power improvement as a function of variation of cells' radius for LTE.

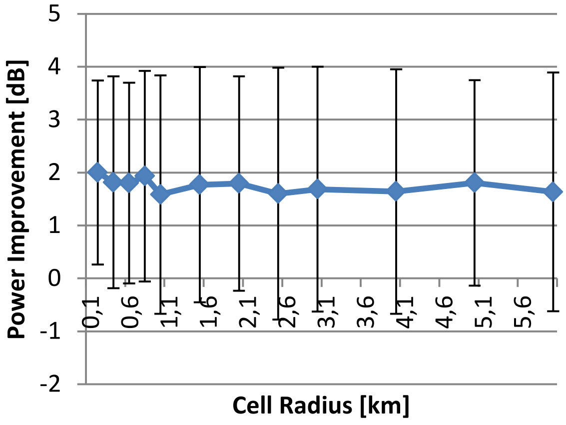

(k): 4 elements, 5 interferers

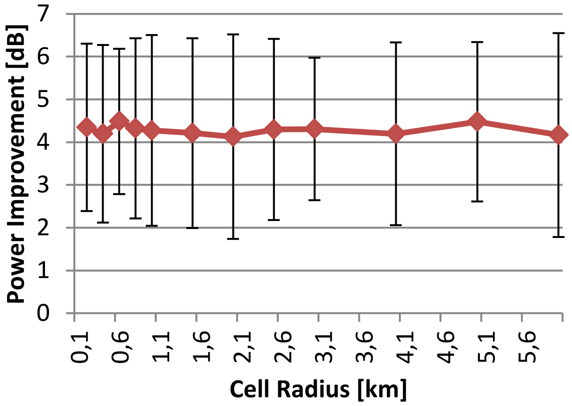

(l): 8 elements, 5 interferers

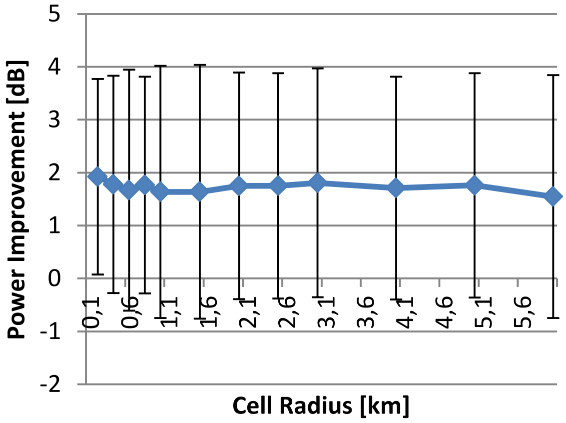

(m): 4 elements, 6 interferers

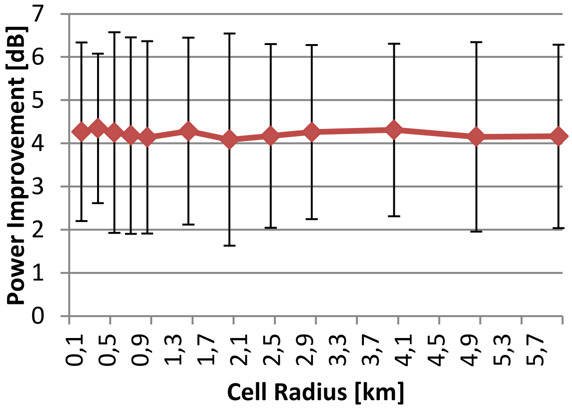

(n): 8 elements, 6 interferers

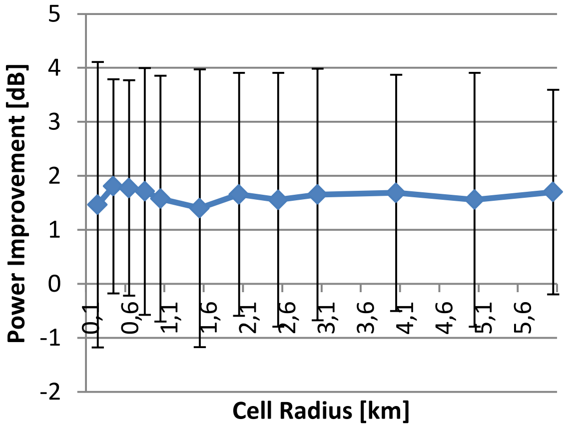

(o): 4 elements, 7 interferers

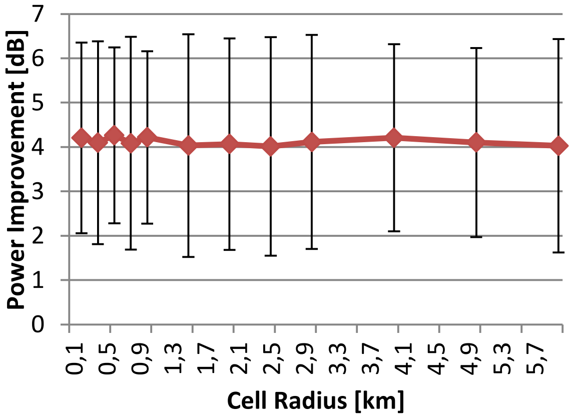

(p): 8 elements, 7 interferers

Figure B.3 (continuation): Variation of power improvement as a function of variation of cells' radius for LTE.

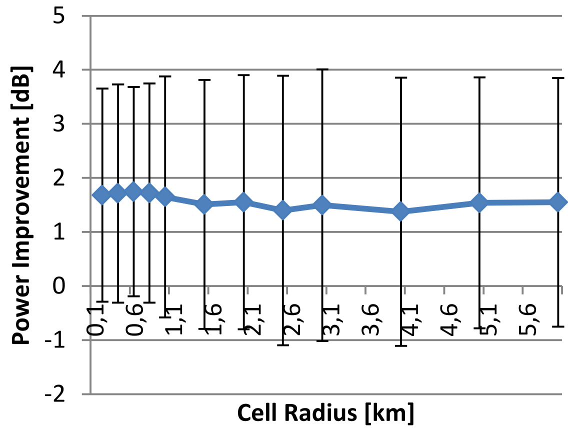

(q): 4 elements, 8 interferers

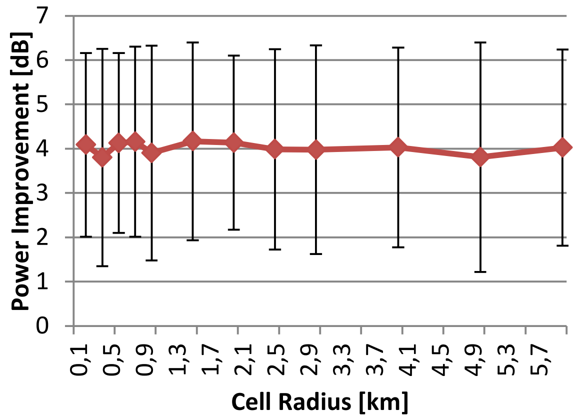

(r): 8 elements, 8 interferers

Figure B.3 (continuation): Variation of power improvement as a function of variation of cells' radius for LTE.

Also the variation of power improvement as a function of interferers' variation were analysed for LTE. Figure B.4 shows the entire set of results for the variation of interferers, for both antennas, scenarios and cells' radius.

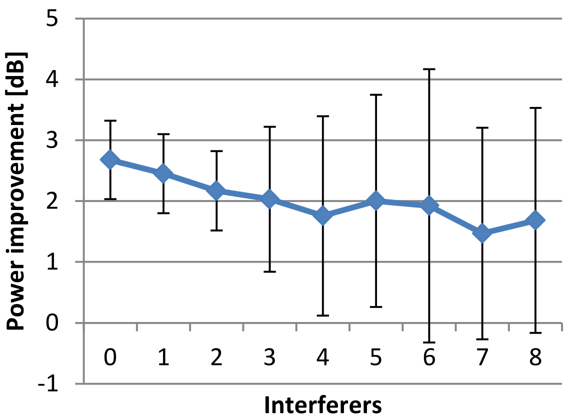

(a): Dense urban (0.2km), 4 elements

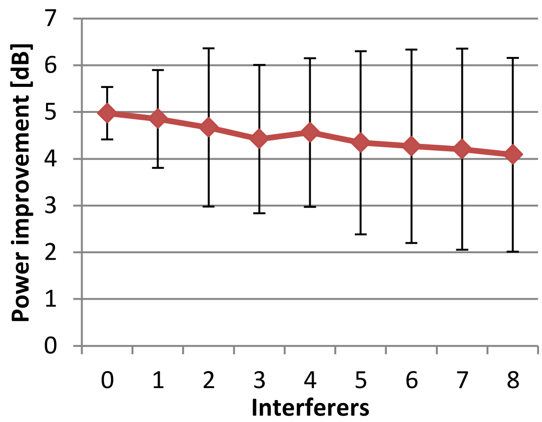

(b): Dense urban (0.2km), 8 elements

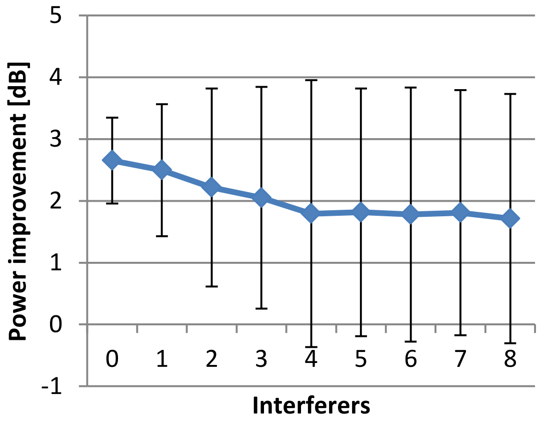

(c): Dense urban (0.4km), 4 elements

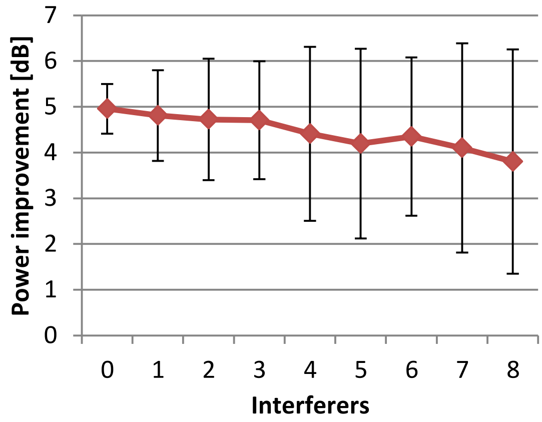

(d): Dense urban (0.4km), 8 elements

Figure B.4: Variation of power improvement as a function of users' variation, for LTE.

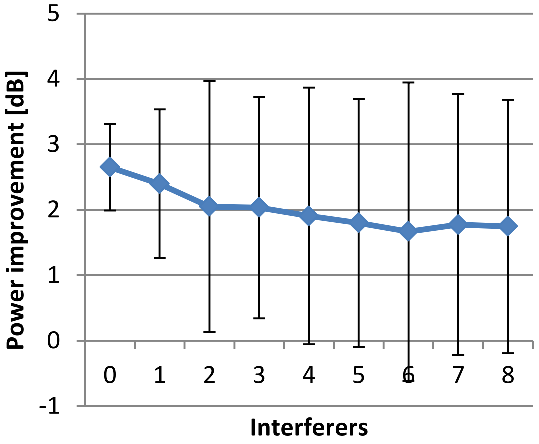

(e): Dense urban (0.6km), 4 elements

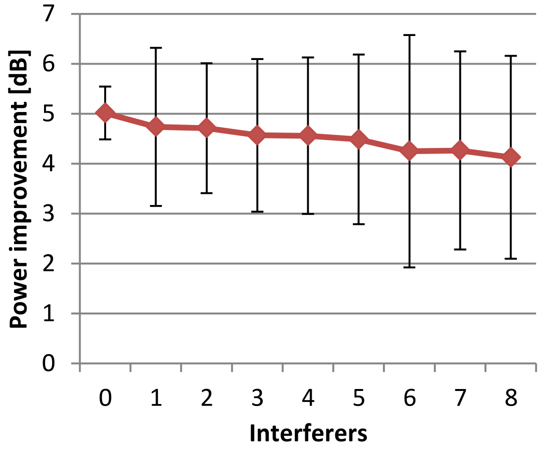

(f): Dense urban (0.6km), 8 elements

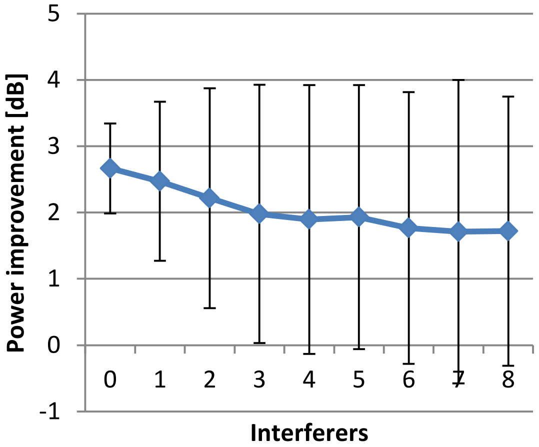

(g): Dense urban (0.8km), 4 elements

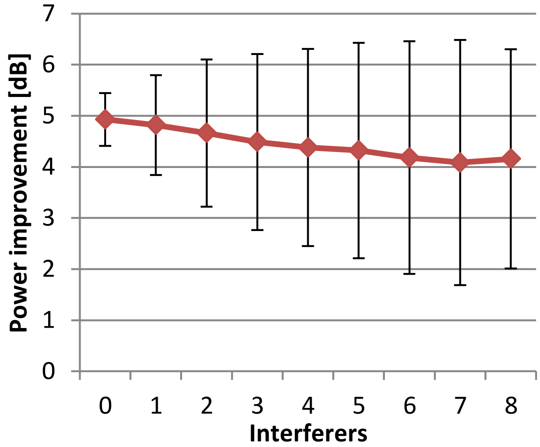

(h): Dense urban (0.8km), 8 elements

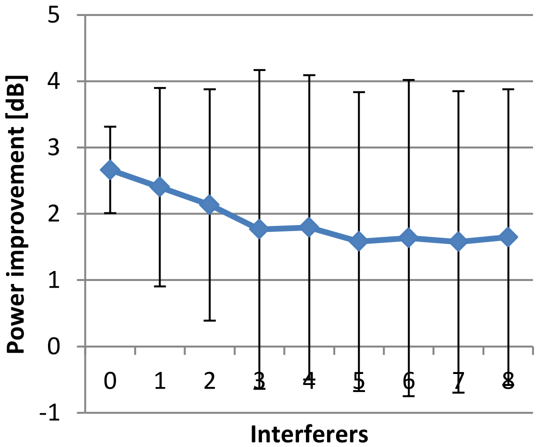

(i): Suburban (1km), 4 elements

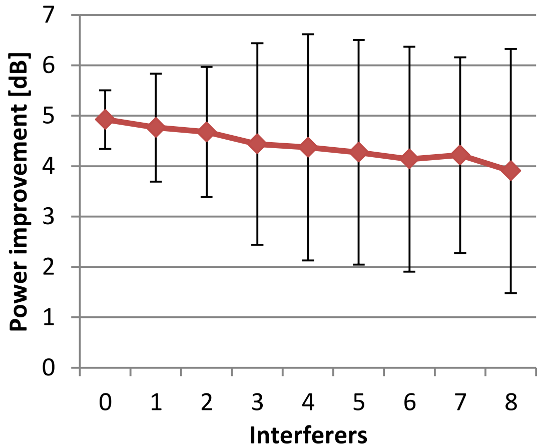

(j): Suburban (1km), 8 elements

Figure B.4 (continuation): Variation of power improvement as a function of users' variation, for LTE.

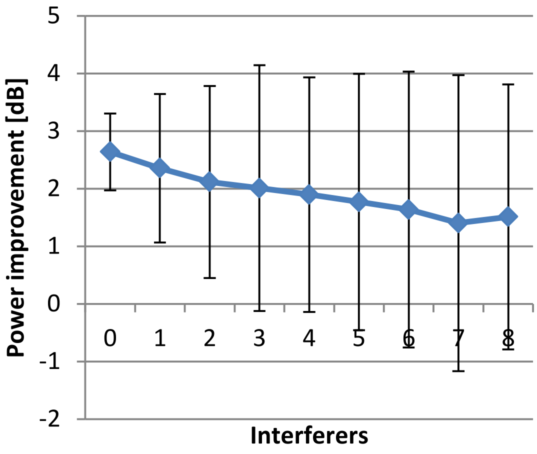

(k): Suburban (1.5km), 4 elements

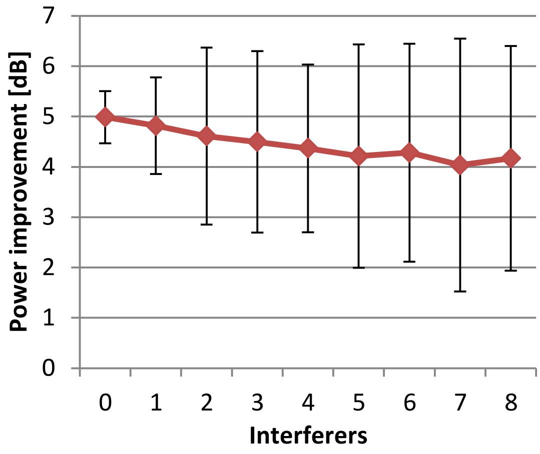

(l): Suburban (1.5km), 8 elements

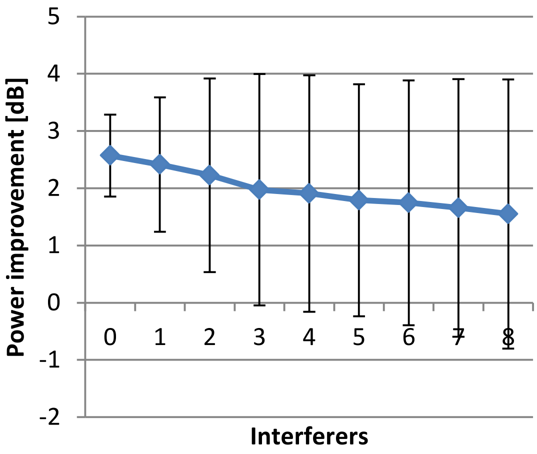

(m): Suburban (2km), 4 elements

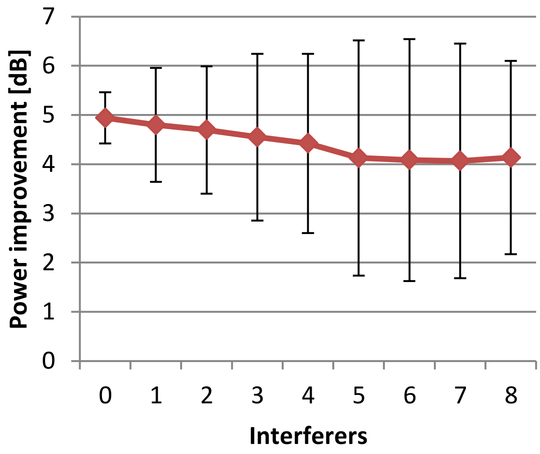

(n): Suburban (2km), 8 elements

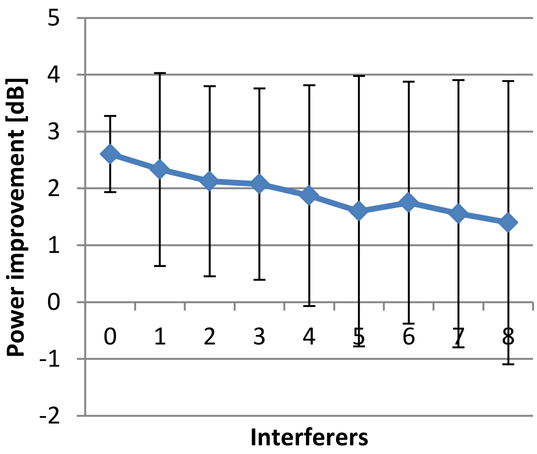

(o): Suburban (2,5km), 4 elements

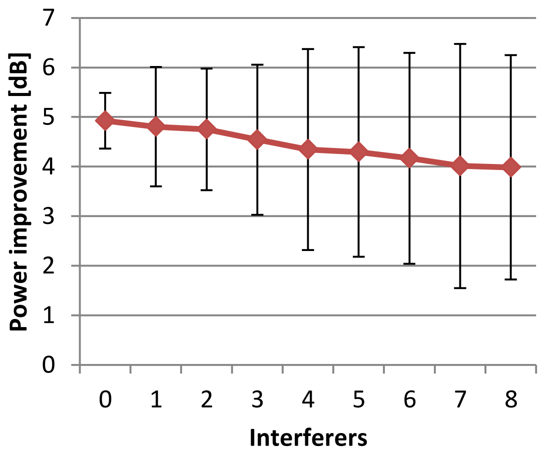

(p): Suburban (2,5km), 8 elements

Figure B.4 (continuation): Variation of power improvement as a function of users' variation, for LTE.

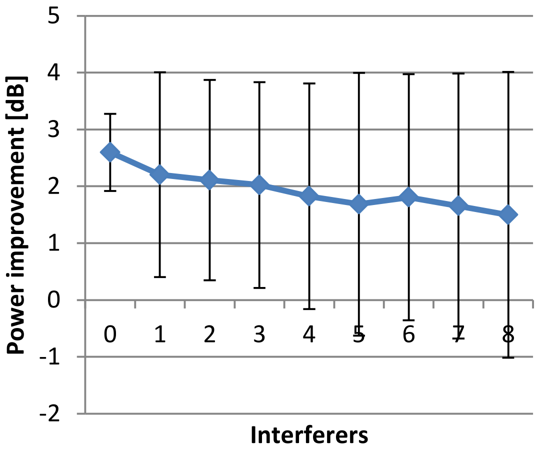

(q): Rural/High Speed (3km), 4 elements

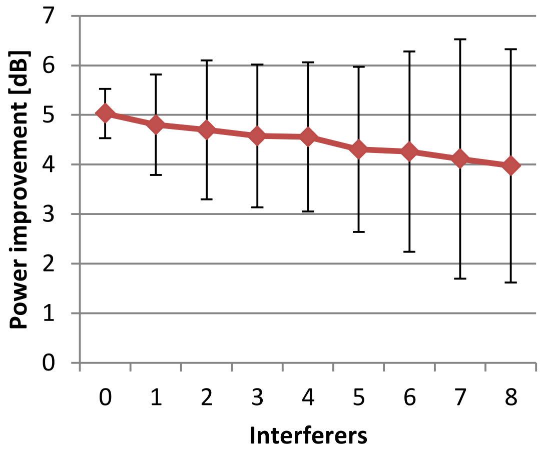

(r): Rural/High Speed (3km), 8 elements

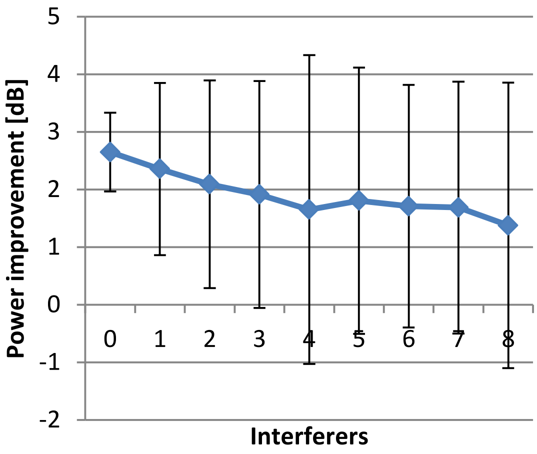

(s): Rural/High Speed (4km), 4 elements

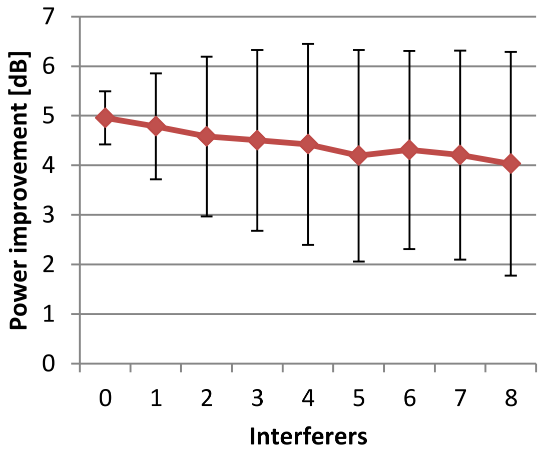

(t): Rural/High Speed (4km), 8 elements

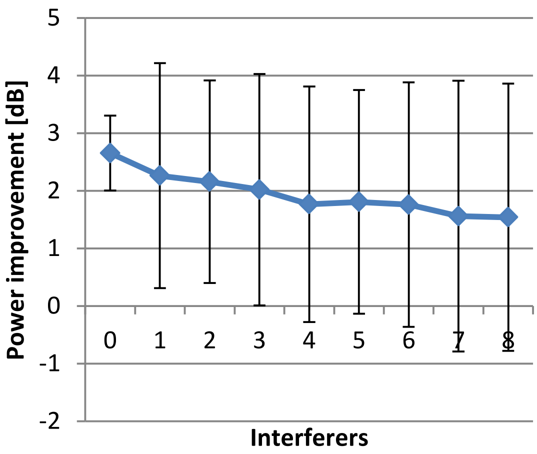

(u): Rural/High Speed (5km), 4 elements

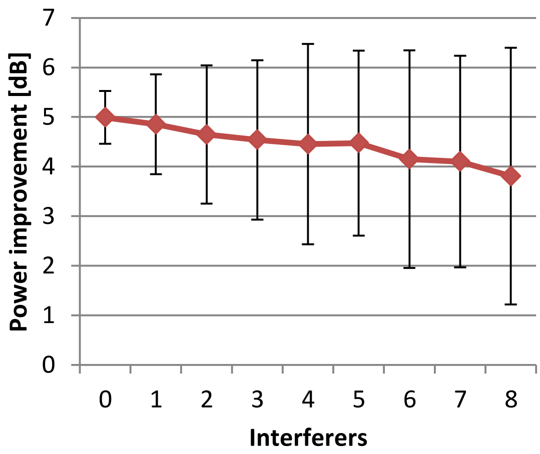

(v): Rural/High Speed (5km), 8 elements

Figure B.4 (continuation): Variation of power improvement as a function of users' variation, for LTE.

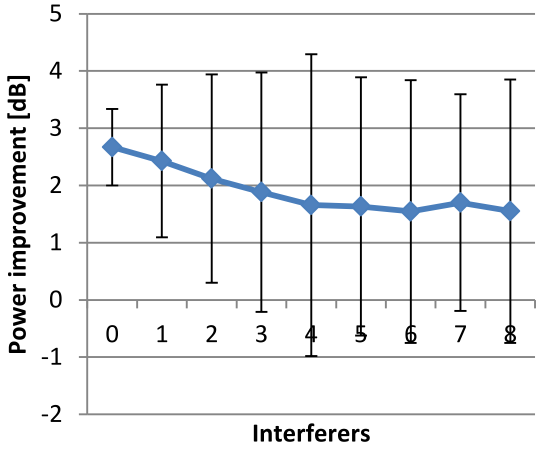

(w): Rural/High Speed (6km), 4 elements

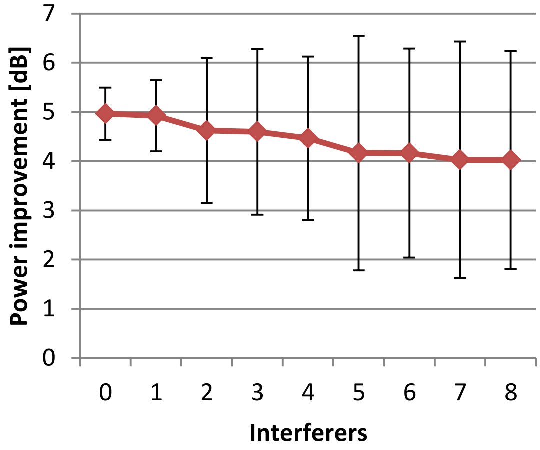

(y): Rural/High Speed (6km), 8 elements

Figure B.4 (continuation): Variation of power improvement as a function of users' variation, for LTE.

References

[3GPP09a] 3GPP, *Technical Specification Group Radio Access Network, Requirements for Evolved UTRA (E-UTRA) and Evolved UTRAN (E-UTRAN) (Release 9)*, Report TS 25.913, V.9.0.0, Dec. 2009 (http://www.3gpp.org/ftp/Specs/html-info/25913.htm)

[3GPP10a] 3GPP, *Technical Specification Group Radio Access Network, Services provided by the physical layer (Release 10)*, Report TS 25.302, V.10.1.0, Dec. 2010 (http://www.3gpp.org/ftp/Specs/html-info/25302.htm)

[3GPP10b] 3GPP, *Technical Specification Group Radio Access Network, Evolved Universal Terrestrial Radio Access (E-UTRA) and Evolved Universal Terrestrial Radio Access Network (E-UTRAN); Overall description; Stage 2 (Release 10)*, Report TS 36.300, V.10.2.0, Dec. 2010 (http://www.3gpp.org/ftp/Specs/html-info/36300.htm)

[3GPP10c] 3GPP, *Technical Specification Group Radio Access Network, Evolved Universal Terrestrial Radio Access (E-UTRA);User Equipment (UE) radio transmission and reception (Release 8)*, Report TS 36.101, V.8.12.0, Dec, 2010 (http://www.3gpp.org/ftp/Specs/html-info/36101.htm)

[3GPP10d] 3GPP, *Technical Specification Group Radio Access Network, Evolved Universal Terrestrial Radio Access (E-UTRA); User Equipment (UE) radio access capabilities (Release 8)*, Report TS 36.306, V.8.7.0, Jun. 2010 (http://www.3gpp.org/ftp/Specs/html-info/36306.htm)

[Agil07] Agilent Technologies, *"Agilent Technologies Solutions for 3GPP LTE"*, Technical Overview, USA, 2007 (http://cp.literature.agilent.com/litweb/pdf/5989-6331EN.pdf)

[AnMC11] Autoridade Nacional de Comunicações, *Draft decision on limiting the number of rights to use frequencies in the 450 MHz, 800 MHz, 900 MHz, 1800 MHz, 2.1 GHz and 2.6 GHz bands and definition of the procedure for allocation* (in Portuguese), Lisbon, Portugal, 2011

[BrSA11] Brisa Autoestradas, Brito S.A, http://www.brisa.pt/

[Chan04] Chandran,S., *Adaptive Antenna Arrays: Trends and Applications*, Springer, Berlin, Germany, 2004

[CoPo11] CP, Comboios de Portugal, http://www.cp.pt/cp/displayPage.do?vgnextoid=3836d5abe2a74010VgnVCM1000007b01a8c0RCRD

[CZBF10] Correia,L.M., Zeller,D., Blume,O., Ferling,D., Jading,Y., Gódor,I., Auer,G., Van Der Perre,L., "Challenges and Enabling Technologies for Energy Aware Mobile Radio Networks", *IEEE Communications Magazine*, Vol.48, Nov. 2010, pp.66-72

[EarP10a] ICT Earth Project, *Most Promising Tracks of Green Radio Technologies*, Deliverable D4.1, version 1.0.0, Dec. 2010. (https://bscw.ict-earth.eu/pub/bscw.cgi/d29584/EARTH_WP4_D4.1.pdf)

[EarP11a] https://www.ict-earth.eu/, Sept. 2011

[EarP11b] ICT Earth Project, *Economic and Ecological Impact of ICT*, Deliverable D2.1, version 2.0.0, Apr. 2011. (https://bscw.ict-earth.eu/pub/bscw.cgi/d38532/EARTH_WP2_D2.1_v2.pdf)

[FaNo98] Farsakh,C., Nossek,J.A., "Spatial covariance based downlink beamforming in an SDMA mobile radio system", *IEEE Transactions on Communications*, Vol.46, No.11, Nov. 1998, pp.1497 - 1506

[Gold05] Goldsmith,A., *Wireless Communication*, Cambridge University Press, UK, 2005

[Hoto04] Holma,H. and Toskala,A., *WCDMA for UMTS* (3rd Edition), John Wiley & Sons, Chichester, UK, 2004

[Hoto07] Holma,H. and Toskala,A., *WCDMA for UMTS – HSPA Evolution and LTE* (4rd Edition), John Wiley & Sons, Chichester, UK, 2007.

[HuAH09] Huang,K., Andrews,J.G. and Heath,R.W., "Performance on Orthogonal Beamforming for SDMA With Limited Feedback", *IEEE Transactions on Vehicular Technology*, Vol.58, No.1, Jan. 2009

[HuGa10] Huq,K.M.S and Gameiro,A., "Resource Allocations For Distributed Broadband Wireless System", in *2nd International Conference on Software Technology and Engineering(ICSTE)*, San Juan, Puerto Rico, USA, Oct. 2010

[Jaci09] Jacinto,N., *Performance Gains Evaluation from UMTS/HSPA+ to LTE at the Radio Network Level*, M.Sc. Thesis, Instituto Superior Técnico, Lisbon, Portugal, Nov. 2009.

[LiK08] Li,K. "Green Thinking Beyond TCO Consideration", in-stat, whitepaper, May, 2008

[LiLo96] Litva,J. and Lo,T.K., *Digital Beamforming in Wireless Communications*, Artech House, Norwood, MA, USA, 1996

[NSNC08] Nokia Siemens Networks Corporations, *Ethiopian Telecommunications Corporation (ETC) A Success Story*, Internal Brochure, Finland, 2008 (http://www.nokiasiemensnetworks.com/sites/default/files/document/ETC_Ethiopian_communications_network_powered_by_renewable_energy_solutions.pdf).

[OhGy00] Ohira,T. and Gyoda,K., "Electronically Steerable Passive Array Radiator Antennas for Low-Cost Analog Adaptive Beamforming", *IEEE International Conference in Phased Array Systems and Technology*, Dana Point, USA, May 2000.

[SeCa04] Sebastião,D. and Cardeiro,J., *Modelation and Traffic Dimensioning in the UMTS Radio Interface*, Graduation Thesis, Instituto Superior Técnico, Lisbon, Portugal, Oct. 2004.

[Kemp11] Kemp.S., lightRadio™ Technology Overview, Alcatel-Lucent - Techzine, May, 2011 (http://www2.alcatel-lucent.com/blogs/techzine/2011/lightradiotechnology-overview/).

[ViTL02] Viswanath,P., Tse,D.N.C. and Laroia,R., "Opportunistic Beamforming Using Dumb Antennas", *IEEE Transactions on Information Theory*, Vol.48, No. 6, Jun. 2002

[ZKTC11] Zeydan,E., Kivanc,D., Turelli,U. and Comaniciu,C., "Joint iterative beamforming and power adaptation for MIMO in ad hoc networks", *EURASIP Journal on Wireless Communications and Networking*, No. 79, Aug. 2011.